Codes And Methods Improvements

for VVER comprehensive safety assessment

Grant Agreement Number: 945081
Start date: 01/09/2020 - Duration: 36 Months

D3.1 - A comprehensive review of the available VVER data for verification and validation of neutronics and thermal-hydraulics codes

Hashymov Artur (Energorisk), Oleksandr Sevbo (Energorisk)

Version 1 – 16/04/2021

This project has received funding from the Euratom research and training programme 2019-2020 under grant agreement No 945081.

CAMIVVER – Grant Agreement Number: 945081

Document title	A comprehensive review of the available VVER data for verification and validation of neutronics and thermal-hydraulics codes
Author(s)	Hashymov Artur (Energorisk), Oleksiy Shumayev (Energorisk),Oleksandr Sevbo (Energorisk), Stanislav Dombrovskyi (Energorisk). Antoaneta Stefanova (INRNE), Neli Zaharieva (INRNE)
Document type	Deliverable
Work Package	WP3
Document number	D3.1 - version 1
Issued by	Energorisk, (ER) Institute for Nuclear Research and Nuclear Energy, (INRNE)
Date of completion	16/04/2021
Dissemination level	Public

Summary

The objective of the H2020 CAMIVVER project is to develop and improve codes and methods for VVER comprehensive safety assessment.

Work Package 3 (WP3) is intended to collect input data and make a comparison between data from different partners, to build common sets of data that will be used for the benchmarks. WP3 is dedicated to establishing a common and shared database for VVER comprehensive safety assessment codes and methods verification and validation.

This WP will allow the partners to share past experiences on VVER safety analysis calculations and to build together a common base for preparing the next phases towards the codes industrializations.

In particular, Task 3.1 is dedicated to the analysis and classification of available VVER data for verification and validation of neutronics and thermal-hydraulics codes.

This Deliverable D3.1 provides an overview of the main VVER experimental and benchmark data available to the International Community (IAEA, OECD/NEA, past European projects, publications, etc.) for verification and validation of neutronics and thermal-hydraulics codes. The information of past experiences on VVER safety analysis, relevant to the project, is summarized to give general information for VVER reactors, to provide data for WP4 and WP5 that additionally will be used in performing of WP6 and WP7 and thus will facilitate the creation of a common and shared database for VVER comprehensive safety assessment codes and methods verification and validation for next phases of the CAMIVVER project.

The report provides data describing the reactor, including the internal devices, the nuclear fuel of the fuel assembly, the thermal and neutron-technical parameters of the core. The set of parameters presented in the report is intended for modeling the core and performing validation and verification of the models. For verification and validation of the models, the report presents data on the neutron-physical characteristics of the fuel load of a serial VVER reactor. Detailed geometrical characteristics, composition and properties of materials are given for the reactor, internal structures, fuel assemblies and absorbing rods.

Approval

Version	First Author	WP leader	Project Coordinator
1	A. Hashymov (Energorisk) 16/04/2021	P.Groudev (INRNE) 16/04/2021	D. Verrier (Framatome) 16/04/2021

-

Table of Contents

List of Figures

List of Tables

Abbreviations

AE	-	Absorbing element
AER	-	Atomic Energy Research
APC	-	Automatic reactor power control system
AR	-	Absorbing rod
ATHLET	-	Name of the calculation code
BMU	-	Name of the project
BOC	-	Beginning of Cycle
BOL	-	Beginning of Life
BST	-	Block of Shielding Tubes
CAD	-	Computer-aided design
CASMO	-	Name of the calculation code
CCVM	-	CSNI Code Validation Matrices
CEA	-	Commissariat a l'Enerige Atomique
CFD	-	Computational fluid dynamics
CHF	-	Critical heat flux
CPS	-	control and protection system
CR	-	Control rod
CSNI	-	Committee on the safety of nuclear installations
DBA	-	Design basis accidents
DNB	-	Departure from nucleate boiling
DNBR	-	Departure from nucleate boiling ratio
DYN3D	-	Name of the calculation code
ECCS	-	System of emergency cooling of active zone
ENDF/B6	-	Name of the cross-section library
EOC	-	End of cycle
EP	-	Emergency protection
ETE	-	Name of the benchmark
FA	-	Fuel assembly
FE	-	Fuel element
FEG	-	Fuel element with gadolinium

FFTBM	-	Fast Fourier transform-based method
FP	-	Fuel pool
FZR	-	Forschungszentrum Rossendorf e.V.
GRS	-	Geselschaft für Reaktorsicherheit
HELIOS	-	Name of the calculation code
HEXNEM	-	Name of the method
HZP	-	Hot zero power
IAEA	-	International Atomic Energy Agency
INRNE	-	Institute for Nuclear Research and Nuclear Energy
IRC	-	in-reactor control
ISP	-	International Standard Problems
ITF	-	Integral Test Facility
KhNPP	-	Khmelnitsky Nuclear Power Plant
KORSAR	-	Name of the calculation code
LB	-	Large break
LES	-	Large eddy simulation
LOCA	-	Loss of Coolant Accident
LWR	-	Light water reactor
MARIKO	-	Name of the calculation code
MCNP	-	Monte Carlo N-Particle Transport Code
MCP	-	Main circulation pipeline
MIDICORE	-	Name of the benchmark
MOC	-	Middle of cycle
MOX	-	Mixed oxide fuel
MPL	-	Minimum power level
MSLB	-	Main steam-line break
NEA	-	Nuclear Energy Agency
NESSEL	-	Name of the calculation code
NFC	-	neutron-physical characteristics
NMC	-	neutron measurement channel
NPP	-	Nuclear power plant

NRC	-	Nuclear Regulatory Commission
OECD	-	The Organisation for Economic Co-operation and Development
OLD	-	Offload and limita- tion device
PACTEL	-	Name of the test facility
PCR	-	Power coefficient of reactivity
PER	-	Power effects of reactivity
PJSC “Impulse”	-	Private joint-stock company
PMK	-	Name of the test facility
PPJ	-	Power prompt jump
PRC	-	Power reactivity coefficient
PSB-VVER	-	Name of the test facility
PWR	-	Pressurized water reactors
RANS	-	Reynolds-averaged Navier–Stokes
RBA	-	rods with burn-out absorber
RC	-	Control rod
RDF	-	Reference discontinuity factors
RELAP5	-	Name of the calculation code
RIA	-	Reactivity insertion accidents
SAR	-	Safety analysis report
SCP	-	
SETF	-	Separate Effect Test Facility
SFR	-	Sodium fast reactor
SG	-	Steam generator
SOU NAEK	-	Standard of the organization of Ukraine "National Atomic Energy Generating
SPE	-	Standard problem exercises
SPM	-	Singularly perturbed method
SRR-1/95	-	Name of the test project
SSTC NRS	-	State Scientific and Technical Center for Nuclear and Radiation Safety
SUNPP	-	South-Ukraine NPP
SUSA	-	Name of the statistical package
TC	-	thermocouple

TECH-M	-	Name of the calculation code
TOX	-	Thorium-plutonium mixed oxide
TPJ	-	Temperature prompt jump method
TRACE	-	Name of the calculation code
TVSA	-	Name of the fuel assembly
TVS-W	-	Name of the fuel assembly
UOX	-	Uranium oxide
VALCO	-	Name of the benchmark
VTT	-	VTT Technical Research Centre of Finland
VVER, WWER	-	Water-Water Energetic Reactor
WIMS	-	Name of the calculation code
WP	-	Work package

1. Introduction

This deliverable D3.1 on the “Analysis and classification of available VVER data for verification and validation of neutronics and thermal-hydraulics codes” is part of CAMIVVER, WP3, Task 3.1 in accordance with the CAMIVVER Grant agreement, NUMBER 945081[1]. Task 3.1 is dedicated to the establishment of a common database required for the development of the core model of the VVER-1000 serial reactor.

The report provides an overview of the main VVER experimental and benchmark data available to the International Community (IAEA, OECD/NEA, past European projects, publications, etc.) for verification and validation of neutronics and thermal-hydraulics codes. The information of past experiences on VVER safety analysis, relevant to the project, is summarized to give general information for VVER reactors, to provide data for WP4 and WP5 that additionally will be used in performing of WP6 and WP7 and thus will facilitate the creation of a common and shared database for VVER comprehensive safety assessment codes and methods verification and validation for next phases of the CAMIVVER project.

The report provides data describing the reactor, including the internal devices, the nuclear fuel of the fuel assembly, the thermal and neutron-technical parameters of the core. The set of parameters presented in the report is intended for modeling the core and performing validation and verification of the models. For verification and validation of the models, the report presents data on the neutron-physical characteristics of the fuel load of a serial VVER reactor. Detailed geometrical characteristics, composition and properties of materials are given for the reactor, internal structures, fuel assemblies and absorbing rods.

Contributors: INRNE, ENERGORISK, FRA, CEA, EDF, KIT, UNIPI

2. Review of existing literature sources

This section provides an overview of the work performed in the thermal-hydraulic and neutron-physical modeling of the VVER-1000 core.

The main sources of information on previously completed work, as well as a brief overview of them, are presented in the table below.

Table 2-1 - Brief description of the main existing data

Title	Context	References	Participants	Summary
PROPOSAL OF A BENCHMARK FOR CORE BURNUP CALCULATIONS FOR A VVER-1000 REACTOR CORE, Proceedings of the 19th AER Symposium on VVER Reactor Physics and Reactor Safety, St. St. Constantine and Elena resort, Bulgaria, Sept. 21÷25, 2009, p.53 T. Lötsch V. Khalimonchuk A. Kuchin	AER	https://inis.iaea.org/collection/NCLCollectionStore/_Public/41/035/41035568.pdf	TÜV Süd Group (IS-ET), SSTC N&RS	In the framework of the project SR2611 supported by the German BMU, the code DYN3D and the associated data libraries was intended to be further validated and verified. The project is based on the results of the work done in the framework of previous BMU projects dealing with the validation and verification of the code packages used for reactor physics calculation within the scope of safety related evaluations and assessments of VVER-1000 reactors. This work presents the continuation of efforts of the projects mentioned to estimate the accuracy of calculated core characteristics of VVER-1000 reactor cores. The codes used for reactor physics calculations of safety related reactor core characteristics should be validated and verified for the cases in which they are to be used. The calculations should, at least, provide reliable information before the reactor startup on the fulfilment of the main safety goals which should be ensured during the reactor operation: 1. Reactivity control 2. Cooling of the fuel assemblies 3. Confinement of radioactive materials 4. Limitation of radiation exposure The paper presents such a proposal for VVER-1000 core burnup calculations on the basis of operational data. The benchmark can be used for integral investigations on the applicability and accuracy of the code package for reactor physics calculations for VVER-1000 reactors. This comprises the FA burnup calculation and few group data preparation as well as the core modelling and cycle burnup calculation. All input data necessary for the FA and core modelling, i.e. FA and

Title	Context	References	Participants	Summary
				reactor core characteristics, loading patterns, load follow etc., are provided. The benchmark proposal specifies a set of operational data such as boron concentration in the coolant, cycle length, measured reactivity coefficients and power density as well as burnup distributions. So the basic data chosen for comparison are given. For calculating the benchmark, at first, the few group data of the FA used in the loadings of the VVER-1000 reactor core should be prepared with the help of codes such as NESSEL [1], CASMO [2], HELIOS [3], WIMS [4] or others. The few group data processing for the preparation of the FA few group data library used in the core calculation is the following step in the benchmark. Next step is the modelling of the reactor core and the cycle burnup. At several burnup steps (usually beginning of cycle - BOC, middle of cycle - MOC, end of cycle - EOC - when the boron concentration Cb ≈ 0, effective end of cycle - EOCeff) core characteristics should be calculated, e.g. reactivity coefficients, power density distributions etc. First results show an acceptable agreement with measured data. But further investigations are necessary to make a conclusion about the quality of the calculations. Statistical analysis is necessary to explain and improve the results as well as to conclude about the accuracy and reliability of the calculation results. Future work comprises the preparation of the data for the third and fourth cycles. This will make it possible to carry out a more reliable statistical analysis of the several sets of calculations. The whole complex of codes used for reactor physics calculations such as codes for FA data preparation and data libraries as well as steady state core calculations can be analysed in relation to the accuracy of the calculated safety parameters for VVER1000 reactors. The benchmark can be extended with other tasks or exercises if required.

Title	Context	References	Participants	Summary
				The benchmark should be completed with information about the measuring errors for a reliable assessment of the quality of the measured and calculated parameters. Such data were not always available during the preparation of the paper presented. Bibliography: 1. Schulz G.: NESSEL Code Manual Version 6.09a, K.A.B. GmbH, Berlin, 1998. 2. Studsvik: CASMO-4 - A fuel assembly burn up program, Version 1.28.05, Studsvik/SOA-95/1, 1995. 3. Casal, J.J. et. al, "HELIOS: Geometric Capabilities of a New Fuel- Assembly Program", Proc. Int. Topl. Mtg. Advances in Mathematics, Computations, and Reactor Physics, Pittsburgh, Pennsylvania, April 28-May 2, 1991, Vol. 2, p. 10.2.1-1. 4. Coll.: WIMS - A Modular Scheme for Neutronics Calculations, User Guide for Version 8, ANSWERS/WIMS(99)9, Winfrith, 1999
THE X2 BENCHMARK FOR VVER-1000 REACTOR CALCULATIONS . RESULTS AND STATUS, International Conference "Novel Vision of Scientific & Technical Support for Regulation of Nuclear Energy Safety:	AER	https://www.researchgate.net/publication/328342155_THE_X2_BENCHMARK_FOR_VVER-1000_REACTOR_CALCULATIONS	TUV SUD, HZDR, SSTC N&RS, IBBS	The paper gives an overview about the tasks defined in the framework of the X2 benchmark, firstly proposed at the 19th symposium of the Atomic Energy Research (AER) in 2009. The X2 benchmark was proposed for validation and verification of the reactor physics code systems for VVER-1000 reactors with loadings of TVSA fuel assemblies. The X2 benchmark comprises all stages of steady state and transient reactor calculations starting with the fuel assembly data preparation. Therefore X2 benchmark specifies the FA and core characteristics as well as the core loading patterns of four consecutive burnup cycles for a Ukraine VVER-1000 reactor core. A set of operational data for comparisons with steady state reactor core burnup calculations and transient neutron kinetics calculations were provided. Such a benchmark is useful for validating and verifying the whole system of codes and data libraries for reactor physics calculations including fuel assembly modelling, fuel assembly data preparation, few group data parametrisation and reactor core modelling. In the framework of several projects supported by the German BMU5) the 3D neutron kinetics code DYN3D and the

Title	Context	References	Participants	Summary
Competence, Transparency, Responsibility" dedicated to the 25th Anniversary of the SSTC NRS, Kiev, Ukraine, 22 – 23 March 2017 T. Lötsch, S. Kliem, E. Bilodid, V. Khalimonchuk, A. Kuchin, Yu. Ovdienko,M. Ieremenko, R. Blank, G. Schultz				coupling of DYN3D with thermo hydraulics system codes were further validated and verified on the basis of the data provided in the framework of the X2 benchmark. In preparing results for the X2 benchmark several organisations have been participated: IBBS, HZDR, SSTC, TUV SUD. The paper presents the current state of the X2 benchmark and discusses results of the work started with the X2 benchmark proposal in 2009. During the work a lack of a benchmark for core burnup calculations for VVER-1000 reactors taking into account all the calculations steps for reactor safety analysis calculations was noticed: FA burnup calculations for the data library preparation, 3D steady state burnup calculations, 3D transient and accident calculations. Whereas well defined benchmarks for FA and steady state core burnup as well as transient calculations for reactors of the VVER-440 type exist (see, e.g., [1], [2], [3], [4]), for VVER-1000 an OECD/NEA benchmark on burnup calculations of theoretical FA with UO_2 and MOX fuel [5] and a benchmark investigating the physics of a mixed VVER- 1000 reactor core using two-thirds low-enriched uranium (LEU) and one-third MOX fuel [6] are published. Another benchmark for VVER-1000 – the Kalinin-3 Benchmark [7] – is focused on the transient calculations with coupled kinetics and thermo-hydraulics system codes using data libraries prepared before for all benchmark participants. Therefore the X2 benchmark for validation and verification of the reactor physics code systems for VVER-1000 reactors with loadings of TVSA fuel assemblies has been developed. The X2 benchmark comprises all stages of steady state and transient reactor calculations starting with the fuel assembly data preparation. The task 1 of the X2 benchmark specifies the FA configurations and designs as well as the results requested for comparison. The reactor core characteristics and the core loading patterns of four consecutive burnup cycles for a Ukraine VVER-1000

Title	Context	References	Participants	Summary
				reactor core were provided for the task 2 of the benchmark. Results of the tasks 1 – the FA burnup calculations and data preparation task - and the task 2 - steady state core burnup calculations. These data sets were completed and reviewed. So, the task 1 results were additionally confirmed by Monte Carlo calculations with the SERPENT code [8], [9]. Task 2 comprises the comparison of operational data and 2D results. As continuation of the work on the X2 benchmark the tasks were extended with task 3 consisting of the comparison of 3D operational data and results of steady state reactor core burnup calculation. That includes pin-by-pin distributions for selected fuel assemblies. Task 4 provides data for 3D stand-alone neutron kinetics calculations as well as calculations with coupled neutron-kinetics and thermo-hydraulics system codes of reactor transients. In preparing results for the X2 benchmark several organisations have been participated: HZDR, SSTC, IBBS, TÜV SÜD. On that basis TÜV SÜD has been provided the analysis and formulation of the specific X2 benchmark tasks. The analysis of the data – experimental, measured and obtained by calculations – showed that on that basis a benchmark for reactor physics calculations of VVER-1000 reactor cores are available for respective model verification and validation. The results of the comparisons between measured and calculated data of the different reactor core parameters showed the sufficiently accurate reactor core calculations using the codes and data libraries mentioned above and used in the framework of the X2 benchmark. The presented results showed further that the whole complex of reactor physics codes used in safety analysis and substantiation as well as in reactor core calculations can be validated:

Title	Context	References	Participants	Summary
				· FA burnup modelling, data preparation and data libraries. · FA shuffling and (may be) history effects. · Calculation of the main safety related core characteristics. · Steady state reactor core calculations. · Transients with 3D kinetic codes and coupled 3D kinetic – thermohydraulic system codes. Bibliography: 1. NP-006-98: Requirements to Contents of Safety Analysis report of Nuclear Power Plant with VVER Reactors (НП-006-98: Требования к содержанию отчета по обоснованию безопасности АС с реактором типа ВВЭР), Gosatomnadzor of Russia, 1995, 2005. 2. P. Mikolas: Summary of Benchmark for VVER-440 with Gd2O3 + UO2 Pins Burnup Comparisons, Proceedings of the 13th Symposium of AER, Dresden, Germany, 22-26 Sept. 2003, p. 29. 3. György Hegyi, András Keresztúri, Csaba Maráczy: Solution of the new Dukovany Benchmark using the new version of KARATE-440 code Proceedings of the 18th Symposium of AER, Eger, Hungary, October 6-10, 2008 4. Kliem, S., Comparison of the updated results of the 6th Dynamic AER Benchmark – main steam line break in a NPP with VVER440. Proceedings of the 13th Symposium of the AER on VVER Reactor Physics and Safety, September 22-26, 2003 in Dresden, Germany. KFKI/AEKI, Budapest, 2003. Pp. 413 - 444. ISBN 963-372-630-1 5. OECD/NEA: A VVER-1000 LEU and MOX Assembly Computational Benchmark. Specification and Results, NEA/NSC/DOC(2002)10 6. OECD/NEA No. 6088: VVER-1000 MOX Core Computational Benchmark. Specification and Results, NEA/NSC/DOC(2005)17.

Title	Context	References	Participants	Summary
				7. V. A. Tereshonok, S. P. Nikonov, M. P. Lizorkin, K. Velkov, A. Pautz, K. Ivanov: KALININ-3 Coolant Transient Benchmark - Switching-off of One of the Four Operating Main Circulation Pumps at Nominal Reactor Power - Specification - First Edition 2008, NEA/NSC/DOC(2009)5, NEA-1848/04. 8. T. Lötsch: Fuel assembly burnup calculations for VVER fuel assemblies with the Monte Carlo code SERPENT, Kerntechnik 79 (2014) 4, p. 295. 9. T. Lötsch, V. Khalimonchuk, A. Kuchin: Consolidated data and status of task 2 solutions of the benchmark for core burnup calculations for a VVER-1000 reactor, Proceedings of the 23. Symposium of AER, 30 September - 4 October 2013, Strbske Pleso, Slovakia, p. 313.
X2 VVER-1000 benchmark revision: Fresh HZP core state and the reference Monte Carlo solution, Annals of Nuclear Energy, Volume 144, 1 September 2020, 107558 Y. Bilodid E. Fridman T. Lötsch	AER	https://www.sciencedirect.com/science/article/pii/S0306454920302565 X2 benchmark dataset: https://rodare.hzdr.de/record/200	Helmholtz-Zentrum Dresden-Rossendorf, Dresden, Germany TÜV SÜD Industrie Service GmbH, Munich, Germany	The X2 VVER-1000 benchmark provides a unique set of the operational data of a VVER-1000 reactor. This includes fresh core hot zero power (HZP) experiments, operational history of first four fuel cycles, and information on the operational transients occurred on the unit during first cycles. Since a publication of the initial versions of the benchmark, numerous updates, corrections and refinements become available. The current paper is a first in a series of publications on the revised X2 VVER-1000 benchmark. It is dedicated to the fresh core HZP experiments and includes description of the fuel and core geometries, the material compositions, description and results of the measurements taken during fresh core start-up. In addition, the paper includes the reference Monte Carlo solution for the HZP experiments obtained with Serpent 2. The calculated and measured values are in a good agreement.

Title	Context	References	Participants	Summary
Optimal Nodalization Schemas of VVER-1000 Reactor Pressure Vessel for the Coupled Code ATHLET-BIPR8KN, 16th Symposium of AER on VVER Reactor Physics and Reactor Safety, Slovakia, Bratislava, Sept. 25-29, 2006. S.Nikonov, K.Velkov, S.Langenbuch, M.Lizorkin, A.Kotsarev,	OECD	https://www.osti.gov/etdeweb/servlets/purl/20909595	RRC KI, GRS	As basis for these analyses, the data of the CEA-NEA/OECD VVER-1000 Coolant Transient Benchmark (V1000CT-2) - vessel mixing problems is applied. The aim of the performed studies is to define an optimal nodalization schema of the VVER-1000 reactor pressure vessel which can correctly describe the mixing phenomena during asymmetric transients. Different downcomer and lower plenum nodalization schemas for the ATHLET code have been analysed and results have been compared with local and integral coolant temperature measurements. For this purpose data is used from the VVER-1000CT-2 Benchmark [1]. These measured data have been collected during the plant-commissioning phase of the Bulgarian Kozloduy Nuclear Power Plant (NPP) Unit 6. The presented work applies the data of Exercise 1 of Phase 2 of the coolant transient benchmark (V1000CT-2). For this Exercise a mixing problem transient has been defined to validate the coupled thermal-hydraulic system codes with integrated 3D reactor core models for VVER-1000 condition with measured plant data. The V1000CT-2 transient is determined by an isolation of one of the four steam generators (SG) from the steam line and from the feed water supply, causing a temperature rise in the affected loop. During the transient all main circulation pumps (MCP) remain in operation. Non-uniform and asymmetric loop flow mixing in the reactor vessel is observed. The results for Exercise 1 obtained by the GRS/KI coupled code system ATHLET-BIPR8KN [2] with a downcomer model consisting of six thermal-hydraulic channels in ATHLET have been reported in [3]. SUMMARY The paper describes the comparisons of results of the coupled code system ATHLET-BIPR8KN for Exercises 1 of the V1000CT-2 Benchmark applying different nodalization schemas of the reactor vessel. Five schemas are developed and compared. The integral reactor parameter histories of the calculated SG isolation transient at low power level agree quite well with the available experimental data in all cases. A systematic study was performed to determine the

Title	Context	References	Participants	Summary
				optimal nodalization schema of the reactor vessel. It was proved that local parameters in the core can be correctly predicted using at least 16 PTHC or higher number to describe the DC (respectively 112 nodes for lower plenum or higher). An optimal VVER- 1000 reactor vessel schema for the coupled system code ATHLET-BIPR8KN can be obtained with 16 DCs or 24 DCs. The studies will be continued with the aim to find not only the optimum number of nodes in the lower plenum but also to determining the correct geometrical form of these nodes in order to reduce the uncertainties by determine the hydraulic losses. The change of flow mixing coefficients during the transient has been evaluated. It is shown that the RMC are not constant during the transient which affects the prediction of the local coolant temperatures. The ATHLET-BIPR8KN model developed for NPP with VVER types of reactors is able to predict correctly not only the overall plant response but also local core parameters. The experience gained for the reactor vessel nodalization will be used for further safety analyses. Bibliography: 1. N. Kolev, S. Aniel, E. Royer, U. Bieder, D. Popov, Ts. Topalov, VVER-1000 Coolant Transient Benchmark (V1000CT), Phase2, Volume I: Specification of the VVER-1000 Vessel Mixing Problems, OECD NEA, March 2004 2. S. Langenbuc h, K. Velkov, S. Kliem, U. Rohde, M. Lizorkin, G. Hegyi, A. Kereszturi, Development of Coupled Systems of 3D Neutronics and Fluid-Dynamic System Codes and Their Application for Safety Analysis, EUROSAFE-2000, Paris, November, 2000. 3. Nikonov S., Lizorkin M., Langenbuch S., Velkov K., Kinetics and Thermal-Hydraulic Analysis of Asymmetric Transients in a VVER-1000 by the Coupled Code ATHLET-BIPR8KN, 15th Symposium of AER on VVER Reactor Physics and Reactor Safety, Znojmo, Chech Republic, Oct. 3-7, 2005
ANALYSIS OF THE	OECD		Penn State University,	In the framework of joint effort between the Nuclear Energy Agency (NEA) of OECD, the United States Department of Energy (US DOE), and the Commissariat

Title	Context	References	Participants	Summary
NEUTRONIC SPECIFICATIONS OF THE OECD/DOE/CEA V1000CT-1 EXERCISE 2 BENCHMARK Boyan D. Ivanov, Kostadin N. Ivanov Eric Royer Sylvie Aniel Yaroslav Kozmenkov Ulrich Grundmann			CEA, RC Rossendorf	a l'Enerige Atomique (CEA), France a coupled three-dimensional (3-D) neutron kinetics/thermal hydraulics benchmark was defined. The overall objective of OECD/NEA V1000CT benchmark is to assess computer codes used in analysis of VVER-1000 reactivity transients where mixing phenomena (mass flow and temperature) in the reactor pressure vessel are complex. Original data from the Kozloduy-6 Nuclear Power Plant is available for the validation of computer codes: one experiment of pump start-up (V1000CT-1) and one experiment of steam generator isolation (V1000CT-2). Additional scenarios are defined for code-to-code comparison. The present paper focuses on the analysis of the observed discrepancies using cross-code comparisons between CRONOS/FLICA-IV, TRAC-PF1/NEM, DYN3D and RELAP-3D. The VVER 1000 core description given in the benchmark specification [1] stays at the assembly level: the core is divided, radially, in 211 hexagonal cells (each corresponding to a fuel assembly or a radial reflector), and axially, in 12 layers (two of them corresponding the axial reflectors). The core is thus described by 283 sets of 2 group cross sections, provided as part of the benchmark specifications. The origin of the observed high discrepancies was found to be due to both the neutronic library and the different nodal methods applied in the participants neutronic models. The present paper describes the path taken to search the origin of the discrepancies and the first conclusions. INTRODUCTION During the second OECD/DOE/CEA V1000CT benchmark workshop conducted in Sofia, Bulgaria in April 2004, it was discovered that two clusters of participants' results for normalized radial power distribution were formed for both Hot Power (HP) conditions and Hot Zero Power (HZP) conditions. The observed difference between these two clusters is approximately in the range of ±11%, while the difference within each of the clusters is in the range of ±1.5%. Compared to the results of PWR MSLB benchmark [2] these deviations are not acceptable.

Title	Context	References	Participants	Summary
				Therefore, steps for solving this problem were taken, which are described in this paper. Comparisons between the following four codes CRONOS/FLICA-IV, TRACPF1/NEM, DYN3D and RELAP-3D were performed in order to investigate this problem. Two of the codes' results (TRAC-PF1/NEM and RELAP5-3D) fall in the one of the clusters with agreement between themselves in the range of 0.5%, while CRONOS/FLICA-IV and DYN3D results fall in the other cluster with comparison between themselves in the range of 0.75%. CONCLUSIONS This paper describes the problem observed during the computation of second exercise of the V1000CT-1 benchmark. Unacceptable high deviations (in the range of ±11%) were discovered when comparisons of 2-D normalized power distributions calculated by different codes were performed. The paper outlined the steps taken for solving this problem. The performed sensitivity studies narrowed down the possible sources of the deviation. It was found out that the deviations are caused mainly by the difference in the methods of solving the Diffusion equation in Hexagonal geometry. The benchmark team has defined also 3-D simple test problems in addition to the presented 2-D test problems, which analysis is underway. The developed simple test problems will be made available to the benchmark participants. The obtained results will be compared as part of 2nd Exercise of V1000CT-1 benchmark to qualify the deviations caused by the hexagonal geometry solution methods. Bibliography: 1. Ivanov B, Ivanov K, Groudev P, Pavlova M, and Hadjiev V, "VVER-1000 Coolant Transient Benchmark (V1000-CT). Phase 1 – Final Specification", NEA/NSC/DOC (2002)6, OECD NEA.
VVER-1000 COOLANT	OECD	https://www.oecd-nea.org/jcms/pl_5063	Penn State University,	This report provides the specifications for international coupled VVER-1000 Coolant Transient (V1000CT-1) benchmark problem based on the scenario of one

Title	Context	References	Participants	Summary
TRANSIENT BENCHMARK – PHASE 1 (V1000CT-1) Volume I: Main Coolant Pump (MCP) Switching On **Final Specifications** NEA/OECD 2002, NEA/NSC/DOC(2002)6 B.Ivanov, K.Ivanov, P.Groudev, M.Pavlova, V.Hadjiev		2/vver-1000-coolant-transient-benchmark-phase-1-vol-1	INRNE, NPP Kozloduy	main coolant pump (MCP) switching on when the other three pumps are working. The reference problem chosen for simulation in a VVER 1000 is a MCP switching on when the other three main coolant pumps are in operation. It is an experiment that was conducted by Bulgarian and Russian engineers during the plant-commissioning phase at the KNPP Unit #6 as a part of the start-up tests. Background Most transients in a VVER reactor can be properly analyzed with a system thermal-hydraulics code like RELAP5, with simplified neutron kinetics models (point kinetics). A few specific transients require more advanced, three-dimensional (3-D) modeling for neutron kinetics for a proper description. A coupled thermal-hydraulics/3-D neutron kinetics code would be the right tool for such tasks. The proposed benchmark problem [1] was analyzed with RELAP5/MOD3.2 [2] and the results were intended to be compared with those obtained with coupled codes with 3D kinetics such as RELAP5-3D [3] and TRAC-PF1/NEM[4]. The reference problem chosen for simulation is a Main Coolant Pump (MCP) switching on when the other three main coolant pumps are in operation, which is a real transient of an operating VVER-1000 power plant. This event is characterized by rapid increase in the flow through the core resulting in a coolant temperature decrease, which is spatially dependent. This leads to insertion of spatially distributed positive reactivity due to the modeled feedback mechanisms and non-symmetric power distribution. Simulation of the transient requires evaluation of core response from a multi-dimensional perspective (coupled three-dimensional (3-D) neutronics/core thermal-hydraulics) supplemented by a one-dimensional (1-D) simulation of the remainder of the reactor coolant system. The purpose of this benchmark is three-fold: • To verify the capability of system codes to analyze complex transients with coupled core-plant interactions.

Title	Context	References	Participants	Summary
				• To fully test the 3-D neutronics/thermal-hydraulic coupling. • To evaluate discrepancies between predictions of coupled codes in best-estimate transient simulations. Definition of three benchmark exercises. In addition to being based on a well-defined problem, with reference design and data from the Kozloduy Nuclear Power Plant Unit 6 (KNPP) [5], the benchmark includes a complete set of input data, and consists of three exercises. These exercises are discussed below. Exercise 1 – Point kinetics plant simulation: The purpose of this exercise is to test the primary and secondary system model responses. Provided are compatible point kinetics model inputs, which preserve axial and radial power distribution, and scram reactivity obtained using a 3-D code neutronics model and a complete system description. Exercise 2 – Coupled 3-D neutronics/core T-H response evaluation: The purpose of this exercise is to model the core and the vessel only. Inlet and outlet core transient boundary conditions are provided. Exercise 3 – Best-estimate coupled code plant transient modeling: This exercise combines elements of the first two exercises in this benchmark and is an analysis of the transient in its entirety. Bibliography: 1.K. Ivanov, P. Groudev, R. Gencheva and B. Ivanov, “Letter-Report on Kozloduy NPP Transient,” US DOE, September 2000. 2. RELAP 5/MOD3.2 Code Manual, INEEL. 3. RELAP-3D Code Manual Volume 1, INEEL. 4. K. Ivanov et al, “Features and Performance of a Coupled Three Dimensional Thermal- Hydraulics/Kinetics Code TRAC-PF1/NEM PWR Analysis Code,” Ann. Nucl. Energy, 26, 1407 (1999).

Title	Context	References	Participants	Summary
				5. Database for VVER-1000, Safety analysis capability improvement of KNPP (SACI of KNPP) in the field of thermal hydraulic analysis, BOA 278065-A-R4, INRNE-BAS, Sofia.
VVER-1000 COOLANT TRANSIENT BENCHMARK (V1000CT) Volume II: Specifications of the VVER-1000 Vessel Mixing Problems, NEA/OECD NEA/NSC/DOC (2004) N .Kolev, E. Royer, U.Bieder, S.Aniel, D. Popov and Ts. Topalov	OECD		INRNE, CEA, NPP Kozloduy	This report provides the specifications of V1000CT-2 Exercise 1. The report is prepared by INRNE and CEA in cooperation with Kozloduy NPP. The work is sponsored by CEA and OECD/NEA. The reference problems for Exercise 1 include a NPP flow mixing experiment and a numerical experiment, as described below. The plant experiment is specially designed to have approximately separable thermal hydraulics and neutron kinetics. The core power distribution is given. The initial state is at BOC and at low power level. The boron concentration corresponds to moderator temperature coefficient close to zero. A transient is initiated by isolation of one steam generator and asymmetric loop heat up, with all main coolant pumps in operation. The computed results were intended to be compared code-to-code and against measured data. A parametric study was intended to be set up to study the importance of modelling the plant specific geometry and vessel asymmetries. For this purpose, two data sets for the reactor vessel and internals were planned to be provided. The numerical experiment is defined so that to study the influence of the disturbance type (coolant heat up or cool down) on the mixing pattern when the geometry is the same. Vessel boundary conditions are given and correspond to asymmetric cool-down at zero core power. Background Most transients in a VVER reactor can be properly analyzed with a system thermal-hydraulics code with point kinetics. A few specific transients require more advanced, three-dimensional (3-D) modeling for neutron kinetics for a proper description. A coupled thermal-hydraulics/3-D neutron kinetics code would be the right tool for such tasks.

Title	Context	References	Participants	Summary
				Recent coupled code benchmarks have identified the vessel mixing as an unresolved issue in the analysis of complex plant transients with reactivity insertion. Phase 2 of the VVER-1000 Coolant Transient Benchmark was thus defined aiming firstly at assessing mixing models in the coupled codes and secondly at analyzing MSLB with improved vessel thermal hydraulic models. The purpose of the V1000CT-2 benchmark is three-fold: • To test flow mixing models (CFD, coarse-mesh and mixing matrix) against measured data and in code-to-code comparison. • To fully test the coupling of 3-D neutronics and vessel thermal-hydraulics. • To evaluate discrepancies between predictions of coupled codes in best-estimate transient simulations. Definition of three benchmark exercises The benchmark includes a complete set of input data, and consists of three exercises. These exercises are discussed below. Exercise 1 – Computation of flow mixing experiments: The purpose of this exercise is to test the capability of vessel thermal hydraulic models to represent the vessel mixing. The reference problem is a pure thermal-hydraulic problem with given vessel boundary conditions and core power distribution, derived from a plant experiment. Exercise 2 – Coupled 3D neutronics/vessel thermal hydraulics response evaluation: The purpose of this exercise is to model the core and the vessel only. MSLB boundary conditions are imposed at the vessel inlet and outlet. Exercise 3 – Best-estimate coupled-code full plant simulation: This exercise is a full plant computation of the transient in its entirety, for a realistic and a pessimistic MSLB scenario.

Title	Context	References	Participants	Summary
VVER-1000 Coolant Transient Benchmark Phase 2 (V1000CT-2) Summary Results of Exercise 1 on Vessel Mixing Simulation N.P. Kolev I. Spasov E. Royer	NEA Nuclear Science Committee	https://www.oecd-nea.org/upload/docs/application/pdf/2019-12/nea6964-ex-l-vessel-mixing.pdf OECD 2010 NEA No. 6964	INRNE, Commissariat à l'énergie atomique	The present volume summarises the results for V1000CT-2 Exercise 1 (single phase vessel mixing calculation) and identifies important modelling issues. The reference problem is a nuclear power plant flow mixing experiment. The fourth volume presents the results for Exercises 2 and 3 (coupled code MSLB analysis using validated flow mixing models). Exercise 1 – Computation of a vessel mixing experiment The vessel mixing problem is based on VVER-1000 plant experiments. The objective is to test the capability of reactor vessel thermal-hydraulic models to represent single-phase flow mixing. The specific objectives are: • understanding the main physics; • qualification of the available data; • understanding the hard point of modelling; • understanding the actual limits of CFD and coarse-mesh simulation. The reference problem is a coolant transient initiated by steam generator isolation at low power, considered as a pure thermal-hydraulic problem. Regarding CFD codes the task is to assess the ability of CFD to reproduce the experimentally observed angular turn of the loop flow centres (swirl) and the core inlet temperature distribution, given the vessel boundary conditions and the pressure above the core. Regarding system codes, the task is to assess the ability of multi-1-D vessel models with cross-flow and coarse 3-D models to reproduce the swirl and the core inlet temperature distribution, as well as the vessel outlet temperatures. Given vessel boundary conditions or full plant simulation can be used. Exercise 2 – Computation of a VVER-1000 MSLB transient with given vessel boundary conditions

Title	Context	References	Participants	Summary
				The task is to model the core and the vessel only, using the validated coolant mixing models and pre-calculated vessel MSLB boundary conditions. A realistic and a pessimistic scenario are considered. The primary objective is to evaluate the response of the coupled 3-D neutronics/core-vessel thermal-hydraulics in code-to-code comparison. A specific objective is to provide an additional test of the vessel mixing models with MSLB boundary conditions, by comparing coarse-mesh solutions and reference CFD results for the core inlet distributions. Exercise 3 – Best-estimate coupled core-plant MSLB simulation This exercise is a best-estimate analysis of the transient in its entirety, for a realistic and a pessimistic scenario. The present volume summarises the comparative analysis of the submitted results for Exercise 1 (computation of a vessel mixing experiment). Conclusions: A detailed evaluation of the CFD results of Exercise 1 was presented in Chapter 4 of this report. The results show that: • There is reasonable agreement for each parameter, with some exceptions for the core inlet velocity. This agreement was achieved under the following conditions: use of the actual and not the conceptual design geometry of the reactor vessel + appropriate treatment of turbulence + compliance with the Best Practice Guidelines. • CFD simulations predict qualitatively well the flow rotation in the lower plenum but the sector formation is predicted with more diffusion than in the measurements. • The maximum error of CFD for temperature prediction at the core inlet is in the range 1-4 K and the average in modulus error is below 1 K, which can be acceptable for industrial applications.

<table>
<tr><th>Title</th><th>Context</th><th>References</th><th>Participants</th><th>Summary</th></tr>
<tr><td></td><td></td><td></td><td></td><td>
• The observed differences depend on the modelling assumptions, summarised in Table 4.1 and Appendix C, and on the degree of compliance with the BPG. The TRIO_U LES results show best agreement in the angular turn of the loop flow. The BUTE CFX SST simulation is the best in terms of maximum and average in modulus temperature deviations at the core inlet. The UNIPI CFX 10 k-ε predicted core inlet radial velocity profile is the closest to that expected.

Table 4.1: Summary of the V1000CT-2 CFD modelling assumptions
<table>
<tr><th>Organi-sation</th><th>Code</th><th>Turbu-lence model</th><th>Discretisation</th><th>Advection scheme</th><th>Mesh type</th><th>Plant specific data</th><th>Use of CEA CAD geom. data</th></tr>
<tr><td>BUTE</td><td>CFX 10</td><td>SST</td><td>3 266 140</td><td>Upwind</td><td>Unstructured tetrahedral</td><td>Yes</td><td>Yes</td></tr>
<tr><td>CEA</td><td>TRIO_U</td><td>LES</td><td>10 000 000 contr. volumes</td><td>High resolution</td><td>Unstructured tetrahedral</td><td>Yes</td><td>Yes</td></tr>
<tr><td>EREC</td><td>REMIX 1.0</td><td>k-ε</td><td>311 394 cells 332 940 vertices</td><td>Upwind</td><td>Unstructured hexahedral</td><td>Yes</td><td>Yes</td></tr>
<tr><td>FZK</td><td>CFX 5</td><td>k-ε</td><td>14 000 000 whole RPV</td><td>Upwind</td><td>Unstructured/ hybrid; core: structured</td><td>Yes</td><td>Yes</td></tr>
<tr><td>FZD</td><td>CFX 10</td><td>SST</td><td>4 700 000</td><td>Upwind</td><td>Unstructured tetrahedral</td><td>Yes</td><td>Yes</td></tr>
<tr><td>PSU/ ORNL</td><td>FLUENT</td><td>k-ω</td><td>541 000</td><td>Upwind</td><td>Unstructured</td><td>Yes</td><td>Yes</td></tr>
<tr><td>UNIPI</td><td>CFX 10</td><td>k-ε</td><td>930 000 nodes 4 200 000 elem.</td><td>Upwind</td><td>Unstructured tetrahedral</td><td>Yes</td><td>Yes</td></tr>
</table>

• The qualitative difference between the computed and plant estimated core inlet velocity distribution requires additional analysis. Further improvement of the core inlet velocity distribution is possible by explicit modelling of the elliptical sieve plate, as well as modelling of the fuel assemblies and using appropriate boundary conditions.

• CFD codes still have limitations but the development work for single phase mixing is on the right track. The quality of the results depends on the experience of the user and the level of compliance with the Best Practice Guidelines.

The coarse-mesh solutions of the mixing problem show that:
</td></tr>
</table>

Title	Context	References	Participants	Summary
				• The disturbed sector formation and the angular turn of loop #1 flow are in reasonable agreement with plant data. The angular turn is somewhat underestimated and the diffusion at the disturbed sector borders is larger than in the experiment. • The predicted downcomer temperature distributions are in generally good agreement with the CFD results and with each other. • The maximal deviations in assembly inlet temperatures are within 1-8 K, which is significantly larger than the observed CFD error range. • The resolution improves with mesh refinement. The solutions are sensitive to azimuth meshing. The available results show that at least 16-18 azimuth sectors are necessary for acceptable accuracy in the core inlet distributions. • For this type of coolant transient, coarse 3-D models do not perform noticeably better than multi-1-D with cross-flow governed by the local pressure drops. Some of the discrepancies between different coarse-mesh results can be explained by the modelling differences summarised in Table 5.1 and the participant's provided calculation details given in Appendix D.

<table>
<tr><th>Title</th><th>Context</th><th>References</th><th>Participants</th><th>Summary</th></tr>
<tr><td></td><td></td><td></td><td></td><td>
Table 5.1: List of participants with coarse-mesh models
<table>
<tr><th>Organisation</th><th>Code</th><th>Model</th><th>Nodalisation</th></tr>
<tr><td>GRS/KI</td><td>ATHLET/BIPR8H</td><td>Multi-1-D</td><td>16 sectors in the vessel
7 radial rings</td></tr>
<tr><td>INRNE</td><td>CATHARE2</td><td>Multi-1-D</td><td>24 sectors in the vessel</td></tr>
<tr><td>KU</td><td>RELAP3D</td><td>Coarse 3-D</td><td>36 sectors in the DC and LP
7 radial rings</td></tr>
<tr><td>ORNL</td><td>RELAP3D</td><td>Coarse 3-D</td><td>6 sectors in the DC and LP
5 radial rings</td></tr>
<tr><td>PSU</td><td>TRACE</td><td>Coarse 3-D</td><td>6 sectors in the vessel
5 radial rings</td></tr>
<tr><td>UNIPI</td><td>RELAP3D</td><td>Coarse 3-D</td><td>20 sectors in the DC
60 sectors in the upper LP
max. 8 radial rings in LP</td></tr>
</table>
Based on this comparison it can be concluded that the considered vessel mixing models in system codes are applicable to the analysis of asymmetric coolant transients characterised by sector formation, such as MSLB.
</td></tr>
<tr><td>VVER-1000 Coolant Transient Benchmark PHASE 2 (V1000CT-2) Vol. III: MSLB Problem – Final Specifications, NEA/NSC/DOC(2006)
N. Kolev, N. Petrov, J. Donov, D. Angelova, S. Aniel,</td><td>OECD</td><td>https://www.researchgate.net/publication/287978519_VVER-1000_Coolant_Transient_Benchmark_Phase_2_V1000CT-2_Vol_III_Final_Specifications_of_the_MSLB_Problem</td><td>INRNE, CEA, NPP Kozloduy, PSU, Kurchatov Institute</td><td>This report provides Volume III of the Specifications of V1000CT Phase 2 devoted to Exercises 2 and 3. The benchmark problem for Exercises 2 consists of reactor vessel and core calculation of large MSLB at hot full power with imposed vessel thermalhydraulics (TH) boundary conditions. Exercise 3 is a coupled full plant MSLB simulation.

Volume III of the V1000CT-2 specifications covers Exercises 2 and 3 and the required output information. In addition to this report provides the crossection libraries for three-dimensional (3D) neutronics calculations. Part of the thermal hydraulic input data is also available in electronic format - files or CD on request from the participants, including: (1) Transient TH boundary conditions for the reactor pressure vessel, supplementary core outlet boundary conditions, SG feed water flow boundary conditions, decay heat input table and (2) Reactor vessel CAD geometry input for CFD calculations.</td></tr>
</table>

Title	Context	References	Participants	Summary
E. Royer, B. Ivanov, K. Ivanov, E. Lukanov, Y. Dinkov, D. Popov, S. Nikonov				
RELAP5/MOD3.2 INVESTIGATION OF A VVER-1000 MCP SWITCHING ON PROBLEM, ICONE10-22443, Proceedings of ICONE 10, The Tenth International Conference on Nuclear Engineering April 14-18, 2002, Arlington, Virginia, USA Pavlin Groudev, Malinka Pavlova	ICONE 10-22443	https://www.researchgate.net/publication/234004819_RELAP5MOD32_Investigation_of_a_VVER-1000_MCP_Switching_on_Problem	INRNE	This paper provides a discussion of various RELAP5 parameters calculated for the investigation of the nuclear power reactor parameter behavior in case of switching on one main coolant pump (MCP) when the other three MCPs are in operation. The reference power plant for this analysis is Unit 6 at the Kozloduy Nuclear Power Plant (NPP) site. Operational data from Kozloduy NPP have been used for the purpose of assessing how the RELAP5 model compares against plant data. During the plant-commissioning phase at Kozloduy NPP Unit 6 a number of experiments have been performed. One of them is switching on MCP when the other three MCPs are in operation. The event is characterized by rapid increase in the flow through the core resulting in a coolant temperature decrease, which leads to insertion of positive reactivity due to the modeled feedback mechanisms. This investigation has been conducted by Bulgarian and Russian specialists on the stage when the reactor power was at 75% of the nominal level. The purpose of the experiment was the complete testing of reliability of all power plant equipment, testing the reliability of the main regulators and defining a jump of the neutron reactor power in case of switching on of one main coolant pump. In general the comparisons indicate good agreement between the RELAP5 results and the experimental data for the "Switching on one main coolant pump to three other working MCPs" test conducted in KNPP, Unit 6. Test facilities are frequently scaled down models of the actual power plant; the scaling can increase the uncertainty of the results of the test facility relative to the reactor performance. In this benchmark based on Kozloduy NPP the scaling is not a factor. The results

Title	Context	References	Participants	Summary
				provide an integrated evaluation of the complete RELAP5 VVER-1000 model. The comparisons indicate that RELAP5 predicts the test results very well. The RELAP5 model developed for the transient analysis of VVER-1000 nuclear power plants has been used to accurately predict the results obtained during the MCP test performed at the Kozloduy NPP, Unit 6. These results are an important part of the validation of the RELAP5 model developed for Kozloduy NPP. The overall conclusion is that RELAP5/MOD3.2 is adequate to simulate the transient phenomena occurring in a VVER-1000 during the "Switching on one main coolant pump to three other working MCPs" test. The results presented in this paper will be used for comparative analysis of a RELAP5 validation benchmark problem.
OECD/DOE/CEA VVER 1000 Coolant Transient (V1000CT) Benchmark for Assessing Coupled Neutronics/Thermal-Hydraulics System Codes for VVER-1000 RIA Analysis, PHYSOR 2004 -The Physics of Fuel Cycles and Advanced Nuclear Systems: Global Developments Chicago, Illinois,	OECD / PHYSOR 2004	https://www.researchgate.net/publication/23 3936097_OECDDOECEA_VVER-1000_coolant_transient_V1000CT_benchmark_for_assessing_coupled_neutronicsthermal-hydraulics_system_codes_for_VVER-1000_RIA_analysis	PSU, CEA, INRNE	The present paper describes the two phases of the OECD/DOE/CEA VVER-1000 coolant transient benchmark labeled as V1000CT. This benchmark is based on a data from the Bulgarian Kozloduy NPP Unit 6. The first phase of the benchmark was designed for the purpose of assessing neutron kinetics and thermal-hydraulic modeling for a VVER-1000 reactor, and specifically for their use in analyzing reactivity transients in a VVER-1000 reactor. Most of the results of Phase 1 were intended to be compared against experimental data and the rest of the results were intended to be used for code-to-code comparison. The second phase of the benchmark is planned for evaluation and improvement of the mixing computational models. Code-to-code and code-to-data comparisons were planned to be done based on data of a mixing experiment conducted at Kozloduy-6. Main steam line break was also planned to be analyzed in the second phase of the V1000CT benchmark and the results to be used for code-to-code comparison. The benchmark team has been involved in analyzing different aspects and performing sensitivity studies of the different benchmark exercises. The paper presents a comparison of selected results, obtained with two different system thermal-hydraulics codes, with the plant data for the Exercise 1 of Phase 1 of the

Title	Context	References	Participants	Summary
April 25-29, 2004, on CD-ROM, American Nuclear Society, Lagrange Park, IL. (2004) B. Ivanov, K. Ivanov S. Aniel, E. Royer N. Kolev, P. Groudev				benchmark as well as some results for Exercises 2 and 3. Overall, this benchmark has been well accepted internationally, with many organizations representing 11 countries participating in the first phase of the benchmark.
SIMULATION OF MIXING EFFECTS IN A VVER-1000 REACTOR, Nuclear Engineering and Design 237(15-17):1718-1728 Ulrich Bieder, Gauthier Fauchet, Sylvie Bétin , Nikola Kolev, Dimitar Popov	OECD / Science Direct	https://www.researchgate.net/publication/223622697_Simulation_of_mixing_effects_in_a_VVER-1000_reactor	CEA, ASTEK, INRNE, NPP Kozloduy	This work has been performed in the framework of the OECD/NEA thermalhydraulic benchmark V1000CT-2. This benchmark is related to fluid mixing in the reactor vessel during a MSLB accident scenario in a VVER-1000 reactor. Coolant mixing in a VVER-1000 V320 reactor was investigated in plant experiments during the commissioning of the Unit 6 of the Kozloduy nuclear power plant. Non-uniform and asymmetric loop flow mixing in the reactor vessel has been observed in the event of symmetric main coolant pump operation. For certain flow conditions, the experimental evidence of an azimuthal shift of the main loop flows with respect to the cold leg axes (swirl) was found. Such asymmetric flow distribution was analyzed with the Trio U code based on the experimental data. Trio U is a CFD code developed by the CEA Grenoble, aimed to supply an efficient computational tool to simulate transient thermalhydraulic turbulent flows encountered in nuclear systems. For the presented study, a LES approach was used to simulate turbulent mixing. Therefore, a very precise tetrahedral mesh with more than 10 million control volumes has been created. The Trio U calculation has correctly reproduced the measured rotation of the flow when the CAD data of the constructed reactor pressure vessel where used. This is also true for the comparison of cold leg to assembly mixing coefficients. Using the

Title	Context	References	Participants	Summary
				design data, the calculated swirl was significantly underestimated. Due to this result, it might be possible to improve with CFD calculations the lower plenum flow mixing matrices which are usually used in system codes.
OECD/DOE/CEA VVER-1000 coolant transient (V1000CT) benchmark - A consistent approach for assessing coupled codes for RIA analysis, Progress in Nuclear Energy 48 (2006) 728-745 B. Ivanov, K. Ivanov, E. Royer, S. Aniel, U. Bieder, N. Kolev, P. Groudev	OECD / Science Direct	https://www.sciencedirect.com/science/article/abs/pii/S0149197006000515	PSU, CEA, INRNE	The rod ejection accident (REA) and the main steam line break (MSLB) are two of the most important design basis accidents (DBA) for VVER-1000 exhibiting significant localized space-time effects. A consistent approach for assessing coupled threedimensional (3-D) neutron kinetics/thermal-hydraulics codes for reactivity insertion accidents (RIA) is to first validate the codes using the available plant test (measured) data and after that to perform cross code comparative analysis for REA and MSLB scenarios. The coupled 3-D neutron kinetics/thermal-hydraulics benchmark presented in this paper is based on data from the Unit #6 of the Bulgarian Kozloduy Nuclear Power Plant (KNPP) and it is entitled the VVER-1000 coolant transient (V1000CT) benchmark. Two real plant transients are selected for simulation in the benchmark: main coolant pump start-up (Phase 1) and coolant mixing tests (Phase 2). In addition to these transients extreme scenarios were defined for better testing 3-D neutronics/thermal-hydraulics coupling: rod ejection simulation with control rod being ejected in the core sector cooled by the switched on MCP (Phase 1) and MSLB transient (Phase 2). The paper presents an overview of the Phase 1 (V1000CT-1) benchmark activities and describes the approach used for assessing the coupled neutron kinetics/thermal-hydraulics codes. Selected comparative analysis of currently submitted participants' results is presented with emphasis on the observed modeling issues and deviations from the measured data. From the performed comparative analysis of all the results, submitted by the participants for the Phase 1 of the V1000CT benchmark, it can be concluded that all the codes are capable of modeling the transient ''MCP switching on when the other three pumps are in operation'' in a VVER-1000 system. There are deviations

Title	Context	References	Participants	Summary
				of the steady-state and transient results from the plant data but almost every compared parameter is within the measurement uncertainties. Overall, this benchmark has been well accepted internationally, with many organizations representing 11 countries participating in the first phase of the benchmark.
Comparison of RELAP5 calculations of VVER-1000 coolant transient benchmark phase 1 at different power, Progress in Nuclear Energy 48 (2006) 790-805 A. Stefanova, P. Groudev	Science Direct	https://www.sciencedirect.com/science/article/abs/pii/S014919700600059X	INRNE	This paper provides comparisons between experimental data of ‘‘MCP switching on when the other three MCPs are in operation’’ and RELAP5 calculations with different initial levels of the reactor power 29.45% and 27.47% from the nominal. The reference power plant for this analysis is Unit 6 at theKozloduy nuclear power plant (NPP) site. RELAP5/MOD3.2 computer code has been used to simulate the investigated transient. Operational data from Kozloduy NPP have been used for the purpose of assessing how the RELAP5 model compares against plant data. During the plant-commissioning phase at Kozloduy NPP Unit 6 a number of experiments have been performed. One of them is switching on MCP when the other three MCPs are in operation. In general the comparisons indicate good agreement between the RELAP5 results and the experimental data for the ‘‘Switching on one main coolant pump to three other working MCPs’’ test conducted in KNPP, Unit 6. These results are an important part of the validation of the RELAP5 model developed for Kozloduy NPP. The overall conclusion is that RELAP5/MOD3.2 is adequate to simulate the transient phenomena occurring in a VVER-1000 during the ‘‘Switching on one main coolant pump to three other working MCPs’’ test. The comparisons indicate that RELAP5 predicts the test results very well. As it is seen from comparison the results in case #2 (using 27.47% reactor power, which is based on the primary side parameters) have better agreement with plant

Title	Context	References	Participants	Summary
				measured data for most parameters when compared to case #1 (using reactor power of 29.45%, which is the reactor power by neutron flux). 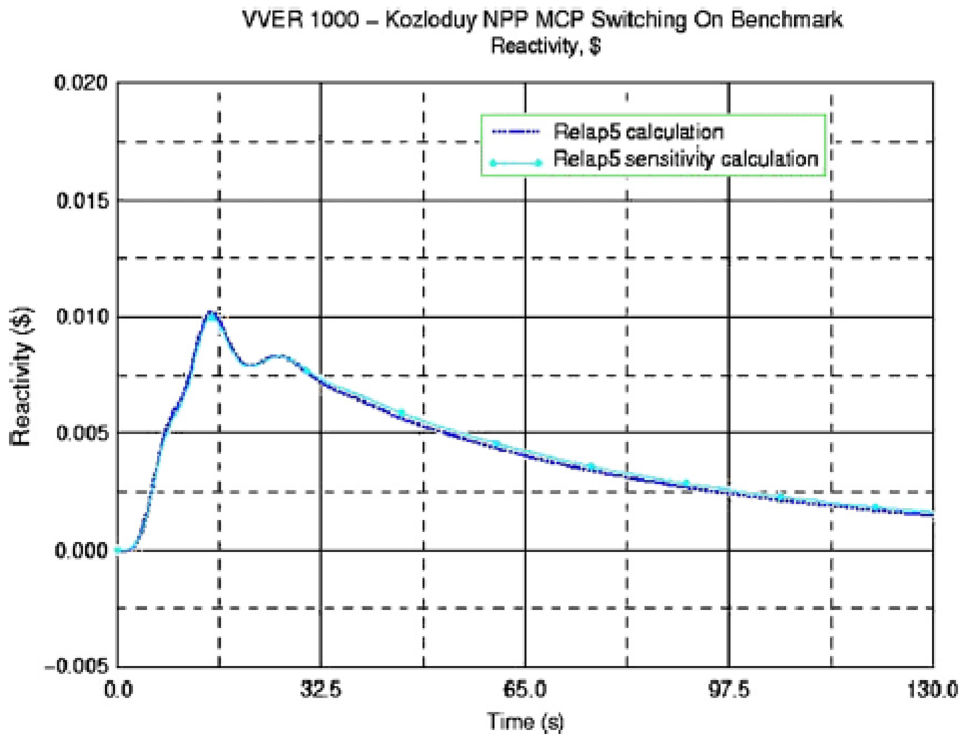 Fig. 19. Reactivity.
BENCHMARKS FOR UNCERTAINTY ANALYSIS IN MODELLING	OECD	https://inis.iaea.org/collection/NCLCollectionStore/_Public/45/026/45026304.pdf	PSU, CEA, UAM Expert Group	Objective of the proposed work is to define, co-ordinate, conduct, and report an international benchmark for uncertainty analysis in best-estimate coupled code calculations for design, operation, and safety analysis of LWRs. The title of this benchmark is: “OECD UAM LWR Benchmark”. The experimental data are used as much as possible (two “interactions” with “known” experimental data are

Title	Context	References	Participants	Summary
(UAM) FOR THE DESIGN, OPERATION AND SAFETY ANALYSIS OF LWRs Volume I: Specification and Support Data for Neutronics Cases (Phase I) Version 2.1 (Final Specifications), NEA/NSC/DOC (2013)7 K. Ivanov, M. Avramova, S. Kamerow, I. Kodeli, E. Sartori, E. Ivanov, O. Cabellos				indicated above but others can be added). The benchmark team identifies Input (I), Output (O) or target of the analysis, as well as provides guidance on assumptions for each step and propagated uncertainty parameters (U). The uncertainty from one step should be propagated to the others (as much as feasible and realistic). This phase is focused on understanding uncertainties in prediction of key reactor core parameters associated with LWR stand-alone neutronics core simulation. Such uncertainties occur due to input data uncertainties, modelling errors, and numerical approximations. Input data for core neutronics calculations primarily include the lattice averaged few group cross-sections. Three main LWR types are selected, based on previous benchmark experience and available data: • PWR (TMI-1). • BWR (Peach Bottom-2). • VVER-1000 (Kozloduy-6, Kalinin-3). Representative designs for Generation 3 PWR (GEN-III) are added to Phase I in order to address the modelling issues and the likely increased prediction uncertainties related to the designs of GEN-III LWR currently being built, both with UOX and MOX fuels. The SNEAK (fast core problem) is added as an optional test case to Exercise I-3 since it has a unique set of experimental data for βeff uncertainties and can be used as an example on how to calculate uncertainty in βeff. The two high-quality reactor physics benchmark experiments, SNEAK-7A & 7B (Karlsruhe Fast Critical Facility) are part of the International Reactor Physics Benchmark Experiments (IRPhE) database.
Benchmark calculation AER VVER-1000 - ETE using BIPR8, ICNRP Volga-2018, IOP Conf.	AER, IOP Science	https://iopscience.iop.org/article/10.1088/1742-6596/1133/1/012043	NRC “Kurchatov Institute”, NRNU “MEPhI” Expert Group	This article presents AER VVER-1000 – ETE benchmark results using the BIPR-8 nodal sparse-grid program. This paper contains a description of the benchmark AER VVER- 1000 – ETE and short description of calculations using the BIPR-8 nodal sparse-grid program. Calculations were carried out at the full scale then the pin-by-pin power distribution was reconstructed, and results are compared with the results obtained in the MCNP program.

Title	Context	References	Participants	Summary
Series: Journal of Physics: Conf. Series 1133 (2018) 012043 P V Gordienko, P K Kiryukhin, and A A Shcherbakov				The VVER-1000 - ETE benchmark [1] was proposed by the ŠKODA JS specialists in 2011 in order to test the VVER fuel cell simulation programs. The main task of this benchmark is to test the pin-by-pin power distribution calculated by different macro-codes in selected fuel assemblies that are placed mainly at and close to the core periphery. Motivation for the benchmark setup is due to an observed phenomenon at calculation of the 9th fuel load of Temelin NPP (VVER-1000 core, fuel load completely composed from TVSA-T fresh fuel assemblies). The task organizers suggested comparing the results with the results of the Monte Carlo MCNP program. This paper presents the solution of the problem with the help of the nodal sparse-grid program BIPR-8 with the pin-by-pin power reconstruction. Benchmark VVER 1000 - ETE was solved with the help of the BIPR-8 code at the full-scale and fuel sampling level. The results of the calculations allow to be made the following conclusions: • Maximum deviation in the full-scale calculation is 1.37%. Deviation of neutron multiplication factor is 0.012%. • Deviation in pin by pin solution is less than 5.1% - it is well result for sparse-grid nodal code. • The results obtained showed the possibility of optimizing the procedure for restoring of energy field into assembly in order to refine this solution. Bibliography: 1. Krýsl V, Mikoláš P,Sprinzl D and Švarný J 2010 'MIDICORE' VVER-1000 core periphery power distribution benchmark proposal Atomic Energy Research Symposium on WWER Physics and Reactor Safety (Espoo: Hanasaari)
Best-estimate simulation of a VVER MSLB core transient using the NURESIM platform codes, Nuclear Engineering and	NURESAFE EU / Science Direct	https://www.sciencedirect.com/science/article/abs/pii/S0029549317301449	INRNE, UPM, KIT, UJV Rez	This paper summarizes the nodal level results from the VVER MSLB core simulation in the NURESAFE EU project. The main objective is to implement and verify new developments in the models and couplings of 3D core simulators for cores with hexagonal fuel assemblies. Recent versions of the COBAYA and DYN3D core physics codes, and the FLICA4 and CTF thermal-hydraulic codes were tested standalone and coupled through standardized coupling functions in the Salome platform. The MSLB core transient was analyzed in coupled code simulation of a core boundary condition problem derived from the OECD VVER

Title	Context	References	Participants	Summary
Design 321 (2017) 26–37 I. Spasov, S. Mitkov, N.P. Kolev, S. Sanchez-Cervera, N. Garcia-Herranz, A. Sabater, D. Cuervo, J. Jimenez, V.H. Sanchez L. Vyskocil				MSLB benchmark. The impact of node sub-division and different core mixing models, as well as the effects of CFD computed core inlet thermal-hydraulic boundary conditions on the core dynamics were explored. The results with coarse-mesh and CFD computed core boundary conditions show that the validated system code models of the RPV are applicable to MSLB analysis but have some limitations in resolution for the local effects. Validated CFD calculations of the down-comer and the lower plenum conditions are found to improve the resolution in the 3D core simulation of asymmetric coolant transients with sector formation. In the considered cases the impact of this refinement is mild and is more pronounced around the periphery of the disturbed sector. It may be stronger in hypothetic scenarios of asymmetric VVER coolant transients with multiple rod perturbations of the core. Authors have presented a sample comparison of MSLB results making use of transient core boundary conditions computed with two particular models: CATHARE 24-sector coarse-mesh and FLUENT with a limited number of cells and rke turbulence model. Based on the lessons from the OECD VVER-1000 vessel mixing benchmark and the studies in related publications one can expect some scatter in the parameters of the core transient when using different computationally efficient CFD models.
CATHARE Multi-1D Modeling of Coolant Mixing in VVER 1000 for RIA Analysis, Science and Technology of Nuclear Installations, Volume 2010, Article ID 457094	Hindawi	https://www.hindawi.com/journals/stni/2010/457094/	INRNE, IRSN	The paper presents validation results for multichannel vessel thermal-hydraulic models in CATHARE used in coupled 3D neutronic/thermal hydraulic calculations. The mixing is modeled with cross flows governed by local pressure drops. The test cases are from the OECD VVER-1000 coolant transient benchmark (V1000CT) and include asymmetric vessel flow transients and main steam line break (MSLB) transients. Plant data from flow mixing experiments are available for comparison. Sufficient mesh refinement with up to 24 sectors in the vessel is considered for acceptable resolution. The results demonstrate the applicability of such validated thermal-hydraulic models to MSLB scenarios involving thermal mixing, azimuthal flow rotation, and primary pump trip. An acceptable trade-off between accuracy and computational efficiency can be obtained.

Title	Context	References	Participants	Summary
Spasov, J. Donov, N. P. Kolev, and L. Sabotinov				This work is motivated by the need for improved single- phase vessel mixing models in system codes that are able to properly represent local effects in reactivity insertion accidents. The study has been performed in Phase 2 of the OECD VVER-1000 coolant transient benchmarks labelled V1000CT-2 [1, 2]. These benchmarks provide a consistent approach to the testing of coupled neutronic/thermal-hydraulic codes. Separate exercises are devoted to stand- alone testing of thermal hydraulic and core physics models. Then the validated models are tested in coupled code simulation of asymmetric MSLB transients. The V1000CT-2 vessel mixing benchmark [1] is based on a steam generator isolation experiment during the plant commissioning phase of Kozloduy-6 in Bulgaria. Local and integral plant data are available for comparison. The objective of this benchmark is to test the capability of system and CFD codes to represent in-vessel thermal hydraulics. The purpose of the V1000CT-2 MSLB benchmark is to test the core neutronics and coupled N/TH calculations. This paper presents results of thermal-hydraulic calculations with CATHARE [3] for the VVER-1000 coolant mixing and MSLB benchmarks. Bibliography: 1. N. P. Kolev, S. Aniel, E. Royer, U. Bieder, D. Popov, and Ts. Topalov, “VVER-1000 Coolant Transient Benchmark (V1000CT-2): Specifications of the VVER-1000 vessel mixing problems,” OECD NEA/NSC/DOC (2004)6; Rev.1, 2006 2. N. P. Kolev, et al., “VVER-1000 Coolant Transient Benchmark (V1000CT-2 Vol.2): Specifications of the VVER- 1000 MSLB problem,” OECD NEA/NSC/DOC(2006) 3. CATHARE 2.5 Manuals, CEA Grenoble, 2006.
Experience and perspective of best-estimate approach application for RIA analysis,	research gate.net	https://nuclear-journal.com/index.php/journal/article/download/15/15/	SSTC N&RS, UJV Rez	The best-estimate computer codes combined with conservative initial and boundary conditions (combined analysis) are used for design basis accident (DBA) analysis in RIA in the framework of safety analysis report (SAR) in Ukraine. For a given purpose, the approach is developed to include all RIA significant

Title	Context	References	Participants	Summary
Nuclear and Radiation Safety, November 2016 Ovdiienko, M. Ieremenko, Y. Bilodid, Jelena Krhounkova				conservative initial and boundary conditions into a realistic model of the reactor core. The conservative values of parameters such as: - reactivity coefficients, - efficiency of control rod (CR) and scram weight, - characteristics of the most loaded fuel pin, and - thermal hydraulic characteristics are introduced into the developed models for DBA analysis. Depending on used neutron kinetics, the approaches slightly differ but are very similar in general. Such an approach complies with IAEA recommendations. The range of conservatism is defined by the Ukrainian regulation "Fuel Handling. Refueling in WWER-1000 Reactor. Nomenclature of Operational Neutronic Calculations and Experiments" (Energoatom, 2013), SOU NAEK 064:2013 [1]. The so-called frame safety parameters are defined. Frame safety parameters are the same for all WWER-1000 (V320+TVSA). There are slight differences only for V302/V338 designs and for fuel loadings with TVS-W (Westinghouse assemblies).
Validation of new CMS5-VVER nuclear data library using critical experiments and X2 full-core benchmark, Kerntechnik, Volume 85, Issue 4, September 2020	KERN - TECHNIK / research gate.net	https://www.researchgate.net/publication/344238980_Validation_of_new_CMS5-VVER_nuclear_data_library_using_critical_experiments_and_X2_full-core_benchmark	Studsvik Scandpower	Studsvik's in-core fuel management code package CMS5- VVER, which includes the CASMO5-VVER lattice physics code and SIMULATE5-VVER three-dimensional nodal code, is currently in use for VVER-1000/1200 reactor analysis. Recently, a new commercially available CASMO5 nuclear data library has been generated based on the ENDF/B-VIII.0 evaluation. The ENDF/B-VIII.0 evaluation represents the state-of- the-art in nuclear data and features new incident-neutron cross section evaluations from the CIELO project for 1H, 16O, 56Fe, 235U, 238U and 239Pu. A summary of the main features and validation of the new ENDF/B-VIII.0-based data library, referred to as E8R0 library, is presented in this work. Comparisons of predicted criticality and fission rate distributions to measurements from various hexagonal-lattice critical experiments, such as the ZR-6 (TIC) and P-Facility, show excellent agreement between the E8R0-based

Title	Context	References	Participants	Summary
R. Ferrer and T. Bahadir				calculations and measurements. In addition, validation results are presented for CMS5-VVER using the new E8R0 library and the X2 VVER-1000 benchmark problem. These results indicate that the E8R0 library provides comparable accuracy to E7R1 results for the various reactor physics parameters such as critical boron concentration, temperature reactivity coefficients, and control rod worth. A new commercially available ENDF/B-VIII.0-based nuclear data library, referred to as E8R0, was generated for Studsvik CMS5-VVER core analysis package. The new ENDF/B- VIII.0 represents the state-of-the-art in nuclear data and features new cross section evaluations for 1H, 16O, 56Fe, 235U, 238U, and 239Pu. Comparisons of calculated criticality and fission rate distributions to measurements from various hexagonal-lattice critical experiments show excellent agreement between the E8R0 CASMO5-VVER calculations and measurements. In addition, X2 benchmark validation results are presented which show that the E8R0 library, used in conjunction with CMS5-VVER, provides comparable accuracy to previous E7R1 results for various reactor physics parameters such as critical boron concentration, temperature reactivity coefficients, and control rod worth. Given the extensive validation and use of the E7R1 library in production calculations, the results presented in this work support the use of the new E8R0 for VVER analysis. Future work involves further validation of CMS5-VVER to VVER-1000/1200 measured plant data.
VALIDATION MATRIX FOR THE ASSESSMENT OF THERMAL-HYDRAULIC CODES FOR VVER LOCA AND	OECD	https://www.oecd-nea.org/jcms/pl_17492	OECD Support Group on the VVER Thermal-Hydraulic Code Validation Matrix	This report deals with an internationally agreed experimental test facility matrix for the validation of best estimate thermal-hydraulic computer codes applied for the analysis of VVER reactor primary systems in accident and transient conditions. Firstly, the main physical phenomena that occur during the considered accidents are identified, test types are specified, and test facilities that supplement the CSNI CCVMs and are suitable for reproducing these aspects are selected. Secondly, a list of selected experiments carried out in these facilities has been set down. The criteria to achieve the objectives are outlined. The construction of VVER Thermal-Hydraulic Code Validation Matrix follows

Title	Context	References	Participants	Summary
TRANSIENTS, A Report by the OECD Support Group on the VVER Thermal-Hydraulic Code Validation Matrix, NEA/CSNI/R(2001)4				the logic of the CSNI Code Validation Matrices (CCVM). Similar to the CCVM it is an attempt to collect together in a systematic way the best sets of available test data for VVER specific code validation, assessment and improvement, including quantitative assessment of uncertainties in the modelling of phenomena by the codes. In addition to this objective, it is an attempt to record information which has been generated in countries operating VVER reactors over the last 20 years so that it is more accessible to present and future workers in that field than would otherwise be the case. Basically the mandate given to the Support Group was to review the level of validation of advanced thermal hydraulic codes applied for the analysis of VVER reactor primary systems in accident and transient conditions. Consequently the aim is to develop a supplement to the existing ITF and SETF CCVMs under consideration of the specific features of VVER reactor systems and their behaviour in normal and abnormal situations. This includes the necessary enlargement of the experimental data base for code assessment with data which were not taken into account in the previous CSNI CCVMs. The report, in this version, is limited to the large and small break LOCAs and transients and therefore does not include shutdown transients and accident management scenarios. Objective of part of this book is to provide an information on the thermalhydraulic phenomena relevant to safety of VVER reactors and to correlate these phenomena to experimental data sets available for code validation and development. In book describes the structure of the VVER matrices and their use in overall terms. An explanation is given of the symbols used in filling in the matrix. In the final sections of the chapter more detailed aspects of each of the three matrices are described as a further aid to their use. A systematic study has been carried out to select experiments for thermal-hydraulic system code validation. The main experimental facilities for VVERs have been identified and described in Chapter 4 and Appendix D.

Title	Context	References	Participants	Summary
				Matrices have been established to identify, firstly, phenomena assumed to occur in VVER plants during accident conditions and secondly, facilities suitable for code validation (Chapter 4). Tables identify the experiments selected for validation of computer codes (Chapter 4). The matrices also permit identification of areas where further research may be justified. Compared with [4], a revision and update of the matrices, have been performed in this report. Additional work has been performed to describe the VVER reactor systems (Appendices A and B), the content of the validation matrices, i.e. the test types (Chapter 2), the phenomena Chapter 2 and Appendix C, and the selected tests (Chapter 4). A periodic updating of the matrices will be necessary to include new relevant experimental facilities and tests (e.g. investigating boron dilution or behaviour of advanced reactors) and to include improved understanding of existing data as a result of further validation. To validate a code for a particular LWR plant application, it is recommended that the list of tests in the relevant matrix be viewed as the phenomenological well founded set of experiments to be used for an adequate validation of a thermal hydraulic computer code. Bibliography: 4. K. Liesch, M. Reocreux Verification Matrix for Thermalhydraulic System Codes Applied for WWER Analysis Common Report IPSN/GRS No 25, July 1995
The VVER Code Validation Matrix and VVER Specificities, THICKET 2008 – Session III – Paper	OECD/CSNI/THICKET	https://inis.iaea.org/collection/NCLCollectionStore/_Public/42/101/42101977.pdf	KFKI Atomic Energy Research Institute	Objectives and structure of the CVMs, along with VVER- specific phenomena are described and an overview of selected test facilities and tests is given. Presents the VVER-related OECD actions: the PSB, Bubbler-Condenser and Paks Fuel projects. Among CSNI's International Standard Problems (ISP) only one was devoted to VVERs: ISP33 based on the PACTEL facility. Therefore also the earlier IAEA activities in this field are reviewed, with the four Standard Problem Exercises (SPE) based on the PMK test facility. The tests and outcome of the

Title	Context	References	Participants	Summary
05 Ivan Tóth				computer code analyses are described. Although not a CSNI action, major conclusions of a series of seminars on horizontal steam generators are also summarised. Cross Reference Matrices related to LOCA and Transients were drawn up with the objective of allowing a systematic selection of tests suitable for code assessment. Since the aim of the Support Group was to review all test facilities which fulfilled the above criteria, no pre- selection was made with respect to availability of the data. The list of test facilities given in Appendix D of the report can be considered as an exhaustive one, from which tests for code validation purposes can be selected. The main emphasis was laid on integral systems, but a large number of separate effect test facilities was also included. For the selection of the phenomena three principles were applied: • The first principle is that the phenomena identified in the CSNI matrices are in general also relevant to VVERs because of common characteristics of PWR and VVER-systems. Therefore it is important to stress that code validation and assessment plans for thermalhydraulic codes to be used for safety assessments of VVERs should be made on the basis of both: the ITF CCVM and SETF CCVM as well as on the VVER-specific matrices. • The second principle for selection of the phenomena for the VVER matrix is their relevance to safety. The selected phenomena have to be important to safety and furthermore their accurate modelling in computer codes crucial to safety analyses. A section of the report provides a tabular overview of the selected phenomena and an appendix gives a detailed description of the phenomena and discusses their safety relevance. • The third principle for selection of phenomena relates to accident scenarios. The phenomena were identified for three separate accident scenario groups and for these separate cross-reference matrices were developed. These groups are large break LOCA, small and intermediate break LOCA and transients. Other scenarios, in particular shutdown and accident management transients should be considered in a future revision of the report.

Title	Context	References	Participants	Summary
				The test facilities listed in the report were selected irrespectively of the fact, whether the facility owners were ready to supply test data to a data bank or not. Criteria for facility and test selection were identified, including guidelines to qualify both facilities and tests.
Validation of Advanced Computer Codes for VVER Technology: LB-LOCA Transient in PSB-VVER Facility, Science and Technology of Nuclear Installations, Volume 2012, Article ID 480948 A. Del Nevo, M. Adorni, F. D'Auria, O. I. Melikhov, I. V. Elkin, V. I. Schekoldin, M. O. Zakutaev, S. I. Zaitsev, and M. Benčík	OECD / Hindawi	https://www.hindawi.com/journals/stni/2012/480948/	University of Pisa, Electrogorsk Research and Engineering Centre, FSUE EDO “GIDROPRESS”, UJV Rez	OECD/NEA PSB-VVER represents the scaled-down layout of the Russian-designed pressurized water reactor, namely, VVER-1000. Five experiments were executed, dealing with loss of coolant scenarios (small, intermediate, and large break loss of coolant accidents), a primary-to-secondary leak, and a parametric study (natural circulation test) aimed at characterizing the VVER system at reduced mass inventory conditions. The comparative analysis, presented in the paper, regards the large break loss of coolant accident experiment. The OECD/NEA PSB-VVER project (2003–2008) has been set with the objective to obtain the required experimental data not covered by the VVER validation matrix The main objectives of the experiments were as follows: • to generate experimental data in order to validate computer codes for transient analysis of VVER reactors, • to address the scaling issue, • to contribute to the investigations of postulated accident scenario and actual phenomena occurring VVER-1000, to support safety assessments for VVER-1000 reactors. The OECD/NEA PSB-VVER project provided unique and useful experimental data for code validation by the scaled- down integral test facility PSB-VVER. In this framework, four participants and three different institutions simulated the test 5a (identification CL-2x100-01), which is the last experiment of the project test matrix. The Western (i.e., ATHLET and RELAP5-3D) and Eastern (KORSAR and TECH-M) advanced computer codes were applied in this context. The initiating event is the double-ended guillotine break in cold leg. The objective of the activity is to collect, analyze, and document the numerical activity (posttest) performed by

Title	Context	References	Participants	Summary
				the participants, describing the performances of the codes simulations and their capability to reproduce the relevant thermal-hydraulic phenomena observed in the experiment. The analysis of the results demonstrates the following: • all code runs were able to predict the primary pressure trend with satisfactory accuracy; • the core cladding temperature was predicted by all posttest analyses. In particular, the maximum cladding temperature was generally overestimated (posttest) with the exception of the ATHLET simulation that highlighted an excellent accuracy; • the primary mass inventories predicted by the simulations resulted in general lower than the experimental (indirect) measurement. The application of the FFTBM, related to the quantification of the accuracy, showed the following: • almost all code simulations have an average amplitude of the primary pressure equal or lower 0.1 and the others are very close to this threshold, • all code simulations showed a good prediction of the experiment (total average accuracy lower than 0.4) or a fair prediction (0.4 < AAtot < 0.5), • the parameter trends of the pressure drops during the transient and the timing of the final cladding temperature excursions affected the total average by increasing the final values. In conclusion, the availability of the experimental data and the present benchmarking activity brought to the following achievements. • The experiment PSB-VVER test 5a, executed in the largest ITF currently available for VVER-1000 type reactors, contributes to extend the experimental database for code validation. • The applications of the numerical models represent an enlargement of the validation activity for computer codes. In this connection, the comparison of Western and Eastern computer codes represenst a further valuable achievement.

Title	Context	References	Participants	Summary
Outcomes of the “steady-state crisis” experiment in the MIR reactor channel, Nuclear Energy and Technology 5(3): 207–212 V. Alekseev, O. I. Dreganov, A. L. Izhutov, I. V. Kiseleva,V. N. Shulimov	NUCET	https://nucet.pensoft.net/article/39288/	JSC “SSC RIAR”	A reactivity-initiated accident (RIA) with an unauthorized release of CPS rods from the reactor core leads to a pulsed channel power increase. This accident can proceed according to two scenarios: without a critical heat flux (CHF) on the fuel element jacket at the final stage and with a dry heat flux. To date, a series of experiments have been carried out according to the first scenario in the MIR reactor channel and the corresponding data on the behavior of fuel elements have been obtained. An urgent task for today is to prepare and conduct reactor experiments according to the second scenario. The main experimental parameter that determines the behavior and final state of the studied fuel elements is their temperature. No experimental data were found on the critical heat flux for the rod bundles in the low coolant mass flow rate region (experiments in the MIR reactor channel can be conducted in the range of 200–250 kg/(m^2s)). The available data are in the extrapolation range. The “steady-state crisis” experiment was conducted to obtain data on the critical heat flux value within the specified coolant mass flow rate range in the MIR reactor channel. The test object was a jacket fuel assembly composed of three shortened VVER-1000 fuel rods with a length of 1230 mm (the fuel part length = 1000 mm) installed in a triangular grid at a pitch of 12.75 mm, which is a cell of the VVER-1000 core. This assembly configuration is used for in-pile tests to study the behavior of fuel elements under emergency conditions. The paper shows the possibility of detecting the start and development of a dry heat flux based on the readings of thermocouples located inside the FE kernel. As a result, the directly measured test parameters were used to determine the critical heat flux value. Using the results of direct measurement, the critical heat flux was determined for specific experimental conditions. Based on the obtained experimental data for Qc calculations under similar conditions, it is recommended to use the published method with the introduction of an upward correction. The experimental data are used to calculate the temperature conditions for testing fuel assemblies in the MIR

Title	Context	References	Participants	Summary
				reactor, particularly, in the experiment with a reactivity-inititated accident (RIA), where, according to the technical requirements, it is necessary to obtain the critical heat flux on the fuel element jacket.
EXPERIMENTAL INVESTIGATION AND ANALYSIS OF THERMAL HYDRAULIC CHARACTERISTICS OF WWER-1000 ALTERNATIVE FA, 6 th International Conference on WWER Fuel Performance, Modeling and Experimental Support, Albena, Bulgaria A.A. Falkov, O.B. Samoilov, A.V. Kupriyanov, V.E. Lukyanov, O.N. Morozkin, D.L. Shipov		https://inis.iaea.org/collection/NCLCollectionStore/_Public/37/098/37098328.pdf	OKBM, Nizhny Novgorod	Thermophysical test facility L-186 is designed for experimental investigations of thermohydraulic characteristics and DNB using electrically heated FA models. The test facility consists of closed water loop designed for working pressure up to 19.6 MPa. TVSA experimental models are 19-rods of fuel rod simulators located in a strong casing. Stainless steel cylindrical tubes are used as fuel rod simulators. The rods in bundle are spaced by cell-type SG. Heat release is provided owing to rods heating by direct current. Parameters in the circulation loop are checked and registered by standard instrumentation. TVSA models are equipped with micro thermal elements for measurement of coolant temperature in cells at bundle outlet and rods temperature in several points along the height. The facility is equipped with automated data acquisition system. More than 20 models including those with TVSA design features were tested: − with simulation of conditions near rigid angle; − with guide thimble; − with various pitch of SG installation; − with radial power non-uniformity; − with axial power non-uniformity. Investigations were performed within the following parameter range: − pressure 7 – 17 MPa; − inlet temperature 200 – 310 °C; − mass velocity 340 – 3550 kg/(m^2·s). Main characteristics of tested TVSA models: − number of fuel rod simulators 19 (18); − heating length 3.0 m;

Title	Context	References	Participants	Summary
				− rod diameter 9.1 mm; − diameter of guide tube simulator 12.6 -13.5 mm; − rod pitch 12.75 mm. During experiments coolant was supplied through the guide tube with flow rate corresponding to that in TVSA WWER-1000. Two types of power non-uniformity were simulated in the experiments, which was provided by fuel rod simulators with various wall thickness. The following investigations were performed using TVSA models: − critical heat flux (CHF) in steady-state modes in view of TVSA design features and power non-uniformity (≈900 modes); − local coolant temperature in fuel rod assembly in the conditions of thermohydraulic non-equivalence of subchannels (≈150 modes); − post-DNB heat transfer in steady-state modes with rod overheating up to Tmax≈550°C; − transients under DNB conditions and fuel rod overheating including modes with power increase and flow rate decrease (≈20 modes). Investigations of emergency modes with power increase and flow rate decrease show that DNB in transients appears slightly later than heat flux becomes critical in steady-state modes. With reference to TVSA WWER-1000 core, coolant velocity and flow rate distributions in the cells across assembly cross-section and in inter-cassette gap of 57-rod TVSA core fragment with 3 segments of adjacent TVSA were investigated in experiments. The experiments show that coolant flow velocity in the various types of TVSA cells are distributed as per their hydraulic characteristics. The maximum axial flow velocity is realized in the inter-cassette gap, the minimum – in the angle and in the guide tube cells. The results of experiments were used for additional verification of certified KANAL code. The reliability of KANAL code prediction of local coolant

Title	Context	References	Participants	Summary
				characteristics and DNBR with account of thermohydraulic non-equivalence of subchannels and TVSA design features shown. Calculation error for critical heat flux does not exceed 15%. The results of experiments and thermohydraulic analyses confirm reliable cooling of fuel rods and high thermal performance margin in TVSA. Statistical procedure which provides joint consideration of random character of parameter deviations allows increasing of DNBR by ~15% as compared with previous deterministic approach. Increased DNBR of TVSA core allows increasing of nuclear peaking factor and enables implementation of effective fuel cycles with low neutron leakage and improved fuel use.
DNB measurements in the Westinghouse Critical Heat Flux Test Facility – ODEN to provide an improved correlation to increase DNB margin for the Westinghouse WWER-1000 fuel design (2013) J. Höglund, S. Andersson, F. Waldermarsson, S. Slyeptsov	Westinghouse	https://inis.iaea.org/collection/NCLCollectionStore/_Public/44/122/44122462.pdf	Westinghouse, Center "Kharkov Institute of Physics and Technology"	Westinghouse has designed and built ODEN, a Critical Heat Flux (CHF) test loop for PWR applications. This loop was used to perform Departure from Nucleate Boiling (DNB) measurements to provide an improved correlation to increase DNB margin for the Westinghouse fuel design for WWER-1000 reactor. Two DNB correlations were developed. The WVHI correlation for predicting DNB for high flow conditions with all four loops in service operation, and the WVLO correlation for predicting DNB for low flow conditions for N-X loop operations. These correlations were incorporated into the Westinghouse 3-D thermal-hydraulic sub-channel code VIPRE-W and used for comparative DNBR analyses. This paper provides an overview of the ODEN loop design as well as the test configuration, the measurement program and results for Westinghouse fuel design for WWER-1000 reactor. Additionally the application of the DNB correlations for WWER-1000 core analyses using the VIPRE-W code are presented. DNB measurements were carried out in the ODEN loop to develop an improved correlation to increase DNB margin for the Westinghouse fuel design for WWER-1000 reactor. The test bundle configuration was a 19 rod hexagonal array. The outside diameter of the heater rod is 9.144 mm and for the thimble rod 12.60 mm. Each rod contains 7 thermo couples (TCs). Two voltage tap rods are positioned in opposite peripheral locations. Each of the 12 peripheral rods has a power output

Title	Context	References	Participants	Summary
				which is 82% (nominal) of that of each of the 7 (or 6 for thimble test) inner rods of the test bundle. The test bundle contained 17 grids. Three DNB tests were conducted on the: Test #1 was performed with cosine axial power shape, typical cell; Test #2 was performed with uniform axial power shape, typical cell; and Test #3 was performed with cosine axial power shape, thimble cell. The nominal range of test conditions is listed below: • Pressure 10.3 to 17 MPa; • Mass Velocity 500 to 4750 kg/m^2s; • Mass Flow Rate 0.82 to 7.83 kg/s; • Inlet Temperature 150 to 325 ºC; • Exit steam quality -2% to 54%. VIPRE-W is the Westinghouse modified version of the Electric Power Research Institute (EPRI) 3-D thermal-hydraulic (T/H) sub-channel code VIPRE-01 developed for light water reactor core design applications. Following the ODEN loop measurements described in Section 3 two DNB correlations were developed by Westinghouse. The WVHI correlation for predicting DNB for high flow conditions with all four loops in service operation, and the WVLO correlation for predicting DNB for low flow conditions for N-X loop operations. These correlations were implemented in VIPRE-W by Center of Reactor Core Design (CRCD) at Kharkiv Institute of Physics and Technology, Ukraine, and used for comparative DNBR analyses of a WWER-1000 core with a proposed Robust Westinghouse WWER-1000 Fuel Assembly (RWFA). In the subsequent sections, a brief description of the VIPRE-W model for a WWER-1000 core is provided. Also, VIPRE-W DNBR comparative analyses carried out by CRCD with the WVHI and with the Russian OKB “Gidropress” DNB correlations are presented at the following operating conditions: • Steady-state hot full power (HFP) with limiting operating parameters.

Title	Context	References	Participants	Summary
				• Complete Loss of Flow, Under Frequency (CLOF UF) transient in 4-Loop WWER-1000 core. The CLOF UF accident is the most DNB limiting transient for a WWER-1000 core. Comparative VIPRE-W DNBR analyses clearly demonstrate that the use of the WVHI DNB correlation with the current analysis methodology allows increasing the current core design limit by 3% without any restrictions. Qualification of the correlations is ongoing for use in safety substantiation analyses for Westinghouse WWER-1000 fuel in Ukrainian NPP´s.
AER Benchmark book, Atomic energy research (AER), Budapest, 1999 P. Dařilek, Korpás,J. Kyncl,L. Maiorov,M. Makai, P. Siltanen	AER	http://aerbench.kfki.hu/aerbench/Preamble.doc	VTT, VUJE, IVO, AEKI, PA Rt, ŠKODA, UJV, IAE.	The present volume intends to collect a volume of VVER related benchmarks, into a unified framework. All submitted cases have been utilized in V&V of VVER codes. The II section provides basic data of VVER-440 as well as VVER-1000 core and fuel assembly. The III section is a short survey of the available tests. Each test has been assigned a mnemonic identification. The first invariable tag is AER. The second tag refers to the nature of the test. The last tag is a three-digit number. Its first digit refers to the reactor type (0/1=VVER-440/VVER-1000), the last two digits make a sequential number. The test specifications are available via internet at http://www.kfki.hu/~aekihp/ where you have to click on AER, there click on Benchmark Book.
AER Benchmark Specification Sheet, Test ID: AER-FCM-101	AER	http://aerbench.kfki.hu/aerbench/FCM101.doc	IAE, CEA Saclay, AEKI, SKODA	The 3D benchmark of Schulz1 models a VVER-1000 core in steady state. The task is to calculate keff, 3D and 2D power distributions normalized to core power density of unity, over a physical grid of 18 fuel assemblies x 10 axial layers. Convergence criteria $\varepsilon f = 10^{-4}$ for the flux and $\varepsilon l = 10^{-6}$ for the eigenvalue are used as iteration limits. Output: • Expected Results:

Title	Context	References	Participants	Summary
				- Keff; - 3D power distribution; - 2D power distribution (axially averaged). • Differences to the reference power distributions. The Appendixs shows CRONOS 2nd-order solutions used to extrapolate the recommended solution, together with selected CRONOS 3rd-order solutions and comparison of CRONOS to FEM-3Di recommended solutions, as follows: 1. CRONOS 2nd-order HXP127#-P72 solution with 54 triangles per hexagon (54TPH) and hz=5.916667 cm; 2. CRONOS 2nd-order HXP61#-P48 solution with 24TPH and hz=8.875 cm; 3. Difference of CRONOS HXP61#-P48 3D solution to the recommended solution; 4. CRONOS 2nd-order HXP19#-P24 solution with 6TPH and hz=17.75 cm; 5. Difference of CRONOS HXP19#-P24 3D solution to the recommended solution; 6. Extrapolated CRONOS 3rd-order solution with hr=0, hz=0; 7. CRONOS finest 3rd-order HXC127#-P72 solution; 8. Absolute difference of CRONOS recommended solutions to FEM-3Di recommended solution; 9. Relative difference of CRONOS recommended solutions to FEM-3Di recommended solution.
AER Benchmark Solution Sheet, Test ID: AER-FCM-101 Forschungszentrum	AER	http://aerbench.kfki.hu/aerbench/FCM101_solfzr.pdf	Institute of Safety Research, Fortum Nuclear	The DYN3D calculations of the AER FCM-101 benchmark [2] were performed with HEXNEM1 and HEXNEM2 by using 10 core layers and 1 node/assembly in each layer. -Neutron Kinetics • Neutron diffusion theory

Title	Context	References	Participants	Summary
Rossendorf, Institute of Safety Research, Germany, 02.06.2005 Ulrich Grundmann			Services Ltd, KFKI Atomic Energy Research Institute	• Two group theory • Nodewise homogenized cross sections - Thermal Hydraulics • One-dimensional four equation model for two-phase coolant flow (momentum equation of mixture, energy equation of mixture, mass balance of mixture and mass balance of vapour phase) • Constitutive laws • Radial heat conduction equation in fuel pin • Map for heat transfer from fuel to coolant - Feedback • Calculation of neutron cross section by using libraries or input data The comparisons were performed with the recommended reference solution of table 2 of [1,2]. • HEXNEM1: Table 3: Deviations of eigenvalue keff, 3D normalized powers Pi, j .

Title	Context	References	Participants	Summary

$\Delta k_{eff} = 41$ pcm

ass i	$(P_{i,j} - P_{i,j,ref}) \cdot 100$									
	axial layer j									
	1	2	3	4	5	6	7	8	9	10
1	-1.95	-2.81	**-4.03**	-3.42	-2.88	-2.06	-1.44	-0.86	-0.64	-0.36
2	-1.50	-2.52	-3.14	-3.25	-2.63	-1.81	-1.30	-0.80	-0.43	-0.21
3	-1.39	-2.31	-2.85	-2.80	-2.21	-1.48	-0.97	-0.56	-0.34	-0.12
4	-1.59	-2.73	-3.36	-3.32	-2.71	-1.95	-1.28	-0.84	-0.49	-0.21
5	-1.29	-1.86	-2.51	-2.36	-1.84	-1.53	-0.83	-0.38	-0.18	-0.15
6	-1.25	-1.95	-2.49	-2.40	-1.85	-1.37	-0.87	-0.45	-0.26	-0.13
7	-0.65	-0.85	-1.14	-1.07	-0.77	-0.52	-0.23	0.09	0.05	0.02
8	-0.98	-1.41	-1.83	-1.81	-1.79	-0.93	-0.45	-0.28	-0.17	-0.06
9	-1.13	-1.42	-2.01	-1.90	-1.32	-1.12	-0.55	-0.17	-0.03	-0.02
10	0.36	1.60	1.70	1.91	1.91	1.81	1.32	1.05	0.76	0.25
11	-0.35	-0.25	-0.46	-0.43	-0.11	0.07	0.14	0.24	0.21	0.11
12	-0.51	-0.59	-0.84	-0.85	-0.45	-0.17	-0.01	0.13	0.19	0.00
13	0.60	1.63	1.84	1.98	1.91	1.49	1.08	0.79	0.64	0.20
14	0.49	1.92	2.11	**2.26**	2.17	1.71	1.28	0.93	0.73	0.29
15	0.36	1.64	1.77	1.97	2.00	1.77	1.26	1.02	0.80	0.26
16	0.03	0.50	0.61	0.61	0.69	0.70	0.56	0.42	0.41	0.17
19	0.64	1.79	1.98	2.12	2.00	1.62	1.25	0.88	0.62	0.26
20	0.57	1.68	1.93	2.10	1.96	1.64	1.18	0.85	0.70	0.25

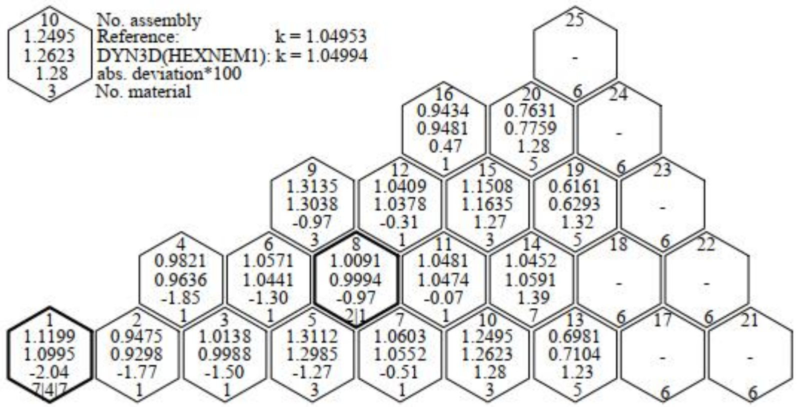

Fig. 1: HEXNEM1 - Absolute deviations of assembly powers P_i^{ass}

- b) HEXNEM2:

Table 4: Deviations of eigenvalue keff, 3D normalized powers Pi, j .

Title	Context	References	Participants	Summary
				(see below)

Δk_{eff} = -13 pcm

ass i	$(P_{i,j} - P_{i,j,ref}) \cdot 100$									
	axial layer j									
	1	2	3	4	5	6	7	8	9	10
1	0.17	**1.73**	1.66	1.55	1.05	0.56	0.08	-0.07	-0.31	-0.27
2	0.26	1.25	1.57	1.09	0.75	0.38	-0.08	-0.19	-0.15	-0.12
3	0.21	1.11	1.47	1.35	0.92	0.27	-0.16	-0.25	-0.24	-0.10
4	0.17	1.05	1.42	1.20	0.77	0.21	-0.15	-0.31	-0.26	-0.13
5	0.27	1.46	1.65	1.54	0.86	-0.40	-0.57	-0.47	-0.35	-0.24
6	0.23	1.22	1.50	1.40	0.92	0.00	-0.35	-0.34	-0.29	-0.16
7	0.25	1.05	1.18	0.96	0.37	-0.49	-0.71	-0.49	-0.40	-0.18
8	0.20	1.10	1.30	1.09	0.19	-0.02	-0.19	-0.31	-0.27	-0.12
9	0.22	1.45	1.56	1.36	0.79	-0.50	-0.68	-0.54	-0.37	-0.18
10	0.24	1.24	0.94	0.58	-0.09	-0.79	-1.19	-0.96	-0.57	-0.31
11	0.20	0.89	0.85	0.53	0.07	-0.62	-0.89	-0.73	-0.48	-0.19
12	0.24	0.98	1.04	0.74	0.30	-0.44	-0.73	-0.63	-0.37	-0.25
13	-0.06	0.10	-0.36	-0.66	-0.88	-1.17	-1.17	-0.90	-0.43	-0.25
14	-0.02	0.71	0.25	-0.14	-0.63	-1.20	**-1.35**	-1.11	-0.60	-0.27
15	0.14	1.08	0.77	0.42	-0.11	-0.76	-1.16	-0.91	-0.48	-0.28
16	0.16	0.73	0.71	0.33	-0.14	-0.61	-0.88	-0.81	-0.43	-0.20
19	-0.08	0.17	-0.34	-0.61	-0.83	-1.02	-0.95	-0.75	-0.42	-0.17
20	-0.04	0.28	-0.11	-0.39	-0.74	-1.01	-1.11	-0.90	-0.42	-0.22

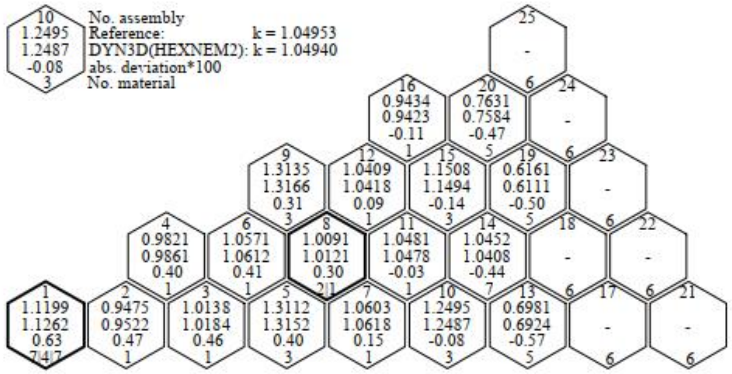

Fig. 2: HEXNEM2 - Absolute deviations of assembly powers P_i^{ass}

c) Overview

Table 5: Deviation of keff, maximum and averaged deviations of node and assembly powers for HEXNEM1 and HEXNEM2.

<table>
<tr><th>Title</th><th>Context</th><th>References</th><th>Participants</th><th>Summary</th></tr>
<tr><td></td><td></td><td></td><td></td><td>
<table>
<tr><th>Method</th><th>$\left|\Delta k_{eff}\right|$ (pcm)</th><th>$100 \cdot \max_i \left|\Delta P_i\right|$</th><th>$\frac{100}{N}\sum_{i=1}^{N}\left|\Delta P_i\right|$</th><th>$100 \cdot \max_i \left|\Delta P_i^{ass}\right|$</th><th>$\frac{100}{N_{ass}}\sum_{i=1}^{N_{ass}}\left|\Delta P_i^{ass}\right|$</th></tr>
<tr><td>HEXNEM1</td><td>41</td><td>4.03</td><td>1.09</td><td>2.04</td><td>1.07</td></tr>
<tr><td>HEXNEM2</td><td>13</td><td>1.73</td><td>0.59</td><td>0.63</td><td>0.31</td></tr>
</table>
Bibliography:
1. N.P.Kolev, R.Lenain, C.Fedon-Magnaud, “CRONOS Solutions of the AER 3D Benchmark for VVER-1000”, CEA Internal Report, Saclay, 1997.
2. N.P.Kolev, R.Lenain, C.Fedon-Magnaud, “AER-FCM-101 Benchmark Specification Sheet”, AER Benchmark Book, AEKI-KFKI (Hungary).</td></tr>
<tr><td>AER Benchmark Solution Sheet, Test ID: AER-FCM-101.
Nuclear Research Institute Rez plc 250 68 Rez, Czech Republic, 16.06. 2006
Jan Hádek</td><td>AER</td><td>http://aerbench.kfki.hu/aerbench/FCM101_solrez.doc</td><td>Nuclear Research Institute Rez plc, Fortum Nuclear Services Ltd</td><td>The document contains:
Short Description of Code DYN3D Version 3.2, Mathematical Model, Features of Techniques Used.
Known approximations:
- Neutronics:
Two group neutron diffusion theory.
Macroscopic cross sections spatially constant in a node.
Feedback dependence of macroscopic cross sections on burnup, fuel temperature, moderator temperature, moderator density and boron acid concentration in a node.
- Thermal-hydraulic:
One dimensional two phase-flow model in parallel coolant channels.
Four equations model (mass, momentum and energy balance equations of the mixture, mass balance equation of the vapour phase).
Constitutive laws for - frictional and local pressure losses, - heat transfer regime mapping including heat transfer correlations in different regimes and criteria for change of heat transfer regimes, - evaporation and condensation rate and consistent phase slip correlation, - mathematical formulation of the equations of state of water and steam including transport properties.</td></tr>
</table>

Title	Context	References	Participants	Summary
				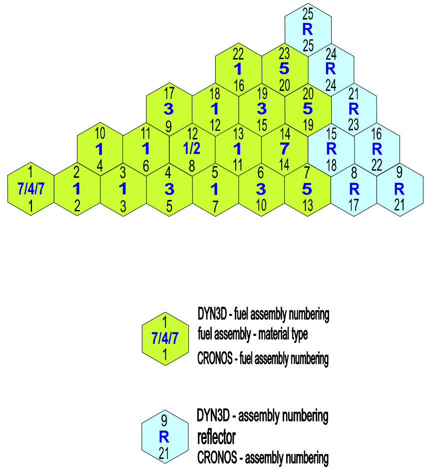 Fig. 1: Benchmark core configuration. DYN3D and CRONOS fuel or reflector assembly numbering **Comparison to Recommended Solution:** **Table 2: CRONOS reference solution** **Recommended reference solution taken from Table 2 of [1]** k_{eff} = 1.049526

Title	Context	References	Participants	Summary

CRONOS numbering Assembly	Normalized 3D power distribution Axial layer 1	2	3	4	5	6	7	8	9	10	Normalized assembly power
1	0.854	1.841	2.299	1.805	1.485	1.108	0.755	0.501	0.385	0.167	1.1199
2	0.627	1.358	1.746	1.693	1.426	1.052	0.709	0.459	0.285	0.119	0.9475
3	0.641	1.397	1.846	1.903	1.613	1.141	0.743	0.470	0.274	0.110	1.0138
4	0.623	1.355	1.781	1.821	1.546	1.112	0.732	0.466	0.274	0.111	0.9821
5	0.843	1.845	2.466	**2.581**	2.159	1.382	0.863	0.541	0.310	0.124	**1.3112**
6	0.673	1.471	1.961	2.045	1.720	1.148	0.728	0.457	0.263	0.105	1.0571
7	0.663	1.456	1.957	2.066	1.751	1.146	0.732	0.462	0.265	0.105	1.0603
8	0.675	1.480	1.985	2.089	1.739	0.916	0.566	0.356	0.204	0.081	1.0091
9	0.836	1.831	2.455	**2.581**	2.168	1.396	0.877	0.551	0.315	0.125	1.3135
10	0.732	1.608	2.169	2.307	2.023	1.490	1.006	0.644	0.370	0.147	1.2495
11	0.630	1.385	1.866	1.980	1.712	1.201	0.795	0.507	0.291	0.115	1.0481
12	0.632	1.389	1.870	1.981	1.703	1.178	0.772	0.491	0.281	0.112	1.0409
13	0.399	0.878	1.185	1.265	1.124	0.856	0.590	0.380	0.218	0.087	0.6981
14	0.602	1.321	1.783	1.902	1.685	1.273	0.873	0.562	0.323	0.128	1.0452
15	0.665	1.460	1.971	2.101	1.857	1.394	0.954	0.613	0.352	0.140	1.1508
16	0.545	1.199	1.617	1.724	1.523	1.142	0.780	0.502	0.288	0.114	0.9434
19	0.349	0.767	1.037	1.109	0.991	0.762	0.529	0.342	0.197	0.078	0.6161
20	0.432	0.950	1.283	1.372	1.227	0.944	0.657	0.425	0.244	0.097	0.7631

Table 3: DYN3D-CRONOS comparison

Δ k_{eff} = k_{eff} (DYN3D) - k_{eff} CRONOS) = -12 pcm

CRONOS numbering Assembly	(DYN3D-CRONOS)*100 Normalized 3D power distribution Axial layer 1	2	3	4	5	6	7	8	9	10	Normalized assembly power
1	0.110	**1.600**	1.540	1.490	1.050	0.620	0.160	0.030	-0.210	-0.220	**0.630**
2	0.210	1.150	1.480	1.040	0.750	0.430	-0.010	-0.100	-0.070	-0.080	0.470
3	0.160	1.010	1.370	1.290	0.920	0.320	-0.080	-0.160	-0.170	-0.070	0.460
4	0.120	0.950	1.320	1.140	0.770	0.260	-0.070	-0.220	-0.180	-0.100	0.400
5	0.200	1.330	1.510	1.450	0.860	-0.340	-0.470	-0.370	-0.270	-0.200	0.390
6	0.170	1.110	1.390	1.340	0.920	0.050	-0.280	-0.250	-0.220	-0.130	0.410
7	0.190	0.940	1.060	0.900	0.370	-0.450	-0.640	-0.410	-0.330	-0.150	0.150
8	0.140	0.990	1.180	1.020	0.180	0.020	-0.130	-0.240	-0.220	-0.090	0.280
9	0.150	1.320	1.420	1.280	0.790	-0.440	-0.590	-0.440	-0.290	-0.140	0.300
10	0.170	1.110	0.810	0.500	-0.100	-0.720	-1.080	-0.840	-0.480	-0.270	-0.080
11	0.150	0.790	0.740	0.460	0.070	-0.560	-0.810	-0.640	-0.400	-0.160	-0.030
12	0.190	0.870	0.930	0.670	0.300	-0.390	-0.650	-0.540	-0.300	-0.220	0.090
13	-0.100	0.030	-0.430	-0.700	-0.880	-1.130	-1.100	-0.830	-0.380	-0.230	**-0.560**
14	-0.080	0.610	0.150	-0.200	-0.630	-1.150	**-1.260**	-1.010	-0.520	-0.230	-0.430
15	0.080	0.970	0.650	0.350	-0.120	-0.700	-1.060	-0.800	-0.390	-0.240	-0.140
16	0.110	0.640	0.620	0.270	-0.140	-0.560	-0.800	-0.720	-0.360	-0.160	-0.110
19	-0.110	0.110	-0.400	-0.650	-0.830	-0.980	-0.890	-0.690	-0.370	-0.150	-0.500
20	-0.070	0.210	-0.180	-0.440	-0.740	-0.970	-1.040	-0.820	-0.360	-0.190	-0.460

Bibliography:

Title	Context	References	Participants	Summary
				1. U. Grundmann, U. Rohde, S. Mittag, S. Kliem: DYN3D Version 3.2 , Code for Calculation of Transients in Light Water Reactors (LWR) with Hexagonal or Quadratic Fuel Elements, Description of Models and Methods, Forschungszentrum Rossendorf, Institute of Safety Research, Germany, August 2005 2.. N.P. Kolev, R. Lenain, C. Magnaud: AER-FCM-101 Benchmark Specification Sheet, AER Benchmark Book, AEKI-KFKI, Hungary, 1999
AER Benchmark Specification Sheet, Test ID: AER-FCM-102 G. Alekova, R. Prodanova	AER	http://aerbench.kfki.hu/aerbench/FCM102.doc	IAE, UJV, AEKI	The test is a mathematical type test for solving the two-group diffusion problem without feed back. It is developed for determination of, 2D- and 3D power distributions in a 30^{o} sector of the WWER-1000 reactor core [1]. Five fictive assemblies with corresponding properties present the real radial reflector (RR). In axial direction the core is divided into 12 slices with thickness of 35.5 cm each. The first and the last slice are the top (TR) and the bottom (BR) reflector correspondingly. Fresh fuel core and equilibrium poisoning of Xenon and Samarium are considered in the test. Two variants of the test are presented (A and B), corresponding to different material composition of the core. Nine material types are considered in the sector loading. The necessary libraries of 4-group effective macroscopic cross sections have been generated by the codes NESSEL [2] and PREPAR [3]. Furthermore, by reduction of energy group and, if necessary, additional spatial homogenisation they are transferred by the code RADMAGRU [4] to prepare for each of the mentioned materials, files of 2-group effective neutron cross sections.

<table>
<tr><th>Title</th><th>Context</th><th>References</th><th>Participants</th><th>Summary</th></tr>
<tr><td></td><td></td><td></td><td></td><td>
Tab.3 Output format for solution
<table>
<tr><td rowspan="2">Ass. N
i</td><td colspan="10">$(k_V)_{ij}$</td><td rowspan="2">$(K_q)_i$</td></tr>
<tr><td colspan="10">Layer j</td></tr>
<tr><td>1</td><td>1</td><td>2</td><td>3</td><td>4</td><td>5</td><td>6</td><td>7</td><td>8</td><td>9</td><td>10</td><td></td></tr>
<tr><td>2</td><td></td><td></td><td></td><td></td><td></td><td></td><td></td><td></td><td></td><td></td><td></td></tr>
<tr><td>...</td><td></td><td></td><td></td><td></td><td></td><td></td><td></td><td></td><td></td><td></td><td></td></tr>
<tr><td>19</td><td></td><td></td><td></td><td></td><td></td><td></td><td></td><td></td><td></td><td></td><td></td></tr>
</table>
Tab.4 Output format for comparison
<table>
<tr><td rowspan="2">Ass. N
i</td><td colspan="10">$\delta(k_V)_{ij}$,%</td><td rowspan="3">$\delta(K_q)_i$
%</td></tr>
<tr><td colspan="10">Layer j</td></tr>
<tr><td>1</td><td>1</td><td>2</td><td>3</td><td>4</td><td>5</td><td>6</td><td>7</td><td>8</td><td>9</td><td>10</td></tr>
<tr><td>2</td><td></td><td></td><td></td><td></td><td></td><td></td><td></td><td></td><td></td><td></td><td></td></tr>
<tr><td>...</td><td></td><td></td><td></td><td></td><td></td><td></td><td></td><td></td><td></td><td></td><td></td></tr>
<tr><td>19</td><td></td><td></td><td></td><td></td><td></td><td></td><td></td><td></td><td></td><td></td><td></td></tr>
<tr><td colspan="12">Summary:</td></tr>
<tr><td colspan="4">$(\delta k_q)^{max}$</td><td colspan="8"></td></tr>
<tr><td colspan="4">$(\delta k_q)^{min}$</td><td colspan="8"></td></tr>
<tr><td colspan="4">$\overline{(\delta k_q)}$</td><td colspan="8"></td></tr>
<tr><td colspan="4">$\sigma(\delta k_q)$</td><td colspan="8"></td></tr>
<tr><td colspan="4">$(\delta k_V)^{max}$</td><td colspan="8"></td></tr>
<tr><td colspan="4">$(\delta k_V)^{min}$</td><td colspan="8"></td></tr>
<tr><td colspan="4">$\overline{(\delta k_V)}$</td><td colspan="8"></td></tr>
<tr><td colspan="4">$\sigma(\delta k_V)$</td><td colspan="8"></td></tr>
</table>
Bibliography:
1.In-Core Fuel Management Code Package Validation for VVERs. IAEA-TECDOC-847, November 1995.
2.G. Schulz, NESSEL-4 Version 6, K.A.B. AG, 1994
3.K.A.B. AG. Berlin, “Programme PREPAR - code manual”, 1996.
4.R. Prodanova. RADMAGRU - a code for transformation of libraries of effective constants of MAGRU type intended to assembly-wise and pin-wise calculations. BgNS Transactions, 1998 (in print).
</td></tr>
<tr><td>AER Benchmark Specification Sheet, Test ID: AER-HOM-101
Mihály Makai</td><td>AER</td><td>http://aerbench.kfki.hu/aerbench/HOM101.doc</td><td>KFKI , PARt, IAE</td><td>Test to verify homogenization and intra assembly flux reconstruction in a regular hexagonal lattice. The test models the geometry of VVER-1000 in 2D. The diffusion cross-sections are given in four energy groups. The goal is to test the assembly homogenization and the full core calculation. Furthermore, the reconstructed cell wise distribution can also be compared to the reference.
Output:</td></tr>
</table>

Title	Context	References	Participants	Summary
				a, Expected Results Primary results: keff, assembly wise power and flux distributions Secondary results: cell wise power and flux distributions b, Files, Format: none The recommended solutions have been obtained by finite difference programs using one point per cell. It was proposed two such solutions, one obtained by SNAP-3D, the other by MOBY DICK. Their results are summarized below. The power distributions are normalized so that in the central assembly the power is unity. The obtained eigenvalues: by SNAP-3D keff=1.133787, by MOBY-DICK keff=1.133759. The assemby averaged power distribution is given in Table 3. The last column may serve as the accuracy of the finite difference solution. Both reference solutions have been scanned from printed output, so they may contain unexpected errors. As to the MOBY DICK solution, the pin power distribution is also available. The normalization corresponds to 0.663 average power in the central assembly. The numbering of the pins starts at the left upper corner and goes from left to right. The results are in Figs. 3.a-3.r. The numbering within an assembly goes parallel with side NW-N and goes from W to E in a line and the lines go parallel with side NW-N, the last line is side S-SE. The last number belongs to corner SE. As to SNAP-3D, the pin power distribution is given only in two subareas. Subarea A includes a 60 deg sector of assembly No. 1 and the attaching 60 deg sector in assembly No. 2. The pin power distribution is given in Fig. 4a. Subarea B includes a 60 deg sector of assembly No. 16 determined by the centre of assembly No. 16 and the shared face between assemblies 16 and 20, and the attaching 60 deg sector of assembly No. 20.

Title	Context	References	Participants	Summary
Validation of coupled neutronic/thermal-hydraulic codes for VVER reactors. Final Report - FIKS-CT-2001-00166 S. Mittag, U. Grundmann, S. Kliem, Y. Kozmenkov, U. Rindelhardt, U. Rohde, F.-P. Weiß, S. Langenbuch, B. Krzykacz-Hausmann, K.-D. Schmidt T. Vanttola, A. Hämäläinen, E. Kaloinen, A. Keresztúri, G. Hegyi, I. Panka, J. Hádek, C. Strmensky, P. Darilek, P. Petkov, S. Stefanova, A. Kuchin,	FP5-VALCO Project	https://inis.iaea.org/collection/NCLCollectionStore/_Public/35/098/35098982.pdf?r=1	FZR, GRS mbH, VTT, AEKI, NRI , VUJE Trnava a.s., INRNE, SSTCNRS, SE, a.s. EBO, SE, a.s.EBO, KI, Serco Assurance	A major objective of VALCO was to study the ability of codes to model the NPP behaviour in different types of transients. For this reason in work package 1 (WP 1), the existing data base, containing already measured VVER transient data from the former EU Phare project SRR-1/95, has been extended by five new transients. Two of these transients 'Drop of control rod at nominal power at Bohunice-3' of VVER-440 type and 'Coast-down of 1 from 3 working MCPs at Kozloduy-6' of VVER-1000 type, were then utilised for code validation. Eight institutes contributed to the validation with ten calculations using five different combinations of coupled codes. The thermal-hydraulic codes were ATHLET, SMABRE and RELAP5 and the neutron kinetic codes DYN3D, HEXTRAN, KIKO3D and BIPR-8. The general behaviour of both the transients was quite well calculated with all the codes. In VALCO work package 2 (WP 2), the usual application of coupled neutron-kinetic / thermal-hydraulic codes to VVER has been supplemented by systematic uncertainty and sensitivity analyses. A respective method was applied to the two transients studied earlier in SRR-1/95: A load drop of one turbo-generator in Loviisa-1 (VVER-440), and a switch-off of one feed water pump in Balakovo-4 (VVER-1000). Results of SRR-1/95 coupled code analyses led to the objective to separate neutron kinetics from thermal-hydraulic feedback effects. Thus, in VALCO work package 3 (WP 3) stand-alone three-dimensional neutron-kinetic codes have been validated. Measurements carried out in an original-size VVER-1000 mock-up (V-1000 facility, Kurchatov Institute Moscow) were used for the validation of the codes DYN3D, HEXTRAN, KIKO3D and BIPR-8. The significant neutron flux tilt measured in the V-1000 core, caused only by radial-reflector asymmetries, was successfully modelled. A good agreement between calculated and measured steady-state powers has been achieved, for relative assembly powers and inner-assembly pin power distributions. Calculated effective multiplication factors exceed unity in all cases. The time behaviour of local powers, measured during two transients that were initiated by control rod moving in a slightly super-critical core, has been well simulated by the neutron-kinetic codes. In VALCO WP 3, the stand-alone neutronic codes have been successfully validated against V-1000 (zero power) measurements. The effect of a strong

Title	Context	References	Participants	Summary
V. Khalimonchuk , P. Hlbocky , D. Sico, S. Danilin, V. Ionov, S. Nikonov, D. Powney				steady-state radial power tilt, measured in the V-1000 core, is described by all codes, when the real boundary conditions (albedos) are applied. These albedos are based on the accurate reflector model, including different water gap widths between fuel assemblies and steel baffle. The powers calculated for the central pins give better agreement with measurements than the node- averaged values, particularly for nodes with control rods inserted. The pin power calculation for assembly 85 is in good agreement with measured pin power distributions. The effective multiplication factor was over-estimated in all calculations by (0.5 … 1.7) %. One reason may be in the error of the boric-acid concentration measurement, which leads to an uncertainty of ± 0.6 % in k-eff. Another source of uncertainty can be errors in the two-group diffusion parameters for the very low operation temperatures in the V-1000 facility. Code validation against experiments is always complicated by measurement errors. For this reason, the nodal diffusion (neutronic) codes, applying homogenized two-group parameters have been additionally verified against a heterogeneous multi-group transport-theory benchmark, which can be considered an "ideal experiment" being clear of any measurement uncertainties. This benchmark test was successful and in accordance with the steady-state validation results. The features that make the Kozloduy VVER-1000 transient interesting, such as lowered power and flow reversals in the loops, also proved to be difficult both for data collection and for modelling. In the comparison of the core outlet temperatures, a linear dependency was found between the assembly power and the difference between measured and the calculated temperatures. The dependency could possibly be explained by a bypass flow through the bundle central tube. Furthermore, in the Kozloduy calculations the initial fuel temperatures and the temperature changes during the transient vary remarkably between the different codes. This supports the conclusion of the previous SRR-1/95 project that more accurate fuel models are needed in the codes. Concerning the first V-1000 transient experiment, where one single control rod cluster was moved, it can be stated that all combinations of neutron-kinetic codes and two-group- parameter libraries successfully simulate the time behaviour of the measured relative power densities (micro fission chambers) and fast-neutron

Title	Context	References	Participants	Summary
				fluxes (ionisation chambers). The rod worth, calculated for the single cluster as the difference in k-eff for this cluster totally inserted and totally withdrawn, is close to the asymptotic value of the measured and calculated dynamic reactivity. Regarding the second transient experiment, a scram with one stuck cluster being later inserted, the calculated results are also close to the detector signals, taking into account the greater statistical errors of the measurement in the scrammed reactor. The validation against measurements in the Moscow V-1000 facility has demonstrated that the neutron-kinetic codes are suitable for the calculation of power distributions and power changes caused by control rod movements in a real VVER-1000. Pin power recovery is necessary to describe the central-channel measurements in strongly heterogeneous fuel assemblies. To cope with the over-estimation of the effective multiplication factor, some adjustment of two-group diffusion parameters may be necessary in practical VVER-1000 calculations.
Validation of coupled neutron kinetic/thermal-hydraulic codes. Part 1: Analysis of a VVER-1000 transient (Balakovo-4), Annals of Nuclear Energy 28 (2001) 857-873 S. Mittaga, S. Kliema, F.P. Weißa, R. Kyrki-Rajamaki, Hamalainen, S. Langenbuch,	EU Phare Project SRR1/95	https://www.researchgate.net/publication/260087946_Validation_of_Coupled_Neutron_KineticThermal-Hydraulic_Codes_Part_1_Analysis_of_VVER-1000_Transient_Balakovo-4	FZR, VTT, GSR, KI, NRI, AEKI-KFKI, STCNRS, INRNE	Three-dimensional hexagonal reactor dynamic codes have been developed for VVER type reactors and coupled with different thermal-hydraulic system codes. In the EU Phase project SRR1/95 these codes have been validated against real plant transients by the participants from several countries. Data measured during a test in the Balakovo-4 WWER-1000 have been analyzed by coupled codes. In the test, one of two working feed water pumps of the steam generators was switched off at nominal power. The steady-state assembly powers measured before and after this transient are reproduced by the codes with a maximum deviation of about 5%. The time behavior of the most safety-relevant parameters, such as total fission power, coolant temperatures and pressures is well modeled. Thermal-hydraulic feedback effects observed in the measurement are described by the codes in a consistent manner. Conclusions: Generally, the physical behavior of the Balakovo-4 VVER-1000, especially of the core and the primary circuit is well described by the coupled codes involved. A good agreement between calculated and measured safety-relevant parameters has

Title	Context	References	Participants	Summary
S. Danilin, J. Hadek, G. Hegyi, A. Kuchin, D. Panayotov				been achieved. The interaction between neutron kinetics (neutron power) and thermal hydraulics that can be observed in the measurement is modelled in a consistent manner by all coupled codes involved.

				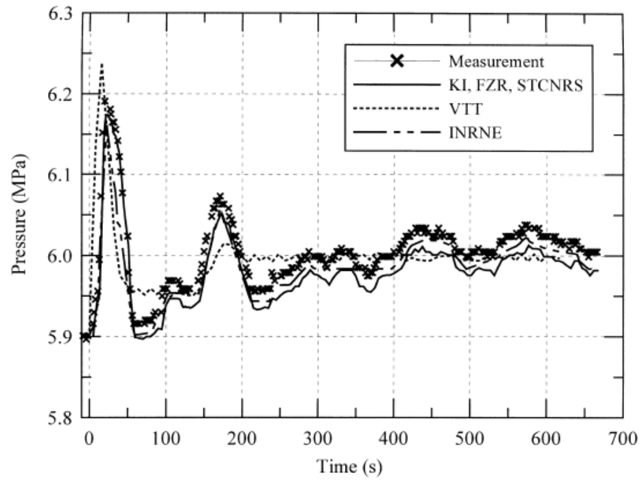 Fig. 6. Main steam header pressure. 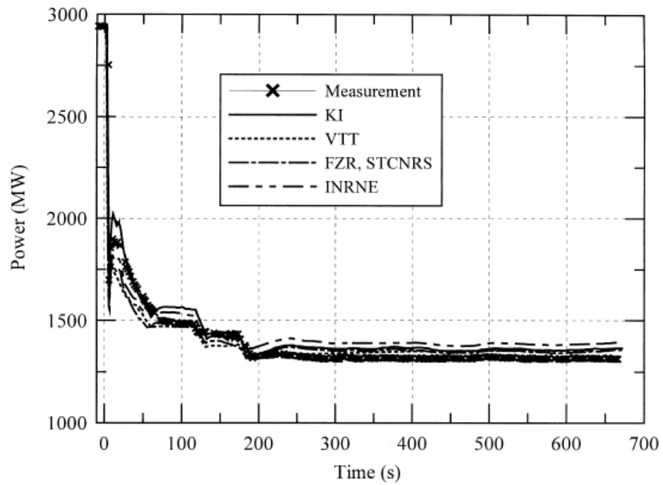 Fig. 7. Nuclear power. The deviation between calculated and measured primary pressure can be explained by uncertainties in the measurement, i.e. the lack of information on the real pressurizer heater operation.

Title	Context	References	Participants	Summary
				The calculated fuel temperature has turned out to be sensitive to the modeling of the gas gap between fuel pellets and rod cladding. Hence, a dynamic treatment of the gap width is necessary.
Development of CrossSection Library for DYN3D Code. I. Ovdiienko, M. Ieremenko, A. Kuchin, V. Khalimonchuk		http://dspace.nbuv.gov.ua/handle/123456789/97633		The DYN3D code is widely used at SSTC NRS in licensing activities both for steady-state calculations in reviews of safety substantiation for fuel reloading and transient calculations for emergency modes of WWER reactors of Ukrainian NPPs. Since 2006 SSTC NRS has been using the modern spectral HELIOS code for preparation of few-group cross-section libraries instead of the out-of-date one-dimensional NESSEL code. It allowed SSTC NRS to increase the accuracy in calculations of the entire complex DYN3D/cross-section library. But, there is an actual problem choosing the appropriate approach to implement the cross-section library into the DYN3D code. The paper overviews the application of approaches used by SSTC NRS, such as a multidimensional table and polynomial dependences. Results with use of the basic parameterization of cross-sections are quite acceptable besides the reactivity coefficient on moderator temperature; particularly on hot zero power states where it shows low absolute values and relative errors more than 100 %. The significant drawback of the basic cross-section library parameterization is the impossibility to use discontinuity factors. The use of discontinuity factors for WWER-1000 fuel assemblies does not have a significant effect. However, the cross-section for the radial reflector without discontinuity factors gives too high discrepancy in power distribution that can reach up to 10 % for peripheral assemblies. This occurs because the HELIOS library for fuel assemblies uses old parameterization for the radial reflector in which cross-sections were additionally adapted by auxiliary program for application without discontinuity factors. The parameterization was improved by adding the third-order polynomial dependence of moderator density β3 and boron acid concentration δ3. Additionally, the linear dependence of change in the moderator density with parameterization coefficients on boron acid concentration was introduced. The third-order polynomial dependence on fuel burnup. The improved basic cross-section library parameterization allowed a slight increase in the accuracy of calculating the boron concentration and axial power

Title	Context	References	Participants	Summary
				distribution. However, the reactivity coefficient on moderator temperature remained unsatisfactory. Further elaboration of the basic cross-section parameterization consisted in introducing the discontinuity factors and pin power distributions from the spectral code with the possibility to increase the calculation accuracy and extend the capabilities of DYN3D code. The new cross-section library was prepared for WWER-1000 based on the OECD/NEA and U.S. NRC PWR MOX/UO2 core transient benchmark. This is a five-dimensional table of cross- section with dependence on burnup, moderator density, boron concentration, fuel and moderator temperature. Use of the multidimensional table cross-section library (with chosen parameters of branches) increases the accuracy of calculating neutron-physical characteristics of reactor core in comparison with the parameterization form of library, first of all accuracy of reactivity coefficient on moderator temperature at HZP. It also covers the whole range of changes in core thermal-hydraulic parameters both for normal operation (hot and cold states) and for accidents with admissible accuracy. But, the use of multidimensional table library significantly increases the DYN3D calculating time — by approximately three times. Moreover, in some calculating cases, the iterations were not converged in contrast to the library with improved parameterization under the same convergence parameters. In addition, the model development and cross-section preparation for the WWER-1000 radial reflector taking into account discontinuity factors are discussed. Introduction of advanced cross-sections for the radial reflector increases the accuracy of power distribution for peripheral assemblies and decreases its maximal discrepancy near the core center. The accounting of spectral effect increases the calculation accuracy both for axial profile and for boron acid concentration and agrees with results of other approaches to spectral effect accounting.
DEVELOPMENT OF A THREE-DIMENSIONAL MODEL OF THE VVER-1000		https://www.researchgate.net/publication/342074824_DEVELOPMENT_OF_A_THREE-		The purpose of this work is to investigate the use of the new Monte Carlo Serpent code for the three-dimensional calculation of the VVER-1000 reactor core. Features of modeling of geometry of fuel assemblies , core and fence in the Serpent code are considered. The first simulation results in the developed three-dimensional model of the core are presented.

Title	Context	References	Participants	Summary
REACTOR USING SERPENT MONTE CARLO CODE FOR NEUTRON-PHYSICAL MODELING. V. Gulik, PhD,V. Galchenko, PhD, I. Shlapak, D. Budik		DIMENSIONAL_MODEL_OF_THE_VVER-1000_REACTOR_USING_SERPENT_MONTE_CARLO_CODE_FOR_NEUTRON-PHYSICAL_MODELING		For the first load of RivneNPP-4, four types of fuel assemblies were modeled: 16FL, 30FL, 42FLB, 44FLB. The Serpent code has the ability to construct the geometry of fuel assembly with the upper and lower reflectors using the so-called “vertical stack”. The lower reflector has a height of 23.1 cm from the lower surface of the fuel. The reflector is divided into six different layers and covers the ends of the fuel elements, the lower grate, part of the bottom nozzle of the fuel assembly and part of the sup- port cylinder. The top reflector has a height of 29.4 cm from the upper surface of the fuel to the bottom nozzle of the fuel assembly. The reflector is divided into five different layers and covers the ends of the fuel elements and the two upper spacer grids. 13 spacer grids that fit into the fuel part evenly smeared on the surfaces of the fuel elements, central tube and guide channels. Fig. 3 shows a horizontal section of the first core loading Rivne NPP-4, and Fig. 4 shows a vertical section of the first core loading Rivne NPP-4. The core zone model was developed in such a way that it could be used to calculate the boundary conditions for the ImCore deterministic code, which is being developed by PJSC JSC “Impulse” for the needs of the Ukrainian NPP incore monitoring systems. The boundary conditions are planned to be calculated in two variants: 1) Coefficients of the albedo (the ratio of neutron currents to the boundary of the active zone – reflector); 2) group constants for two rows of hexagonal prisms (with a turnkey size similar to a fuel assembly) surrounding the core and including the reactor wall. The obtained modeling result suggests that the developed model of the VVER-1000 reactor core is suitable for neutron-physical calculations. Fig. 1 shows the so-called mesh rendering of the Serpent code for Rivne NPP-4 first loading, where warm tones (red-yellow) reflect “fission reaction density” and cold tones (blue and white) reflect “scattering reaction density”. The modeling of the core zone in the Serpent code for the 28th loading of SUNPP3 was per- formed for the purpose of the albedo coefficients used to determine the boundary conditions in the InCore deterministic code, which is being developed by PJSC JSC “Impulse” for the needs of the Ukrainian NPP in-core monitoring systems. A model for Rivne NPP-4 was used to develop the model of the SUNPP-3 core. Westinghouse production facilities were used for the 28th loading of SUNPP-3.

Title	Context	References	Participants	Summary
				As a result of Serpent simulation, albedo coefficients can be obtained for each of the 90 lateral faces of the core, albedo coefficients for different types of symmetry, and albedo coefficients for the upper and lower reflectors both for the entire core and for each of the 163 fuel assemblies. The obtained data allow us to set the boundary conditions for the ImCore deterministic code with high accuracy, which will allow to increase the accuracy of the calculation of the basic neutron- physical characteristics in the in-core monitoring system. 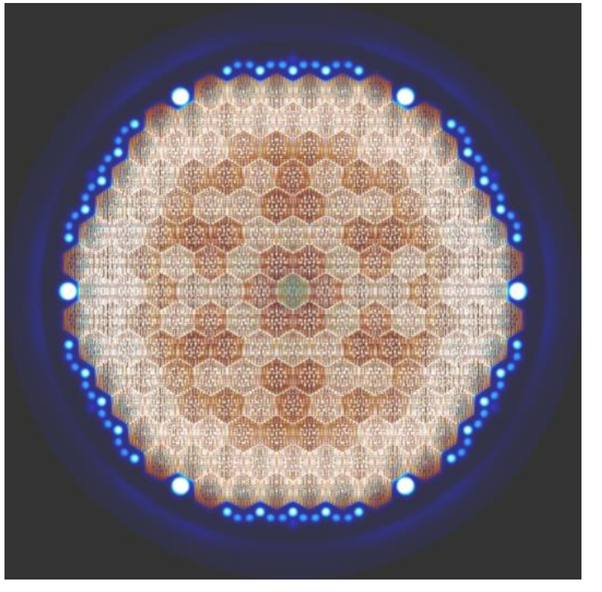 Fig. 1. Serpent mesh visualization of the horizontal section of the core
Explicit decay heat calculation in the nodal diffusion code DYN3D Y. Bilodid, E. Fridman, D. Kotlyar, E. Shwageraus		https://www.researchgate.net/publication/316510818_Explicit_decay_heat_calculation_in_the_nodal_diffusion_code_DYN3D		Simulation of residual decay heat is important for the analysis of accident scenarios such as loss of coolant, main steam line break, station blackout, etc. The decay heat of spent fuel is also an important parameter for the design and analysis of facilities such as spent fuel storage pools, transportation systems, intermediate spent fuel storage and final disposal sites. The residual decay heat is produced by a radioactive decay of nuclides which could be subdivided into two main groups (Tobias, 1980): - fission products and nuclides produced by the neutron capture in fission products, - actinides produced by the neutron capture in heavy metals.

Title	Context	References	Participants	Summary
				This paper describes a new general decay heat calculation model implemented in DYN3D. The radioactive decay rate of each nuclide in each spatial node is calculated by recently implemented depletion module and the cumulative released heat is used to obtain the spatial distribution of the decay power for every time step. Such explicit approach is based on first principles and is free from approximations and, thus, can be applied to any reactor system (e.g. thermal and fast) and fuel type. The proposed method is verified through code-to-code comparison with the Serpent 2 Monte Carlo code results. Numerous methods of the decay heat calculation have been developed and mainly utilize the following two approaches or their combination: • the actual concentration of each relevant radioactive nuclide is calculated explicitly. Then, the decay heat is obtained as a sum over all nuclide decay rates multiplied by their corresponding energy released in each decay branch. • the time-dependent decay heat power produced by fission products of main fissile nuclides is described by a set of semi-empirical exponential fits (or lump Decay Heat Precursors). The decay constants and weight coefficients of each exponent are evaluated based on assumptions regarding reactor spectra (e.g. light water reactors - LWR) and operational power history (power pulse or long-term constant power operation). This work proposes an explicit approach to calculate the decay heat power and describes its recent implementation in time-dependent nodal diffusion code DYN3D. This method relies on “first principles” – it utilizes detailed information on each nuclide concentration in the fuel and does not require approximations or assumptions regarding the initial fuel composition and its evolution with burnup. In order to demonstrate the validity of the method, a code-to-code verification is performed against the Serpent code. The method explicitly accounts for the heat from the decay of each nuclide in the fuel. Detailed nuclide content, required for the decay heat estimation, is calculated by DYN3D using recently implemented micro-depletion solver, while taking into account the local operational history of each node. The presented

Title	Context	References	Participants	Summary
				method is more computationally expensive than methods based on the decay heat standards, but it is based on “first principles”, does not involve any assumptions about the fuel content or operational history and, therefore, its applicability is not restricted to any particular fuel type. It is important to emphasize that high fidelity decay heat calculations typically require coupled Monte Carlo depletion codes (e.g. Serpent), which are computationally expensive because they require multiple neutron transport solutions. In this work however, the transport solution is replaced by a computationally efficient multi-group diffusion solution that allows predicting the 3-dimensional decay heat generation with only modest computational requirements. The presented method was applied to a number of 2D infinite lattice test cases with thermal spectrum PWR UOX, MOX and TOX fuel, VVER UOX fuel with burnable absorber as well as fast spectrum SFR MOX fuel and was verified against reference Serpent solutions. The test cases have demonstrated a notable dependence of the decay heat on the fuel initial composition and burnup operational history. In all test cases, the deviation of DYN3D decay heat from Serpent 2 reference stayed within 1%. This indicates that DYN3D is able to accurately estimate the decay heat power distribution during burnup and shutdown periods for a wide range of reactor systems. Future work will be focused on testing the method in realistic full core cases as well as depletion system compression and performance optimization.
Power coefficient of reactivity: definition, interconnection with other coefficients of reactivity, evaluation of results of transients in power nuclear reactors		https://www.researchgate.net/publication/329194916_Power_coefficient_of_reactivity_definition_interconnection_with_other_coefficients_of_reactivity_evaluation_of_results_of_transients_in_power_nuclear_reactors		There exist well-known problems in the use of nuclear reactors in the manoeuvrable operation mode, which include the task shared by all types of nuclear reactors. It is advisable to have a unified indicator weakly power-dependent and fairly easy to measure, which would make it possible to formulate the judgement about the nature of the transient processes within the entire power range and to assess the reactivity required for changing the power level by the preset value. Power reactivity coefficient (PRC) can be used as such indicator. The purpose of the present study is to investigate dependence of PRC on the temperature reactivity effects and on the technological parameters associated with the steady-state control program of the power unit, using the example of VVER-1000. Analysis was made of existing definitions and under- standing of PRC in relevant references. It turned out that there is no generally accepted definition of

Title	Context	References	Participants	Summary
Yury A. Kazansky, Ya.V. Slekenichs				the PRC. Based on the performed study, the following definition was suggested: the PRC is the ratio of the low reactivity introduced into the reactor to the power increment at the end of the transient process. It is assumed here that variation of reactivity is dependent on the energy released in nuclear fission but is not related to the changes of reactivity induced by feedback signals in the automatic reactor power control system. Analysis of the relationship between the PRC and temperature coefficients and technological parameters associated with the steady-state control program was performed taking the above suggested definition into account. Calculation code was written in SciLab environment for estimation of PCR dependences for widely spread SCPs during operation with four, three and two cooling loops of the primary cooling circuit representing for the example of VVER-1000 under typical assumptions for reactor core models with lumped parameters: • Half-sum of coolant temperatures at the reactor inlet T_{ci} and outlet T_{co} is accepted as the average coolant temperature; • There is no non-uniformity of coolant flow rate and energy output in the reactor core; • Parabolic distribution of fuel temperature in the fuel pin is valid, i.e. mean fuel temperature exceeds the external temperature of the fuel rod by the value equal to two thirds of the maximum temperature differential inside the fuel rod. Analysis of the obtained calculated dependences demonstrates that specific operational conditions of the power unit, including the preset SCP and operation of OLD, affect the PCR value and its dependence on the reactor power. For instance, SCP with constant average coolant temperature in the reactor weakens PER because temperature effect of coolant is practically neutralized. For constant coolant flow rate in the primary cooling circuit dependence of PCR on power is fairly weak and does not exceed 10% within the whole range of its variation, which is comparable with accuracy of the performed calculations of heat exchange in the reactor core. Therefore, PCR can be regarded in the first approximation as constant and not dependent on the reactor power. Reduction of coolant flow rate due, for

Title	Context	References	Participants	Summary
				instance, to the operation of the old system, results in the increase of PCR absolute value which, in turn, increases self-regulation properties of the reactor and produces favorable effect on the power unit safety. More noticeable variation of PCR (about 40%) takes place when SCP is changed, for instance, in the case of transition from SCP with constant steam throttle pressure to SCP with constant average coolant temperature in the reactor core. This fact must be taken into account in constructing combined SCPs, because change of set- tings of automatic control devices such as APC may be required.
Solution of Point Reactor Neutron Kinetics Equations with Temperature Feedback by Singularly Perturbed Method Wenzhen Chen, Jianli Hao, Ling Chen, and Haofeng Li		https://www.researchgate.net/publication/258391643_Solution_of_Point_Reactor_Neutron_Kinetics_Equations_with_Temperature_Feedback_by_Singularly_Perturbed_Method		The analysis of variation of neutron density (or power) and reactivity with time under the different conditions is an important content of nuclear reactor physics or neutron kinetics. Some important achievements on the super- critical transient with temperature feedback with big ($\rho 0 > \beta$) or small ($\rho_0 < \beta$) reactivity inserted have been approached through the effort of many scholars. In present work, the singularly perturbed method (SPM) is proposed to obtain the analytical solution for the delayed supercritical process of nuclear reactor with temperature feedback and small step reactivity inserted. The variation law of power, reactivity, and precursor density with respect to time at any level of initial power is obtained by the singularly perturbed method (SPM). The PWR with fuel 235U is taken as an example with parameters $\beta = 0.0065$, $l = 0.0001$ s, $\lambda = 0.0774$ 1/s, Kc =0.05 K/MW·s, and $\alpha = 5 \times 10{-}5$ 1/K. The relation between the reactivity and time is derived. Also, the neutron density (or power) and the average density of delayed neutron precursors as the function of reactivity are presented. The variations of neutron density (or power) and temperature with time are calculated and plotted and compared with those by accurate solution and other analytical methods. It is shown that the results by the SPM are valid and accurate in the large range and the SPM is simpler than those in the previous literature. All the results are compared with those obtained by the numerical solution which tend to the accurate solution under very small time step size. It is proved that the SPM is correct and reliable and is simpler than the analytical methods by the related literature.

Title	Context	References	Participants	Summary
				Can be concluded that very good results cannot be obtained by the precursor prompt jump (PrPJ) method to calculate the delayed supercritical progress with small step reactivity and temperature feedback. For small step reactivity, the results by the small parameter (SmP) method are close to those by the power prompt jump (PPJ) method and are better than those by the precursor prompt jump (PrPJ) method, but the accuracy of results by the small parameter method decreases with the increase of the reactivity inserted. The power is negative when the small parameter method is used to calculate the transient process in the vicinity of prompt supercritical state. The small parameter method is more suitable for the calculation of reactivity and temperature increase than for that of power. The results are quite precise using the power prompt jump (PPJ) method for the delayed supercritical process, but the main problem compared to the accurate solution is that some displacement exists along time axis. Furthermore it should be pointed out that each power peak value obtained by the precursor prompt jump (PrPJ) method, power prompt jump (PPJ) method, or small parameter (SmP) method is lower than that obtained by the accurate solution or singularly perturbed method (SPM). The temperature prompt jump method (TPJ) and the singularly perturbed method (SPM) in this paper are the two most precise methods for the delayed supercritical process with small step reactivity and temperature feedback. The reactivity inserted increases to the vicinity of prompt supercritical process, the total discrepancy of power by the TPJ method is larger than that by the SPM or PPJ method, and the irrelevant phenomena that the power jumps at first and then decreases monotonously from the peak will appear in the TPJ method.
Validation of Pin Power Calculations Using DYN3D on MIDICORE Benchmark Kuchyn O., Ovdiienko I.,		https://nuclear-journal.com/index.php/journal/article/download/170/166/		The MIDICORE calculation benchmark was presented on the 20th Symposium of AER by Mr. P. Mikolas . It is based on the calculation of restricted part of the VVER-1000 core in cold state. Proposed benchmark consists of fresh fuel assemblies surrounded by real VVER-1000 radial reflector. The reflection boundary conditions are used in axial directions. MCNP-4C Monte Carlo computer code and ENDF/B6 cross-section library were used to obtain benchmark solution. The main issue of MIDICORE benchmark is to provide the reference solution for validation of pin-by-pin power distribution at the VVER- 1000 reactor

Title	Context	References	Participants	Summary
Khalimonchuk V., Ieremenko M.				core periphery calculated by few-group diffusion codes. The MIDICORE benchmark objectives are: • Keff calculation; • Assembly-wise power distribution; • Pin-by-pin power distribution in FA No. 6 (A200), FA No. 7 (P36E9), FA No. 9 (P40E9). In accordance with MIDICORE benchmark description, input file for DYN3D calculation was developed. To find neutron flux distribution inside the nodes, two different approximations are used in DYN3D. The first one is HEXNEM1 method in which the nodes are coupled only by the averaged fluxes and currents at the hexagon sides. In the second approximation, side-averaged and corner- point values of fluxes and currents are used for the coupling of nodes for flux definition (HEXNEM2). In that way, HEXNEM2 method additionally includes the corner points in comparison with HEXNEM1 method and uses functions that are more exponential in the flux expansion. The main difference of the HEXNEM3 method is the additional use of tangentially weighted exponential functions and the coupling of neighboring nodes by tangentially weighted fluxes and currents on node surfaces. Hence, one should expect that HEXNEM3 is more accurate method than HEXNEM1 and HEXNEM2. To model MIDICORE reflector, two-group diffusion cross- section sets and RDF values were used for real geometry of VVER-1000 reflector. These sets were obtained by P. Petkov using HELIOS and MARIKO codes. DYN3D does not allow modeling reflection boundary conditions in 60º symmetry of reactor core (only rotational symmetry is possible). At the outer boundary of reflector, the vacuum boundary conditions are put. The reflection boundary conditions are used in axial direction. Results of calculations and Conclusions • HEX NEM1/HEX NEM2/HEX NEM3 methods implemented in DYN3D code predict the calculation of effective multiplication factor for MIDICORE benchmark with the accuracy 520/640/580 pcm, respectively.

Title	Context	References	Participants	Summary
				• HEXNEM1/HEXNEM2/HEXNEM3 methods yield mean square deviation from benchmark solution for assembly-wise power distribution 0.56 % / 1.36 % / 0.67 %, respectively. • HEXNEM2 method yields more accurate calculation of pin-by-pin power distribution for non-periphery fuel assembly (A200) in comparison with HEXNEM1 method. • For periphery fuel assemblies (P36E9 and P40E9), more great deviations of pin-by-pin power calculation are observed compared with non-periphery fuel assembly. Maximal deviation in pin power distribution is observed in the area of fuel assembly close to the radial reflector.

Table 2-1 presents an overview and summary of the main collected published materials available to the International Community (IAEA, OECD/NEA, past European projects, publications, etc.), relevant to the project, aimed to provide general information for VVER reactors and VVER experimental and benchmark data for verification and validation of neutronics and thermal-hydraulics codes. Previous works were considered to provide the information useful for the database establishing for next phases of the CAMIVVER project.

The X2 benchmark [2], [3], [4] proposed for validation and verification of the reactor physics code systems for VVER-1000 reactors (the Unit 2 of the Khmelnytska NPP in Ukraine) with loadings of TVSA fuel assemblies was considered to provide very useful information for validating and verifying the whole system of codes and data libraries for reactor physics calculations including fuel assembly modelling, fuel assembly data preparation, few group data parametrisation and reactor core modelling. The X2 benchmark provides a set of operational data for comparisons with steady state reactor core burnup calculations and transient neutron kinetics calculations and comprises all stages of steady state and transient reactor calculations starting with the fuel assembly data preparation. Thus, the X2 benchmark provides valuable information for the CAMIVVER project, especially for WP4 and WP5.

Other important report - "Benchmarks for Uncertainty Analysis in Modelling (UAM) for the Design, Operation and Safety Analysis of LWRs - Volume I" [16] that presents benchmark specifications for Phase I (Neutronics Phase) of the of the OECD LWR UAM benchmark would provide useful information for the work planned in WP4 and WP5 due to the exercises performed: "Cell Physics" focused on the derivation of the multi-group microscopic cross-section libraries and their uncertainties; "Lattice Physics" focused on the derivation of the few-group macroscopic cross-section libraries and their uncertainties and "Core Physics" focused on the core steady-state stand-alone neutronics calculations and their uncertainties.

One of the main sources of information, considered as very important to the activities in the project, is the VVER-1000 Coolant Transient Benchmark (V1000CT) [7, 8, 9, 10] consisted of two parts: V1000CT-1, which is a simulation of the switching on of one main coolant pump (MCP) when the other three MCPs are in operation; and V1000CT-2, which is a calculation of coolant mixing experiments and a main steam line break (MSLB) transient. V1000CT Benchmark provides data and information relevant to the selected in the CAMIVVER project nuclear power plant transients and thus adresses mainly WP6 and WP7 but provides information for WP4 and WP5 as well.

In parallel with the above-mentioned benchmarks, Table 2-1 summarizes a number of published works referring to codes verification and validation that provide useful information for different work packages.

In addition, different types of tests relevant to the CAMIVVER project were considered, as for example thermal hydraulic tests for validation of VVER-1000 for LOCA and transient compiled in the Report by the OECD Support Group on the VVER Thermal-Hydraulic Code Validation Matrix [22] deals with an internationally agreed experimental test facility matrix for the validation of best estimate thermal-hydraulic computer codes applied for the analysis of VVER reactor primary systems in accident and transient conditions; VVER-Related OECD projects including the PSB Project and main characteristics of the PSB facility [23], LB-LOCA Transient in PSB-VVER facility presents PSB facility and the tests[24]; critical heat flux (CHF) tests [25], [26], [27] and for neutronics tests - some tests by AER working group for VVER reactors [28 – 33].

3. Technical description and design serial reactor V-320

The main parameters of the core are shown in Table. 3-1.

Table. 3-1 - Operational limits on the technological parameters of the control unit in the state of "Operation at the power»

№ p/p	Parameter name	Parameter value with the number of operating MCPs			
		4	**3**	**2 opposite**	**2 related**
1	The maximum permissible thermal power of the reactor, taking into account the accuracy of its maintenance by the control system	(100+2)% N_{nom} 3060 MW	(67+2)% N_{nom} 2070 MW	(50+2)% N_{nom} 1560 MW	(40+2)% N_{nom} 1260 MW
2	Thermal power of the reactor set (permitted), no more	100% N_{nom} 3000 MW	67% N_{nom} 2010 MW	50% N_{nom} 1500 MW	40% N_{nom} 1200 MW
3**	Maximum permissible heat output of a single loop	770 MW			
4	Maximum allowable heating of the coolant in the reactor	30..7°C	26.0 °C	25.0 °C	25.0 °C
5	Maximum permissible heating of the heating agent in the loop	31.5 °C	28.0 °C	27.0 °C	27.0 °C
6	Heating of the coolant at fuel assemblies, no more:				
	– for TVSA without thermometric head without AE;	39.0 °C	36.0 °C	41.0 °C	41.0 °C
	– for TVSA without thermometric head with AE;	42.0 °C	39.0 °C	44.0 °C	44.0 °C
	– for TVSA with a thermometric head.	44.0 °C	41.0 °C	46.0 °C	46.0 °C
7	Neutron power (EP actuation setpoint)	107% N_{nom}	77% N_{nom}	60% N_{nom}	50% N_{nom}
8	The neutron output (Power limit controller actuation setpoint)	102% N_{nom}	69% N_{nom}	52% N_{nom}	42% N_{nom}
9	Coolant pressure above the core reactor	от 158 до 162 kgf/cm^2			
10	Maximum allowable coolant temperature at the reactor inlet in any of the operating loops	288 °C			
11	Average temperature of coolant at the outlet of the reactor, no more	320 °C			
12	Coolant level in Pressurizer, within	H_{nom} ($T_{1k\ medium}$) ±150 мм			

№ p/p	Parameter name	Parameter value with the number of operating MCPs			
		4	3	2 opposite	2 related
13	Steam pressure in the working SG, within	от 60 до 64 kgf/cm^2			
14	Feed water level in SG, within	*H_{nom} ±50 мм			
15	Temperature of feed water to SG, not less	160 °C			
16	Non-uniformity coefficient of energy release ***, no more	$K_{q\ perm}$ = 1.35 (for N = 100 % N_{perm})			

Notes.

1 At current power values ($N_{current}$) less acceptable (N_{perm}) permissible values of the coefficients of non-uniformity of energy release over the core volume ($K_{vi\ current}{}^{perm}$) should not exceed the value $K_{vi\ perm} \cdot \Psi$, where

$$\Psi = 1/(0{,}83 \cdot N_{current} / N_{perm} + 0.17) \text{ for power } N_{current} = (0.0\text{-}1.0)\ N_{perm};$$

$K_{vi\ perm}$ - permissible value of the coefficient of non-uniformity of energy release over the volume of the core in the i-th section of the core height when the reactor is operating at a power level permissible from the number of operating MCPs.

N_{perm} - permissible value of the thermal power of the reactor depending on the number of operating MCPs. Any other limitations on the power of the reactor plant caused by failure of systems or equipment, operation on the power effect of reactivity, etc. not to be associated with the value of N_{perm} used in the calculation of Ψ, MW;

N_{curr} - current value of reactor thermal power, MW.

2 When exceeding $K_{vi\ curr}$ acceptable values ($K_{vi\ current}{}^{perm}$), the current value of the power Reactor plant should be reduced according to the expression:

$$N_{current} = N_{perm} \cdot \Psi \cdot K_{vi\ perm} / K_{vi\ current}, \text{ (MW)}.$$

3 When the maximum coefficient of non-uniformity of energy release in the core by fuel assembly is exceeded (K_q) permissible value, the thermal power of the reactor must be reduced until the ratio:

$$K_{q\ max} \leq K_{q\ perm} \cdot \Psi,$$

where $K_{q\ max}$ - maximum value of the coefficient of non-uniformity of energy release in the core determined for fuel assemblies for the current power level of the reactor plant.

4 When controlling the power of the reactor, the power N_{core} specified in paragraph 1.2 of the Tables should be used, calculated by the RCS, as the weighted average value of the powers obtained by two or more methods, of which calculations must be made according to the parameters of the first and second circuits.

5 ** H_{nom} - nominal level in the SG equal to 270 mm along the two-chamber balance vessel (2400 mm reduced to the bottom of the SG).

6 *** The total power value for all loops should not exceed the values for items 1 and 2.

7 **** Limitations on the coefficient of non-uniformity of power release come into force when the power is more than 10% N_{nom}.

3.1.Reactor vessel

The reactor vessel is a vertical cylindrical vessel with an elliptical bottom and is designed to accommodate internal devices and cassettes. The cylindrical part of the body consists of 4 zones in height. Lower zone with a wall thickness of 192.5 mm and an outer diameter of 4535 mm. An elliptical bottom with a thickness from 192.5 mm to 237 mm is welded to it. The middle zone is a support shell with wall thicknesses of 285 mm and 192.5 mm. Next is the pipe zone and the solid-forged flange. The inner surface of the case is covered with anti-corrosion surfacing. The parameters of the body with regard to surfacing are shown in Table. 3-2.

Table. 3-2 - General data of the reactor vessel

Title	unit	Value
The height of the reactor vessel	m	10.897
The height of the axis of cold nozzles	m	7.247
Inner diameter		
• upper cylindrical part	m	3.640/3.680
• cylindrical part of the pipe area	m	3.986
• cylindrical part of the lowering section	m	4.136
• spacer ring	m	3.630
Outer diameter		
• the outer diameter of the upper flange	m	4.580
• outer diameter of the upper cylindrical part and the pipe area	m	4.570
• outer diameter of the thrust ring	m	4.690
• outer diameter of the lower part of the reactor vessel	m	4.535
Thickness of reactor vessel walls		
• in the area of the MCP pipes (including surfacing 0.007 m)	m	0.292
• in the area of saoz pipes (including surfacing 0.007 m)	m	0.322
• in the cylindrical part (including surfacing 0.007 m)	m	0.1995
• elliptical bottom (including surfacing 0.009 m, at the edge / center)	m	0.224 / 0.246
Main body material		Steel 15Х2НМФА
Surfacing material		steel 04Х20Н10Г2Б

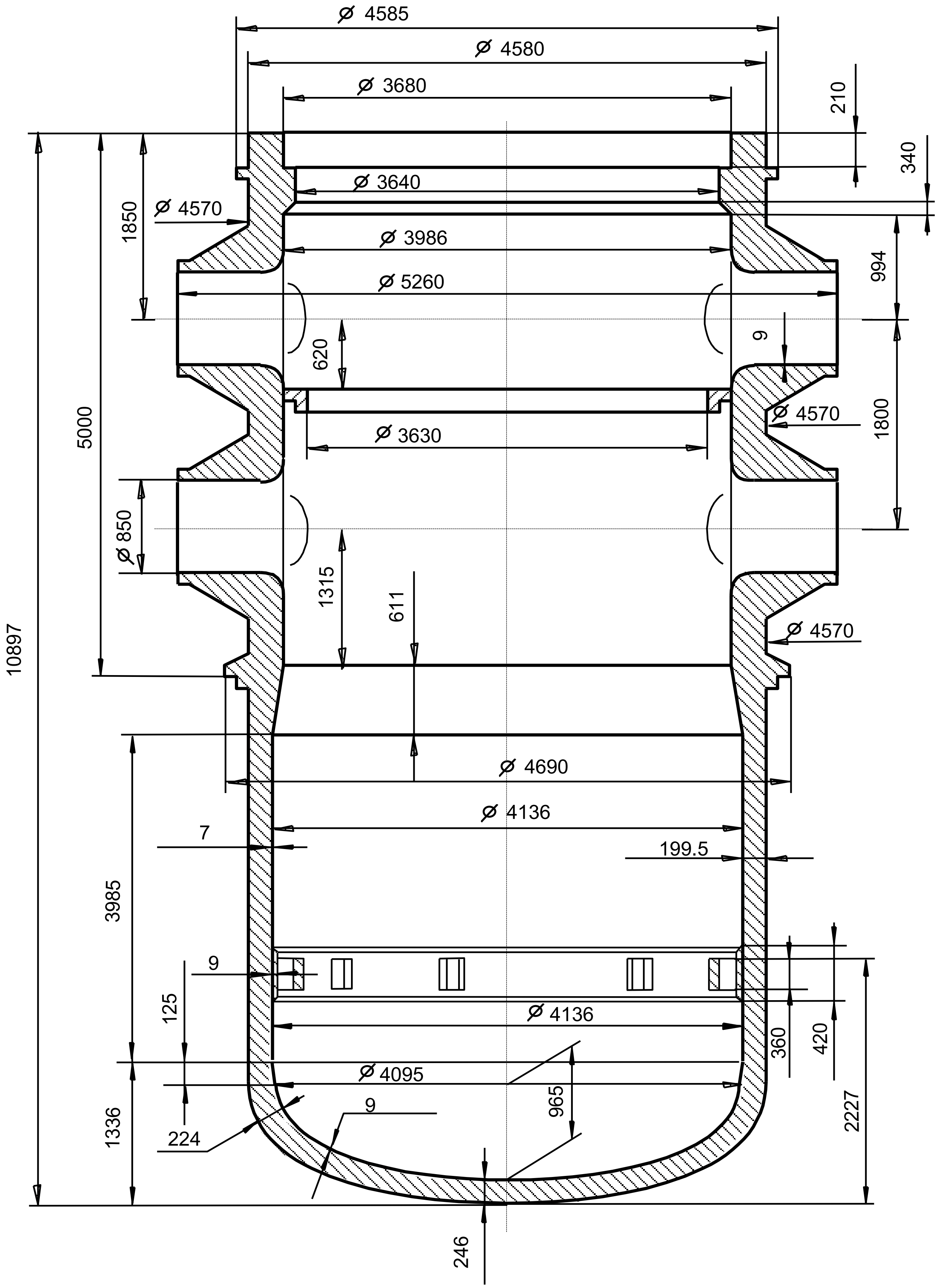

Figure 3.1 – Reactor vessel. Main dimensions

3.1.1.reactor shaft

The shaft (Figure 3.2, Figure 3.3and Table. 3-3) is a vertical cylinder with a perforated elliptical bottom, in which the support cups are fixed. The upper cylindrical part of the shaft between the flange and the flow separator is perforated with holes that serve to exit the coolant into the outlet pipes of the vessel. Opposite the upper pipes of the ECCS vessel, 2 holes with a diameter of 300 mm are made in the shaft, through which water supplied to the reactor when the ECCS is triggered passes into the inter-tube space of the BST.

The lower part of the shaft consists of a perforated elliptical bottom and support cups fixed in it, the upper parts of which, together with the spacing grid, form the lower support plate. The extreme support cups are fixed with a faceted belt attached to the lower shoulder of the cylindrical part of the shaft. The faceted belt has holes for fixing the fence, for orienting the fence in the plan and for supplying water for cooling the witness samples and the metal of the fence.

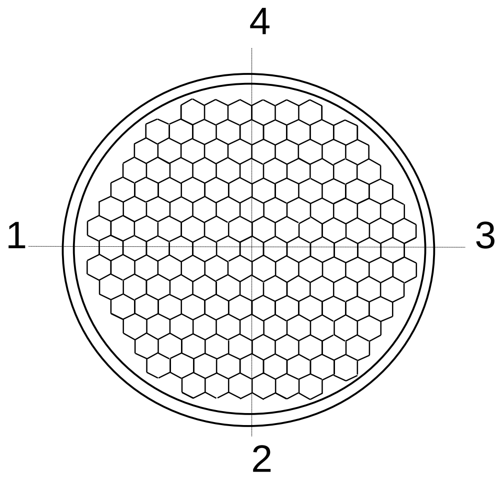

Figure 3.2 - The reactor shaft the top view (holes in glasses and faceted belt are not shown)

Table. 3-3 - General data of the reactor shaft

Title	unit	Value
Height	m	10.425
Distance from the flange to the axis of the hot pipes of the MCP	m	1.730
Gap between the bottom of the mine and the reactor vessel in the cold state	m	0.106
Gap between the bottom of the mine and the reactor vessel in the hot state	m	0.080
Distance from the vertical axis of the shaft to the parallel axis of the extreme hole in the bottom of the shaft	m	1.597
Inner diameter		
• at the level of the hot pipes of the MCP	m	3.500
• at the center of the active zone	m	3.490
Outer diameter		
• by flange	m	3.670
• at the level of the hot pipes of the MCP	m	3.630

Title	**unit**	**Value**	
• at the level of the separation ring	m	3.626	
• at the core level (major axis of the outer surface of the elliptical bottom of the mine)	m	3.620	
Value of the small half-axis of the bottom ellipse	m	1.100	
Wall thickness of the reactor shaft			
• at the level of the hot pipes of the MCP	m	0.065	
• at the center of the active zone	m	0.065	
Thickness of the elliptical bottom of the mine			
• at the level of the faceted mine belt	m	0.100	
• at the bottom of the bottom	m	0.120	
Elliptical bottom perforation		Number	D
• openings, free passage of the heat carrier into the space between the support cups	m	1344	0.040
Perforation of the cylindrical part of the shaft (7 rows of holes)			
• holes, free passage of the heat carrier to the hot pipes of the gas turbine engine	m	278	0.180
• openings for the free passage of coolant from the accumulators to the ECCS	m	2	0.300
Material		08X18H10T	

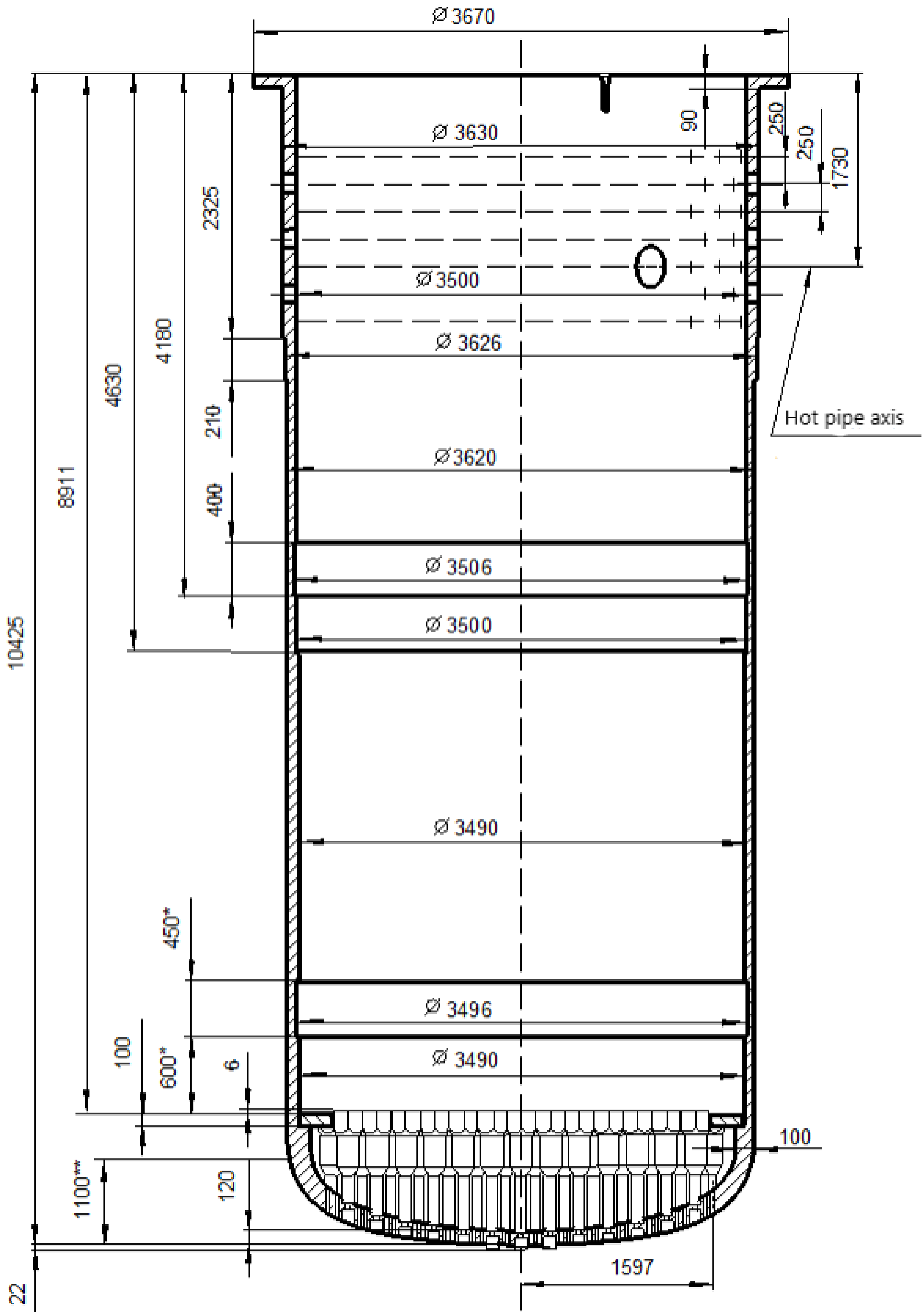

Figure 3.3 - Reactor shaft. Main dimensions

3.1.2.Enclosure of the reactor

The enclosure of the reactor (Figure 3.4 and Table. 3-4) is intended for forming the field of energy release and spacing of peripheral fuel assemblies. Together with the mine, it serves as a neutron protection for the reactor vessel, and also reduces coolant leaks past the core.

The fence is a shell consisting of 5 rings. The rings are fastened together with pins and fixed relative to each other with pins. The rings have longitudinal channels that are designed to cool the metal of the fence. When installing the fence on the faceted belt of the mine, the channels in the fence coincide with the holes in the faceted belt of the mine. The fence in the plan is fixed by 3 pins evenly located on the faceted belt of the mine. The outer surface of the fence has transverse grooves for cooling the metal of the fence. The number of channels in one row is 6 (sections A-A in Figure 3.7).

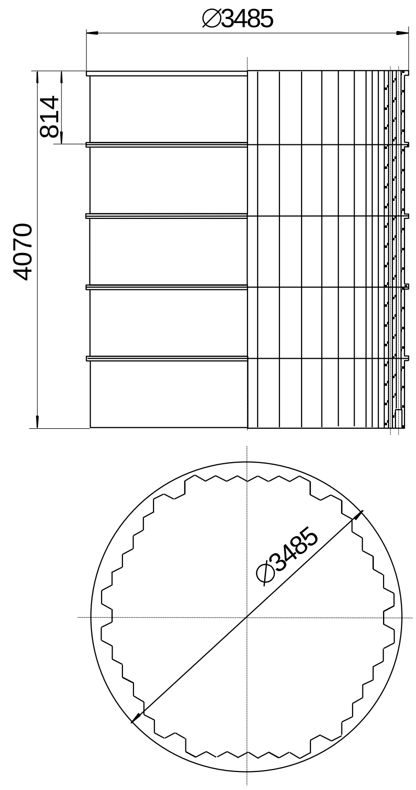

Figure 3.4 - The reactor enclosure. The basic dimensions. (Channels are not shown in the fence)

Table. 3-4 - General data of the reactor enclosure

Title	**unit**	**Value**	
Position of the bottom of the fence from the bottom of the shaft	m	1.514	
The height of baffle reactor	m	4.070	
Overall outer diameter	m	3.485	
Gap between the peripheral cassettes and the surface of the fence	m	0.004	
Perforation		Number	Diam.
• holes along the fence metal (30 pipes with samples of body steel, the remaining 54 are hollow, see Figure 1.5)	m	84	0.070
• holes for pressure pipes (see Figure 3.6)	m	6	0.130
Cross-section of 30 containers with samples of body steel	m^2	0.16	
Material		08X18H10T	

The design scheme of the reactor enclosure channels is shown in Figure 3.6. to calculate leaks between the reactor enclosure and the mine in, the design scheme shown in Figure 3.7 was used.

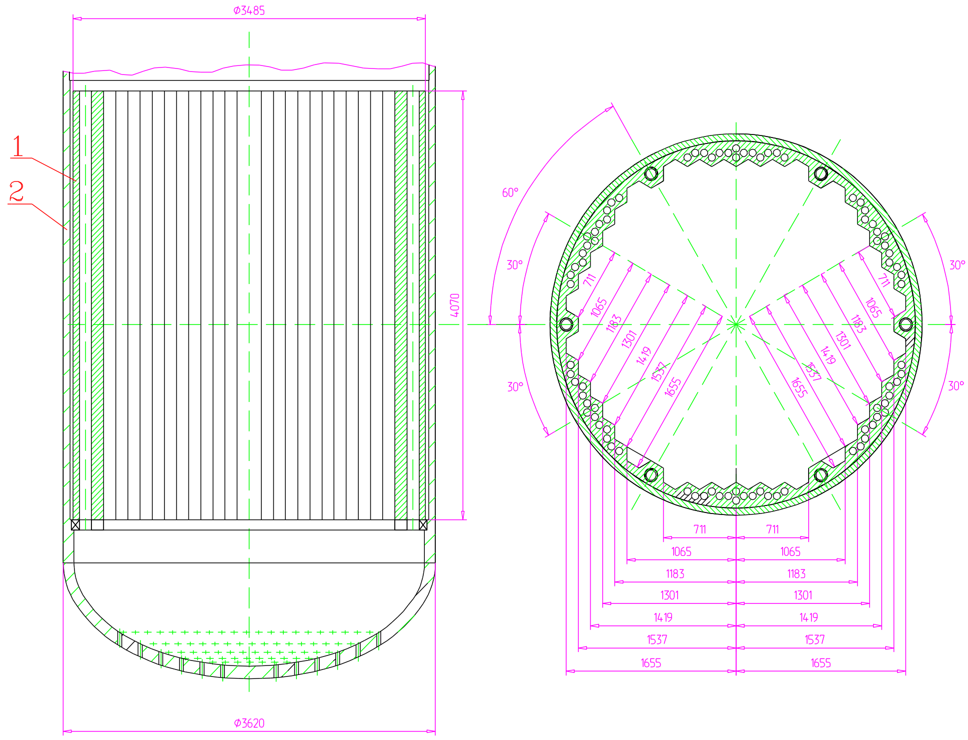

Figure 3.5 - Location of the enclosure in the reactor shaft (1-reactor shaft, 2-enclosure)

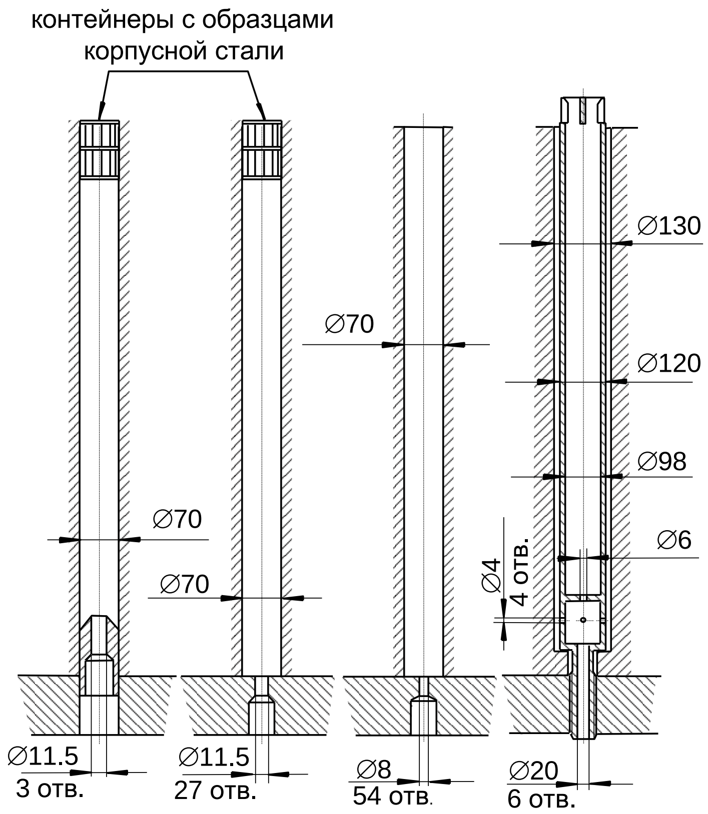

Figure 3.6 - Design scheme of reactor enclosure channels

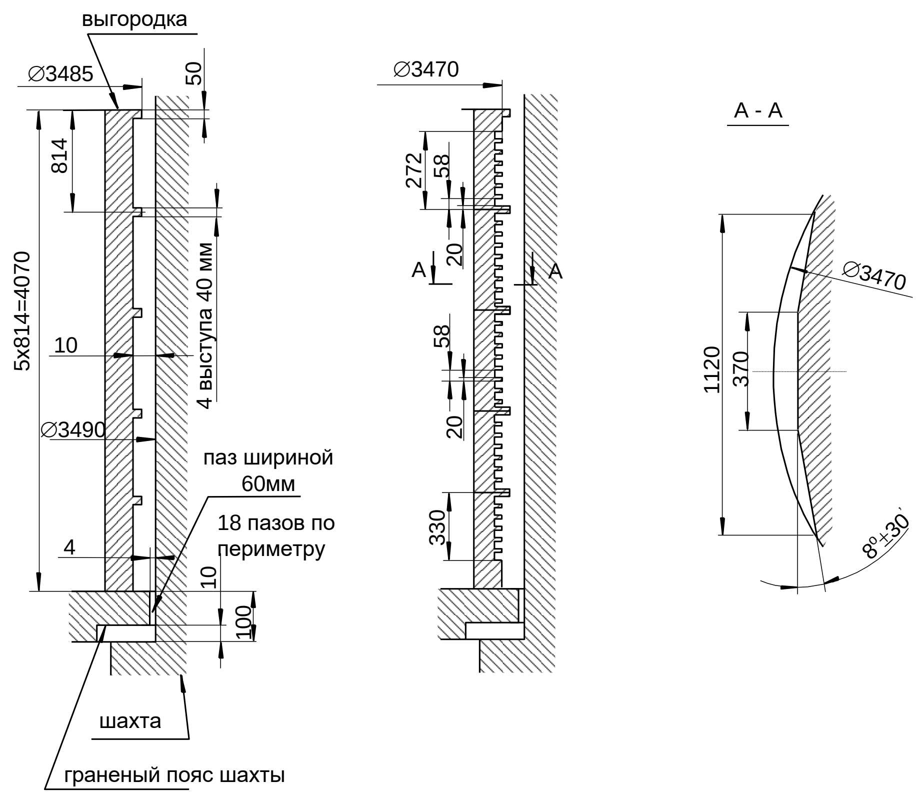

Основные размеры (упрощенно)   Размеры проточек

Figure 3.7 - Design scheme of the leak channel between the shaft and the enclosure

Table. 3-5 - Chemical composition 08X18H10T

Content of elements in %								
C	Si	Mn	Cr	Ni	Ti	S	P	Cu
no more than						no more than		
0,08	0,8	2,0	17,0-19,0	9,0-11,0	5C-0,7	0,02	0,035	0,3
Note – C - carbon content, %								

3.1.3.Design of alternative fuel Assembly (TVSA)

Alternative fuel Assembly (TVSA) (Figure 3.8) consists of a power frame, a bundle of fuel elements and fuel rods, a head and a shank. The power frame is formed by 15 spacer grids and 6 corners, to which the spacer grids are welded by contact spot welding. The frame also includes 18 guide channels and a Central tube, which, with a guaranteed gap, pass through the spacing grilles. Power frame receives the load from the internal forces caused by friction in fuel cells spacer grid with heat and bending moments of the guide channels formed by the forces from the compression springs.

18 guide channels and a Central pipe serve as power elements connecting the head and the shank and receiving loads during transport and technological operations (lowering and removing fuel assemblies from the reactor). The bundle of fuel elements is made up of 312 cylindrical fuel elements and fuel rods located in the corners of a regular triangular grid with a step of 12.75 mm.

Spacing of fuel rods is carried out by 15 cell-type spacer grid, structurally similar to the spacer grid of serial VVER-1000 fuel assemblies, but optimized in terms of the force of dragging the fuel element through the cells of the spacer grid by reducing the contact surface of the fuel element with the spacer grid.

Figure 3.8 shows the overall drawing of the fuel Assembly with the main dimensions in accordance with. See Table. 3-6 below provides General data for TVSA.

The use of fuel assemblies in comparison with the fuel assemblies of the basic design allows:

- increase the efficiency of nuclear fuel use at nuclear power plants by increasing the fuel burn-up depth and ensuring a long operational life of the fuel assembly structure;
- reduce the amount of curvature of the fuel assemblies in the reactor core;
- increase the speed of movement of fuel assemblies in the reactor core and FP and thereby reduce the time of reloading operations;
- increase the representativeness of the thermal monitoring of the coolant at the outlet of the fuel assembly;
- eliminate the costs of handling the RBA;
- increase the value of the burn-in reactivity margin, taking into account that the integrated absorber, unlike the RBA, burns out almost completely during a single fuel campaign.

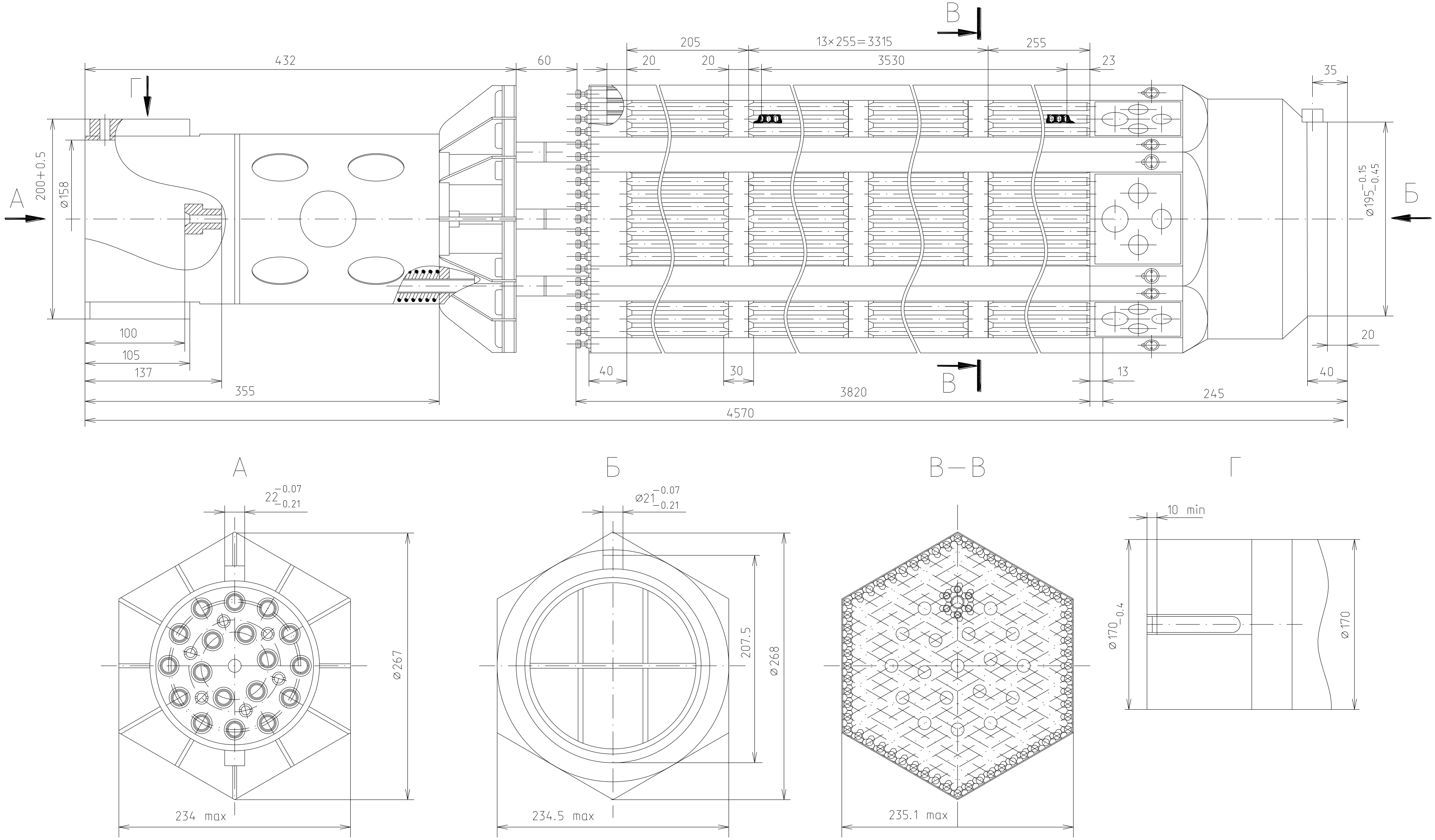

Figure 3.8 - TVSA. Dimensional drawing

Table. 3-6 - General TVSA data

Title	Unit	Value		
Number of fuel elements in the cassette (FE)	pieces	306		
Number of fuel elements with gadolinium in the cassette (FEG)	pieces	6		
The spacing of the FEL (FEG)	m	0.01275		
TVSA length	m	4.570±0.0011		
Size TVSA «for wrench»:				
- on the grid of the head	m	0.234 max		
Inner diameter:				
- shank TVSA	m	0.180		
- the upper cylindrical part of the head of TVSA	m	0.158		
Outer diameter:				
- shank TVSA	m	0.195		
- the upper cylindrical part of the head of TVSA	m	$0.170_{-0.4}$		
Characteristics of pipes		number	Outer diam.	Thickness wall
- FE	m	312	0.00913	0.0007
- Guide channels of absorbing rods	m	18	0.0126	0.00085
- Central tube	m	1	0.013	0.001
Lower spacing grid				
- Thickness	m	0.0136		
- position relative to the bottom of the TVSA	m	0.245		
Perforation of the lower spacer grid		number	Outer diam.	
- slots, free passage of the heat carrier into the inter-shaft space *	m	252	--*	
- peripheral openings, free passage of the heat carrier into the inter-tunnel space	m	20	0.0063	
- holes, free passage of the heat carrier into the inter-tunnel space	m	76	0.0063	
Intermediate spacer grids:				
- Number		14		
- the width of the grid	m	0.020		
- rim width	m	0.030		
- distance from the lower spacing grid to the first intermediate one	m	0.255		

Title	Unit	Value	
- distance between intermediate spacer grids	m	0.255	
Upper spacer grid:			
- Number		1	
- the width of the grid	m	0.020	
- rim width	m	0.040	
- distance between the upper spacer grid and the last intermediate one	m	0.205	
Head of TVSA			
- height	m	0.432	
- Perforation of the lower plate of the TVSA head		number	Diam.
- holes, free passage of the heat carrier	m	324	0.0085
- holes on the periphery, free passage of the heat carrier	m	126	0.0058
- Perforation of the intermediate plate of the TVSA head			
- holes, free passage of the heat carrier	m	6	0.008
- Perforation of the upper plate of the TVSA head			
- holes, free passage of the heat carrier	m	6	0.008
- Characteristics of pipes between the upper and middle plates of the TVSA head			
- central tube	m	1	0.016
- guide channel	m	18	0.0156
- Characteristics of pipes between the middle and lower plates of the TVSA head			
- central tube	m	1	0.015
- guide channel	m	18	0.0163
- Distance from the top of the TVSA to the top plate of the TVSA head	m	0.137	
- Distance from the top of the TVSA to the beginning of the Central tube	m	0.100	
- Thickness of the upper grid of the TVSA head (consists of two plates)	m	0.024	
- Thickness of the middle grid of the TVSA head	m	0.013	

Title	Unit	Value
- Height of the free space between the upper and middle plates of the fuel Assembly head (the cassette is not preloaded, this distance decreases when it is preloaded)	m	0.194
Stiffeners (corners of the power frame)		
- Number	шт.	6
- length in the heated part	m	3.530
- width	m	0.052
- thickness	m	0.00065
Fuel Assembly cross-section	m^2	0.0254
Mass of the main elements of the fuel Assembly		
- TVSA without absorbing rods	kg	710
- TVSA with absorbing rods	kg	~730
- Head of TVSA	kg	24
- Fuel Assembly shank	kg	11.2
- 15 Spacer grids	kg	7.5
- 6 corners	kg	8.4
- 18 guide channel	kg	15.5
- Central tube	kg	0.88
- FEG shells	kg	138.8
- Total alloy Э635	kg	24.8
- Total alloy Э110	kg	146.3
- UO_2	kg	491.4±5
TVSA construction materials:		
- Details of the head and shank		Steel 08X18H10T
- guide channel, central tube, corners		alloy E635
- Spacer grids, FEG shells		alloy E110
- Pressure springs		EK 173-ID

Table. 3-7 shows the hydraulic characteristics of the fuel assembly, determined by the results of hydraulic tests of fragmentary and full-scale models of the fuel assembly. The table shows the values of the hydraulic resistance coefficients obtained on the basis of the test results at an average coolant temperature of 305°C and a flow rate through the fuel assembly equal to 515 m3/h.

Table. 3-7 - Hydraulic resistance coefficients of the fuel assembly

Name of the TVSA section	The coefficient of hydraulic resistance
The entrance to TVSA	0.7
The active part of the TVSA	8.3
Spacer grid	0.3
Exit from the fuel assembly (including the non-heated part of the fuel elements)	2.5
TVSA generally	11.5

Figure 3.9 below shows the design of the fuel element of the fuel Assembly, indicating the main dimensions.

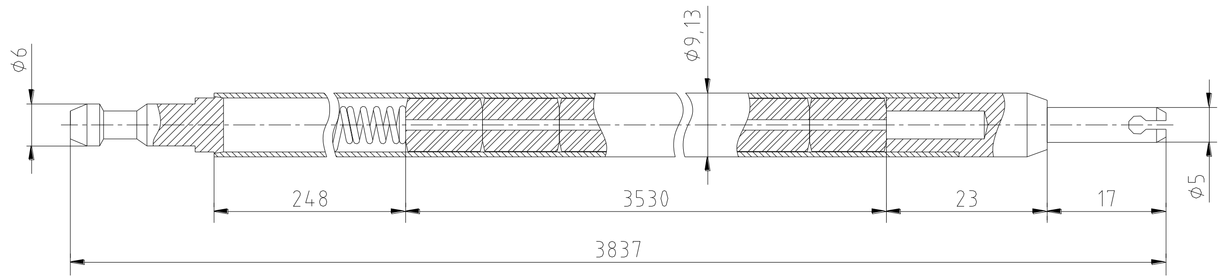

Figure 3.9 - Construction of FE TVSA

Table. 3-8 describes the design of the fuel element of the fuel Assembly.

Table. 3-8 - Design of the fuel element of the TVSA

Title	Unit	Value
Position of the beginning of the fuel column from the bottom of the fuel Assembly (lower unheated section of the fuel Assembly)	m	0.2816
Position of the beginning of the fuel column from the bottom of the lower spacer grid of the fuel Assembly	m	0.0366
Length of the fuel column in a cold state	m	3.530
Length of the fuel column in the hot state	m	3.550
Inner diameters		
• shell FE (FEG)	mm	7.73
• axial hole in the fuel tablet	mm	1.5+0.2
Outer diameter		

Title	Unit	Value
• shell FE (FEG)	mm	9.13
• fuel tablet	mm	7.57
The material of the fuel pellet		
• FE		UO_2
• FEG		$UO_2 + Gd_2O_3$

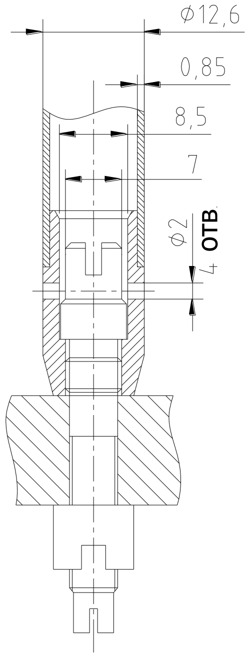

Figure 3.10 - Bushing of the guide channel of the absorbing element (AE) of the TVSA

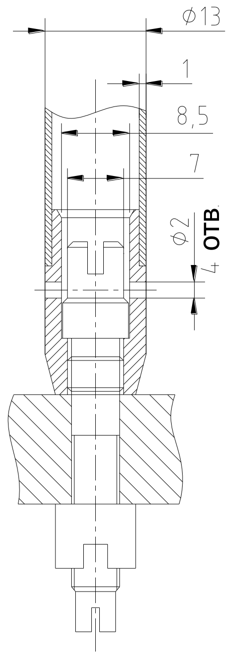

Figure 3.11 - Bushing of the central pipe of the TVSA

Table. 3-9 - Design of the AE TVSA guide channel

Title	Unit	Value	
Length of the free part of the channel	m	4.175	
The outer diameter	m	0.0126	
Wall thickness	m	0.00085	
Perforation	m	number	diameter
• holes in the lower sleeve of the channel for the intake of coolant for cooling the absorbing rods of the CPS	m	4	0.002
Annular gap in the inner cavity of the bushing (between the bushing and the bolt)			
• inner diameter of the bushing	m	0.0085	

Title	Unit	Value
• the outer diameter of the bolt at the level of the bushing holes	m	0.007

Table. 3-10 - Design of the central pipe of the TVSA

Title	Unit	Value	
Length of the free part of the central pipe	m	4.189	
The outer diameter	m	0.013	
Wall thickness	m	0.001	
Perforation		number	diameter
• holes in the lower sleeve of the pipe for the intake of coolant for cooling the neutron measurement channel (NMC)	m	4	0.002
Annular gap in the inner cavity of the bushing (between the bushing and the bolt)			
• inner diameter of the bushing	m	0.0085	
• the outer diameter of the bolt at the level of the bushing holes	m	0.007	

Table. 3-11- Basic data of the AEs bundle

Title	Unit	Value
Quantity in the absorbing rod of the control and protection system	n	18
The length of the rod	m	4.215
An absorbent material in the AE		
• top part		B_4C
• lower part		$Dy_2O_3TiO_2$
The height of a column of the absorbing material		
• total	mm	3500
• top part	mm	~3200
• lower part	mm	~300
Density of the absorbing material		
• top part (B_4C), nevertheless	g/sm^3	1.7
• lower part ($Dy_2O_3TiO_2$), nevertheless	g/sm^3	4.9
Outer diameter of the AE shell	m	0.0082
The thickness of the shell AE	m	0.0005
The shell material of AE		42XHM
Working speed of movement of the absorbing rod of the control and protection system	m/s	0.02

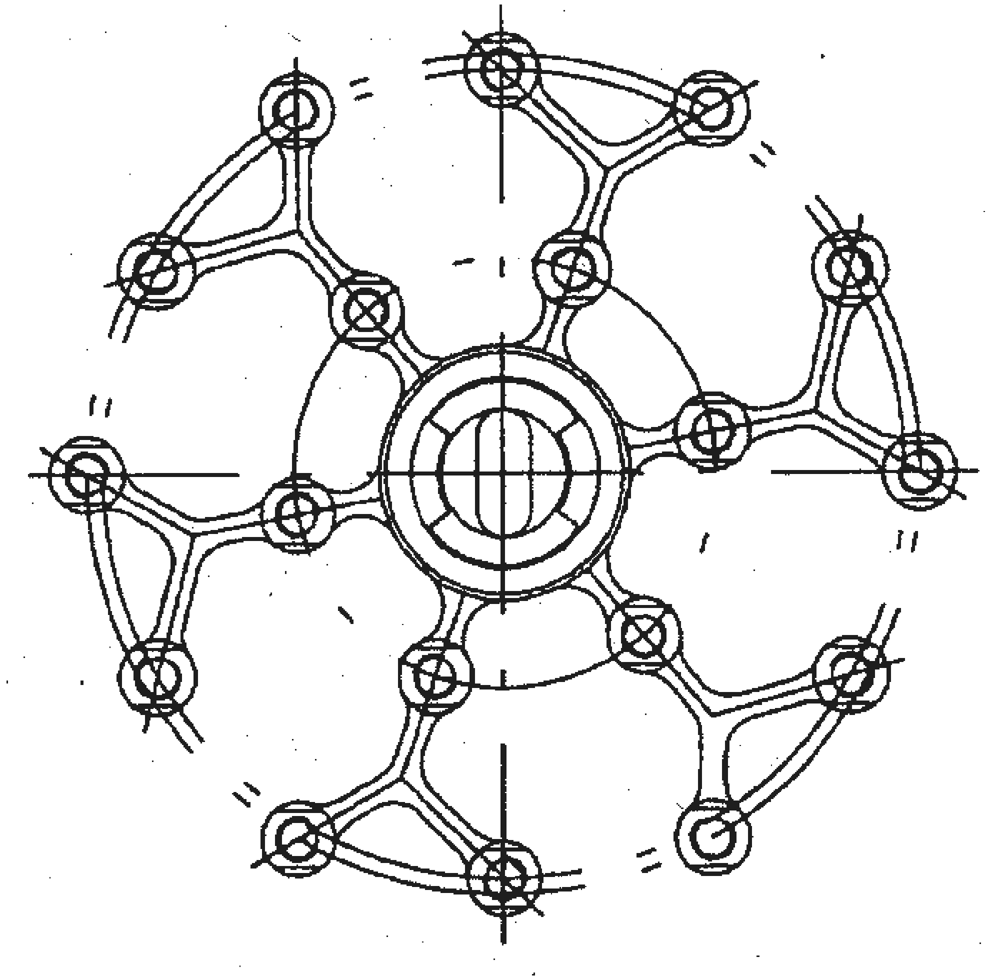

Figure 3.12 - absorbing rod of the control and protection system TVSA

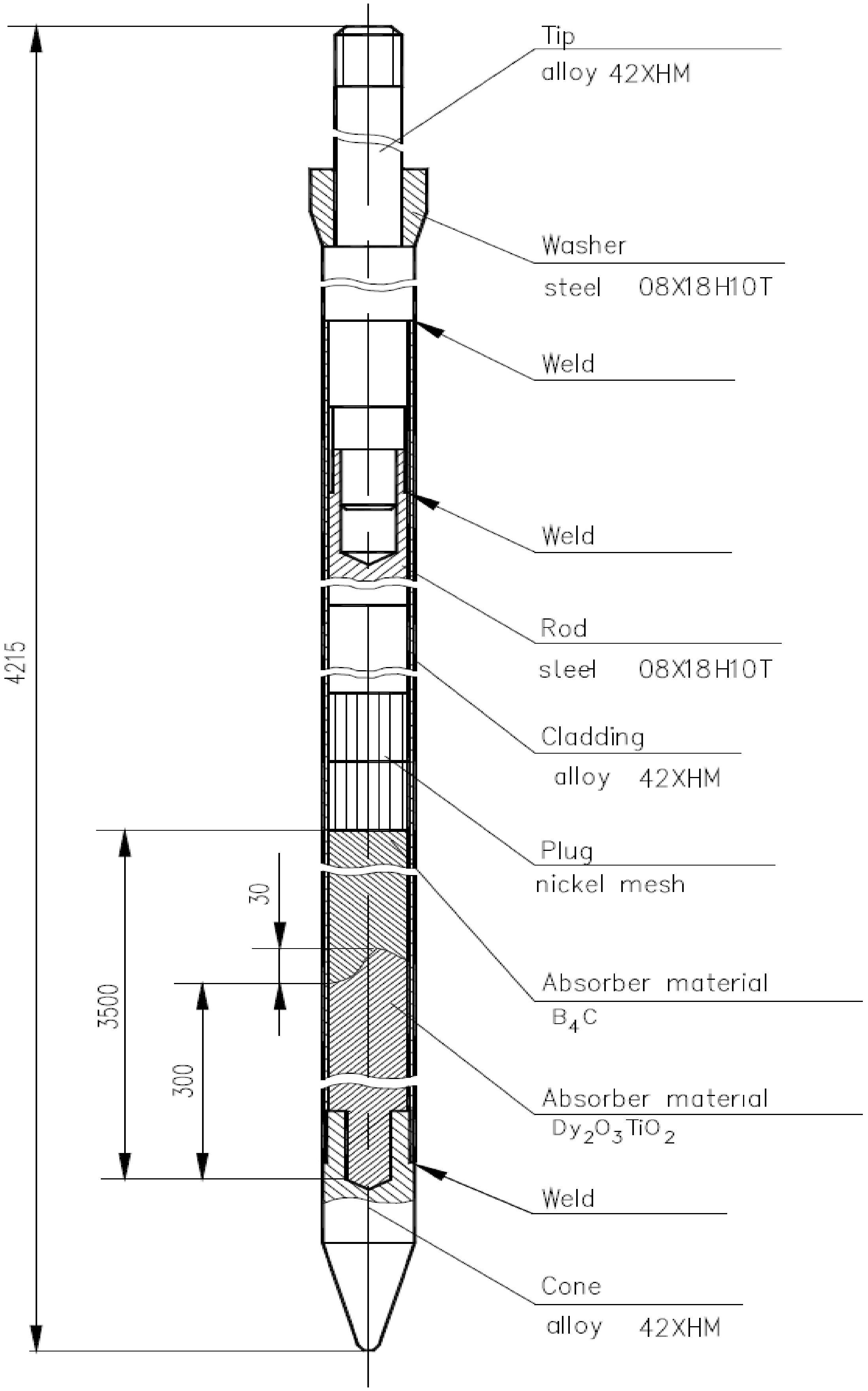

Figure 3.13 - Design of the absorbing element

3.1.4.The Block of Shielding Tubes

The Block of Shielding Tubes (BST) is intended for:

- fixing and spacing of the heads on the tapes;
- keeping cassettes from surfacing in all operating modes, including emergency situations;
- ensuring the prevention of dynamic impact on regulatory bodies and their free and reliable movement in regulation and emergency protection modes;
- provision of routing of guides and measuring channels of the RC system;
- ensuring a uniform cross-section of the core outlet of the coolant.

PTB is a welded metal structure consisting of three plates connected to each other by shells, protective pipes and pipes of the in-reactor control system.

In 61 protective pipes, guide frames are installed in which the control bodies move. The design of the guide frame provides a channel in which a tight cover is installed for the thermocouple of the temperature control system at the exit from the core.

In the pipes of the in-reactor control (IRC) system, tight covers for thermocouples and guide channels for NMC assemblies are placed. Part of the neutron measurement channel (NMC) and thermocouple assemblies are installed in protective guide channels welded on the outer surface of the BST throttle cylinder connecting the lower and middle plates of the BST. In total, 64 NMC assemblies and 98 thermocouples can be placed in the protective tube block.

The lower plate is a grid with 163 holes for interfacing with the cassette heads and a perforation that provides the output of the coolant to the upper mixing chamber.

To ensure the circulation of the coolant under the cover of the upper block, a perforation is provided in the middle and upper plate.

Above the upper plate, the IRC channels are grouped into 30 bundles: 14 TC bundles with 7 dense covers in each and 16 NMC bundles with 4 guide channels in each. The bundles are attached to risers that are fixed to the top plate.

General data of the BST are shown in Figure 3.14. If all or part of the holes are occupied by any devices, this must be indicated next to the name of the hole (for example: "14 of them are occupied for thermocouples, 16 for NMC"). If this is not indicated or "free passage of the heat carrier" is indicated, then all openings are open for the heat carrier.

Table. 3-12 - General data of the base (lower) plate of the BST

Title	**Unit**	**Value**	
Diameter	m	3.490	
Thickness	m	0.260	
Perforation (top view, against the movement of the coolant)		number	Diam.
• peripheral openings, free passage of the coolant	m	24	0.074
• peripheral openings, free passage of the coolant	m	78	0.120
• peripheral holes, free passage of the heat carrier (14 of them are occupied for thermocouples, 16 for NMC)	m	168	0.033
• Central openings, free passage of the coolant	m	72	0.108

Title	Unit	Value	
• peripheral openings, free passage of the coolant	m	12	0.092
• specially shaped Central openings, free passage of the coolant		186	*
• the holes under the protective pipe absorption rods	m	61	0.170
• openings for protective pipes for in-reactor monitoring	m	60	0.108
Total weight of the base plate	kg	8400	
Material		08X18H10T	

Table. 3-13 - General data of the middle plate of BST

Title	Unit	Value	
Diameter	m	3.400	
Distance between the middle plate and the base plate of the BST	m	3.575	
Thickness	m	0.200	
Perforation (top view)		number	Diam.
• peripheral openings, free passage of the coolant	m	42	0.100
• peripheral openings, free passage of the coolant	m	90	0.090
• peripheral holes, free passage of the heat carrier (14 of them are occupied for thermocouples, 16 for NMC)	m	30	0.0225
• the holes under the protective pipe absorption rods	m	61	0.185
• openings for protective pipes for in-reactor monitoring	m	60	0.115
Total weight of the meddle plate	кg	9300	
Material		08X18H10T	

Table. 3-14 - General data of the spacer plate (upper) BST

Title	Unit	Value	
Diameter	m	3.280	
Distance between the spacer (upper) plate and the middle plate of the BST	m	1.302	
Thickness	m	0.090	
Perforation (top view)		number	Diam.
• Central openings, free passage of the coolant	m	36	0.200
• peripheral holes for M80 thread, free passage of coolant	m	12	0.080

Title	Unit	Value	
• peripheral openings free passage of the coolant	m	6	0.150
• holes for thermal control racks	m	14	0.100
• holes for neutron measurement channel racks	m	16	0.165
• the holes for the covers CPS	m	61	0.165
• peripheral holes for the M74 thread, are occupied by bolts securing the plate to the shell, there is no passage of the coolant	m	9	0.064
Total weight of the spacer plate (upper)	кg	3600	
Material		08X18H10T	

Table. 3-15 - General data of PTB shells

Title	Unit	Value	
The cylindrical part between the upper and middle plate of the BST (see Fig. 1.5)			
Outer diameter (from the top to the thrust collar)	m	3.360	
External diameter (from the thrust shoulder to the middle plate)	m	3.400	
Inner diameter	m	3.280	
Height	m	1.392	
Perforation		---	
Mass	кg	6185	
Material		08X18H10T	
Data of the shells between the middle and the base (lower) plate of the BST (from top to bottom)			
Cylindrical part			
• outer diameter	m	2.950	
• Thickness	m	0.050	
• Height	m	2.035	
Perforation		number	diameter
• openings, free passage of the coolant	m	780	0.032
• openings, free passage of the coolant	m	1422	0.040
• openings, free passage of the coolant	m	40	0.060
Mass	кg	6360	
Material		08X18H10T	
Conical part			
• upper / lower outer diameter	m	2.950/3.480	
• thickness	m	0.050	

Title	Unit	Value	
• height	m	0.990	
Perforation		number	diameter
• openings, free passage of the coolant	m	742	0.040
• slots for peripheral TC and NMC	m	30	*
Mass	кg	3290	
Material		08X18H10T	
Cylindrical part			
• outer diameter	m	3.480	
• Thickness	m	0.050	
• Height	m	0.540	
Mass	кg	2850	
Material		08X18H10T	

Table. 3-16 - General data of PTB pipes

Title	Unit	Value		
Pipes located between the reactor cover and the upper plate of the BST		number	Outer diam.	Wall thickness
TC stands (height 0.492 m from the plate)	m	14	0.121	0.016
Thermocontrol protection pipes extending from the TC racks and above to the cover pipes	m	14	0.074	-
Racks (height 0.496 m from the plate)	m	16	0.146	0.008
Protective covers of neutron measurement channels (NMC) extending from the EV racks and higher into the cover pipes, without a protective pipe	m	64	0.022	0.002
Covers for CPS drives	m	61	0.078	-
Pipes located between the upper and middle plate of the BST				
• CPS protective pipes	m	61	0.063	0.006
• NMC protective pipes	m	64	0.022	0.002
• Thermopars protective pipes	m	95	0.016	0.0014
Pipes located between the middle and lower plate of the BST				
• CPS protective pipes	m	61	0.180	0.008
• Protective pipes for in-reactor control channels	m	60	0.108	0.006
• Peripheral NMC protective pipes	m	14	0.022	0.002

Title	Unit	Value		
• protective pipes for peripheral thermocouples	m	16	0.022	0.002

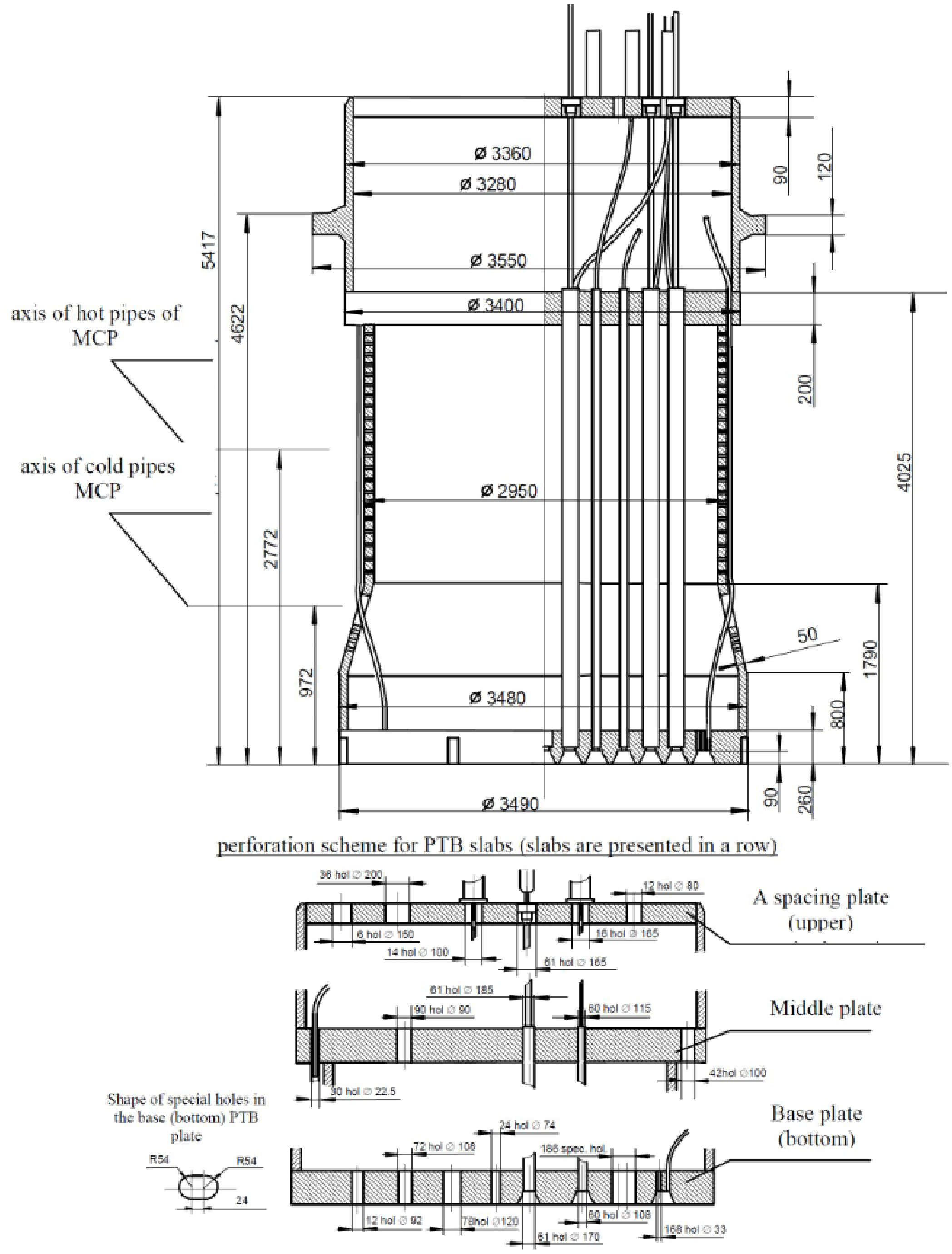

Figure 3.14 - BST. Main sizes. BST plate perforation

3.2.Chemical composition of materials

3.2.1.Chemical composition in % of material 08X18H10T

C	Si	Mn	Ni	S	P	Cr	Cu	-
up to 0.08	up to 0.8	up to 2	9 - 11	up to 0.02	up to 0.035	17 - 19	up to 0.3	(5 C - 0.7) Ti, else Fe

3.2.2.Chemical composition in % of material EK 173-ID

element	C	S	P	Mn	Cr	Si	Ni	Fe
	0.04-0.08	≤0,02	≤0,02	1-1.7	17-19	≤0,5	39-42	base
element	**Al**	**V**	**B**	**Ti**	**Mo**	**Nb**	**Co**	**N**
	0,9-1,3	0,05-0,2	0,005-0,008	1,8-2,5	4,5-5,5	0,25-0,6	≤0,02	≤0,05

3.2.3.Alloy E635

Chemical composition (in % of mass):

element	Nb	Sn	Fe	O	Si	Zr
min, %	0.90	1.10	0.30	0.05	0.0050	-
max, %	1.10	1.40	0.47	0.12	0.0200	other

3.2.4.Alloy E110

Chemical composition (in % of mass):

element	Nb	Zr
min, %	0.90	-
max, %	1.10	other

4. Neutron-physical characteristics of the VVER-1000 reactor core

This section provides brief information on the neutron-physical characteristics of the core of the power unit No. 2 of the KhNPP.

The estimated duration of the 8th fuel campaign until the burnout reserve is exhausted on the boron control is 293.59±8.81 eff. days, the estimated duration of the campaign, taking into account the operation in the campaign extension mode on the power effect of reactivity, is 323.59 eff. days.

The following fresh fuel nomenclature is used for recharge:

- TVSA of medium enrichment 4.38% (439MT) with 6 fuel rods – 24 pcs;
- TVSA medium-enriched fuel rods 4.30% (430MO) with 6 fuel rods – 12 pcs;
- TVSA of medium enrichment 3.99% (398MO) with 6 fuel rods – 6 pcs;
- TVSA of medium enrichment of 2.20% (22AUM) -1 pc.

All fuel assemblies in the core in the 8th fuel load of the alternative type.

The layout of the control rods in the reactor core and their distribution into groups is shown in Figure 4.1.

As a working group, the 10 group of the CPS AR is used. The position of the working group when working at a stationary, nominal power level is 90% of the bottom of the core.

The layout of the NMC and thermocouples in the core is shown in Figure 4.2 and Figure 4.3. The maximum permissible heating of the coolant on the fuel assembly at the locations of the TC at 4 operating MCPs is shown in Figure 4.4.

The critical concentration of boric acid at the first critical state at the MPL and at the critical state after experimental measurements of the NFC at the beginning of the campaign, at the position of the working group 70% from the bottom of the core - 9.91 g/kg .

To ensure the criticality analysis of the reactor not less than 1%, with the cocked to the operating position of CPS, after actuation when carrying out experimental measurements PH in the beginning of the campaign, it is necessary to increase the concentration of boric acid in the primary coolant to a value of not less than 0.80 g/kg higher than the critical concentration of boric acid recorded during the measurement of temperature reactivity coefficient at the position of the working group 80÷90% from the bottom of the core.

Stationary poisoning of Sm149 in the 8th campaign (compensated reactivity) •

* at the beginning of the campaign – 0.817%,

• at the end of the campaign – 0.682%.

Comparison of the values of the main neutron-physical characteristics of the fuel load with the permissible values is given in Table. 4-1.

Table. 4-1 - Comparison of the values of the main neutron-physical characteristics of the fuel load with the permissible values

Parameter	The values of the parameters	Acceptable limits for changing parameters
Effective operating time of the fourth-year TVSA at the end of the campaign, eff. hour	29424.72	□□31500
Kq (maximum value during the campaign)	1.30	□1.35
Kr (maximum value during the campaign)	1.49	□1.50
Margin to Kv setpoint (minimum value during the campaign)	0.207	>0
Margin to the Ql setpoint for fuel rods (minimum value during the campaign), W/cm	35.39	>0
The maximum burnup in TVSA, MW·day/kgU.	53.57	□55.0
The maximum burnup in FE TVSA, MW·day/kgU.	57.07	□59.1
The maximum burnup in FEG TVSA, MW·day/kgU.	50.34	□51.4
Coefficient of reactivity according to the temperature of the coolant (T=0 eff.day., Minimum controlled power level, H1-10=100%), %/°C.	$-5.73\cdot10^{-3}$	<0
Coefficient of reactivity according to the density of the coolant (T=0 eff.day, Minimum controlled power level,, H1-10=100%), %/(г/см^{3}).	5.05	>0
Subcriticality of the reactor in the state of t=20°C, Cв=16 g/kg, Xe=0, $Sm=Sm^{n}$, H1-10=100%, %.	-9.343	□-2
Re-criticality temperature, °C.	196/178	□220
The magnitude of the change in the linear energy release, %.	11.988	□15
Subcriticality of the reactor in the state of t=20°C, Cв=16g/kg, Xe=0, $Sm=Sm^{n}$, H1-10=100%, %.	29424.72	□□31500
Re-criticality temperature (TK1/TKW), °C.	1.30	□1.35

The unevenness of the distribution of energy releases in the reactor core is determined by the following set of coefficients:

- coefficient of unevenness of energy releases by FA’s, Kq;
- coefficient of unevenness of energy release across the fuel elements of the FA, Kk;
- coefficient of unevenness of energy release by fuel rods of the core, Kr;
- coefficient of unevenness of energy releases by the volume of the core, Kv;

- coefficient of unevenness of energy releases along the height of the FA, Kz;
- total coefficient of unevenness in the local heat flow, Ko.

The coefficients of nonuniformity of energy release are determined by the following formulas:

$k_q = \frac{Q_i \cdot N}{\sum_{i=1}^{N} Q_i}$, where N is the number of FA's in the core; Q_i is the power of the i-th cassette;

$k_k = \frac{Q_i \cdot n}{\sum_{i=1}^{n} Q_i}$, where n is the number of fuel rods in this FA; Q_i is the power of the i-th fuel rod;

$k_z = \frac{Q_i \cdot m}{\sum_{i=1}^{m} Q_i}$, where m is the number of sections along the height of the FA; Qi is the power of the i-th section.

Relations between the coefficients of unevenness:

$K_v = K_q \cdot K_z$;
$K_r = K_q \cdot K_k$;
$K_o = K_v \cdot K_k$.

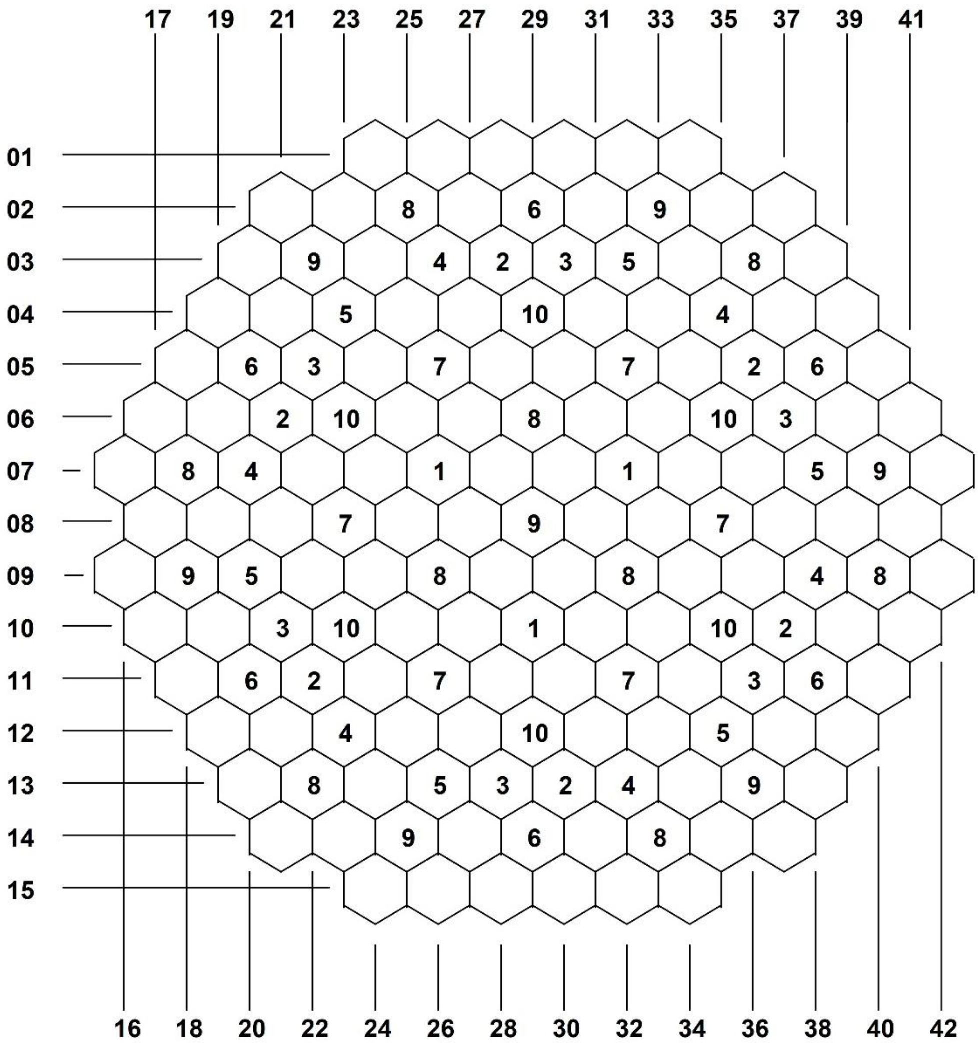

Figure 4.1 - Diagram of the location of the control rods in the reactor core (the cells indicate the numbers of the CPS CR groups)

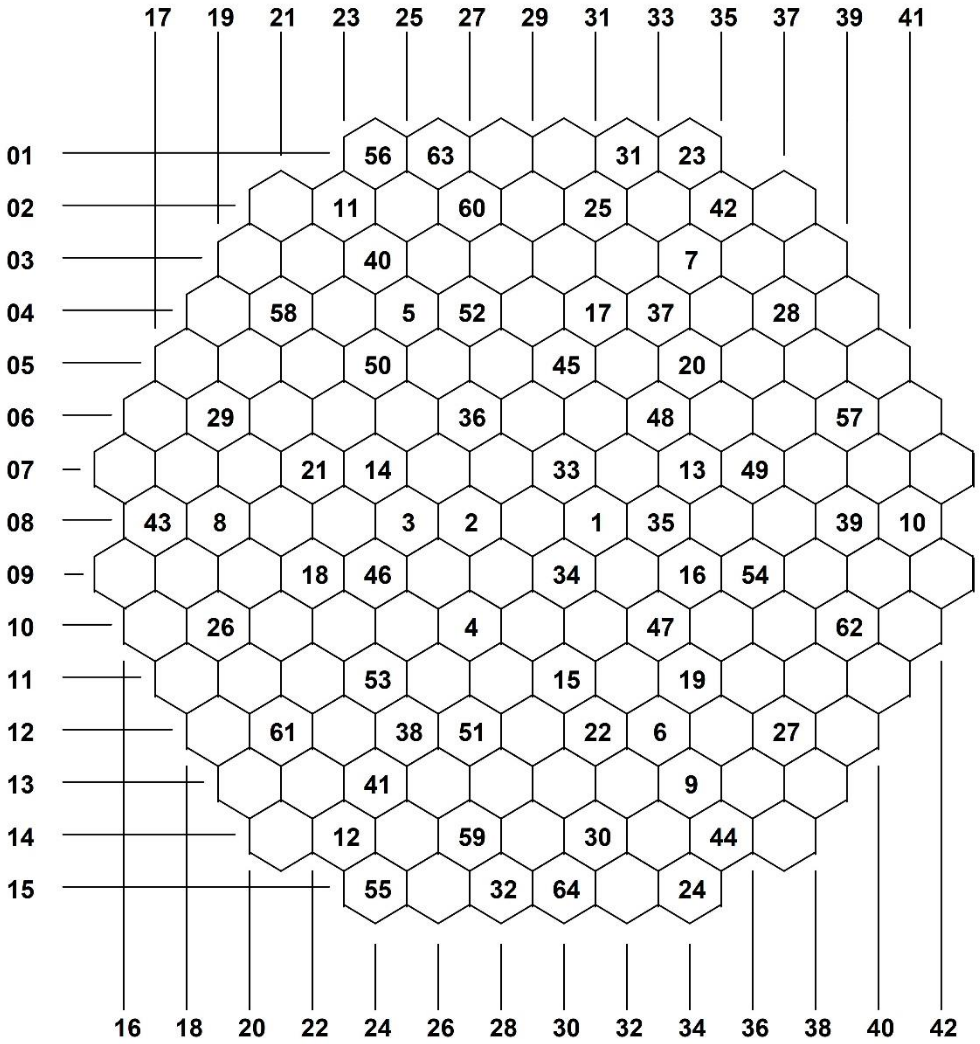

Figure 4.2 - The layout of the CNM in the reactor core (the cells contain the CNM numbers)

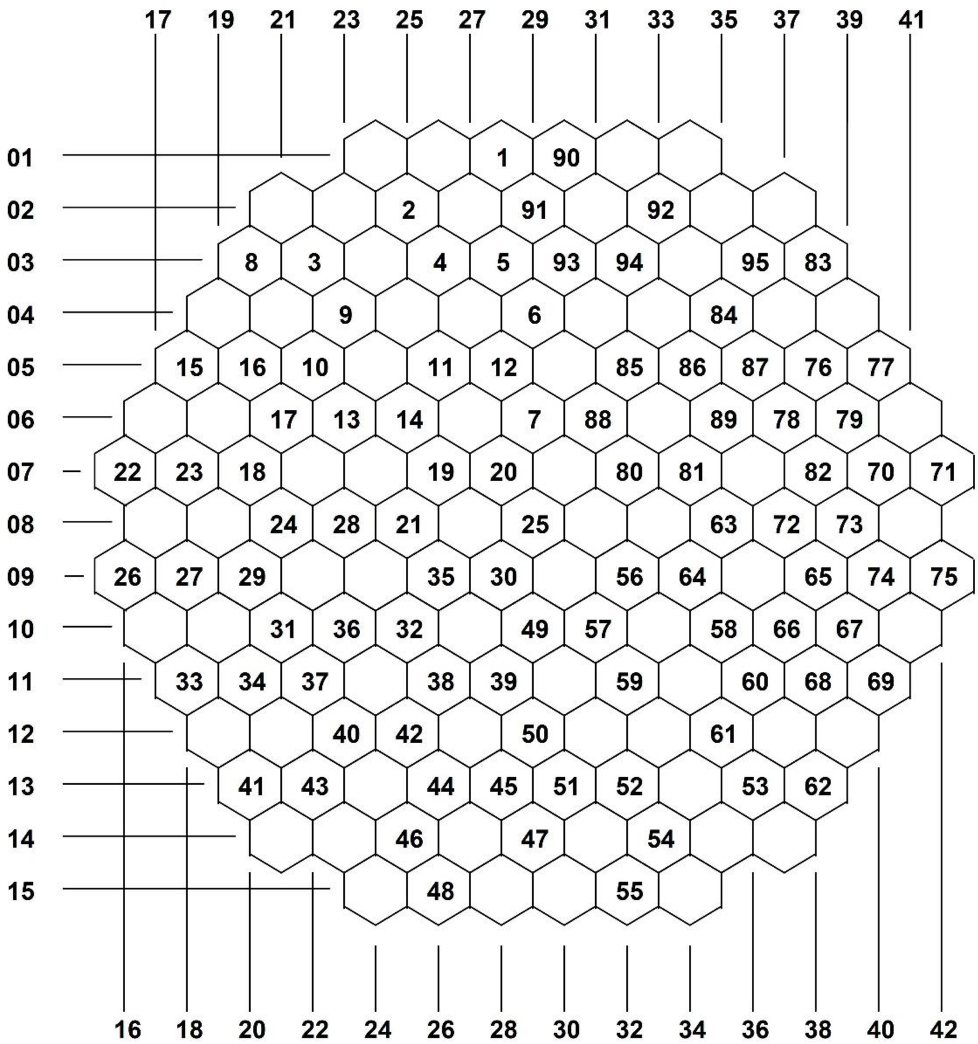

Figure 4.3 - Diagram of the location of the thermocouples in the reactor core (the cells contain the numbers of the thermocouples)

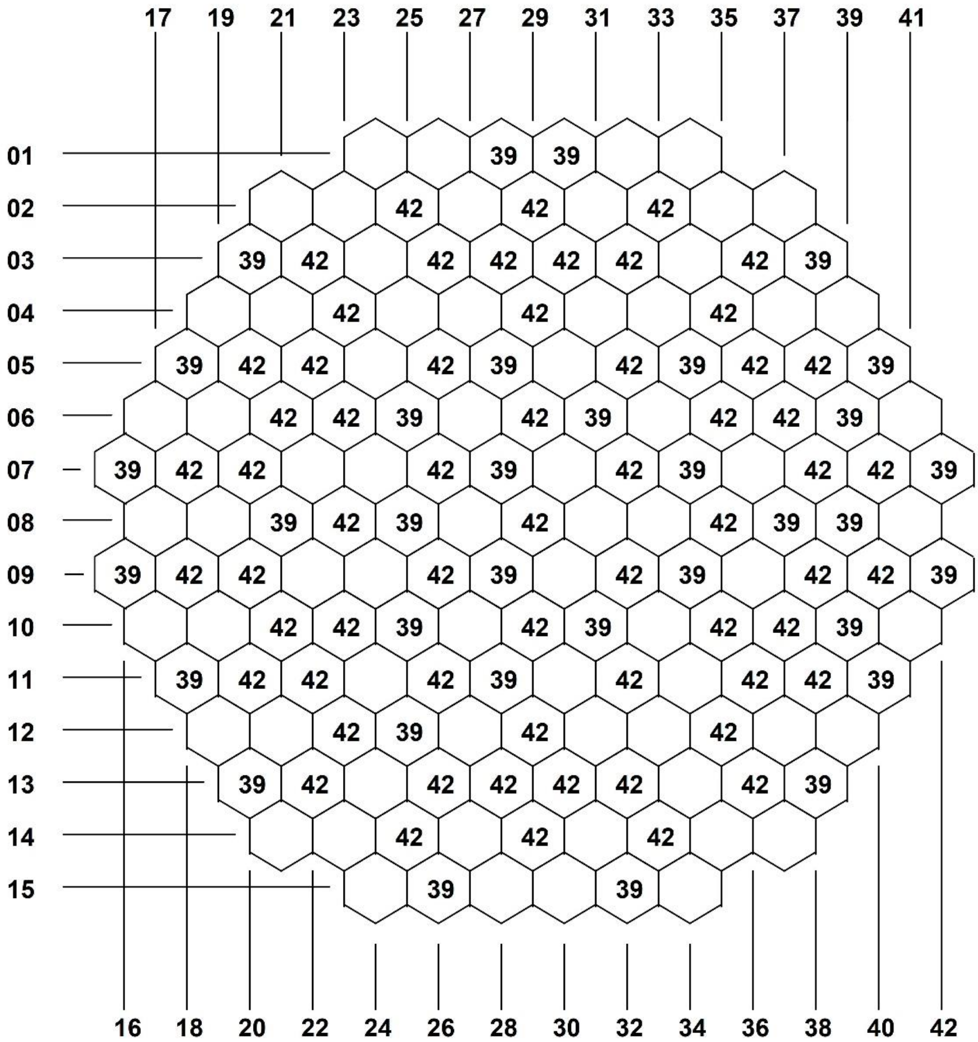

Figure 4.4 - The maximum permissible heating of the coolant on the TVSA in the locations of the TC (with 4 operating MCPs)

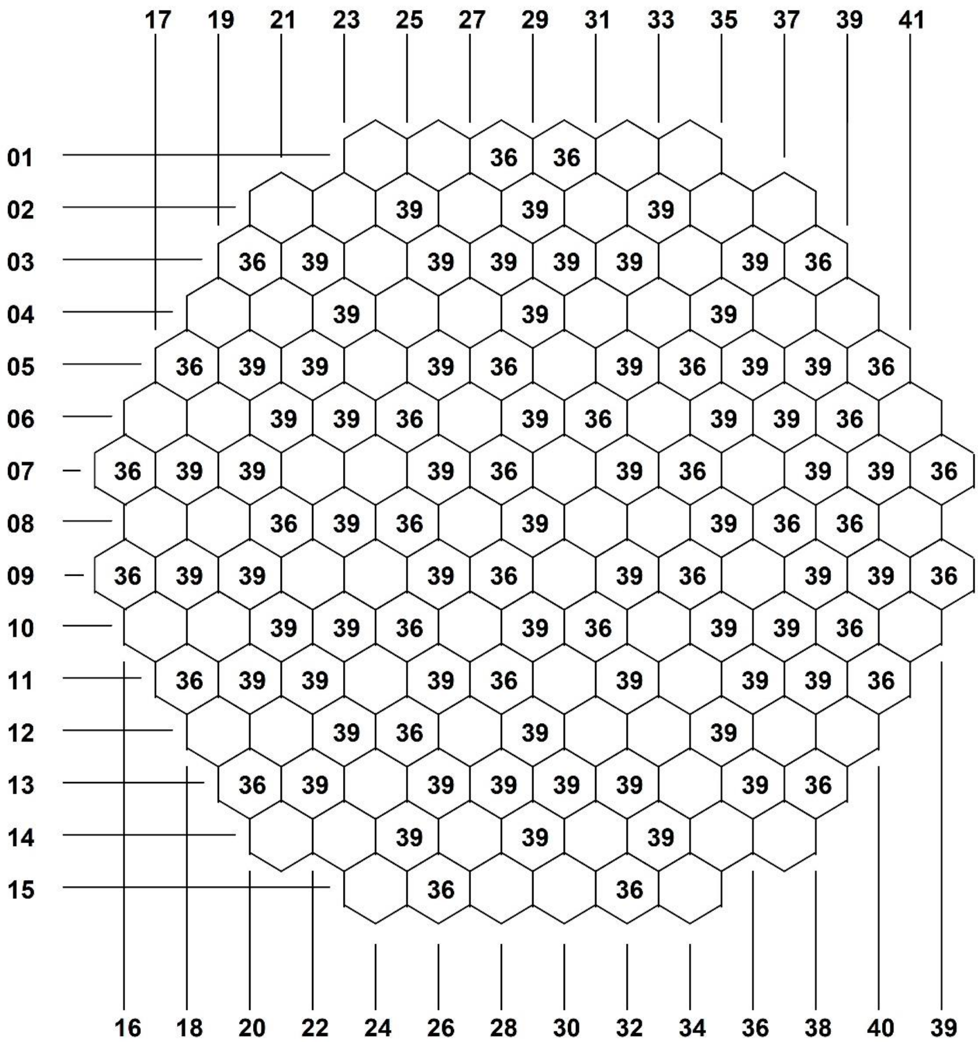

Figure 4.5 - The maximum permissible heating of the coolant on the TVSA in the locations of the TC (with 3 operating MCPs)

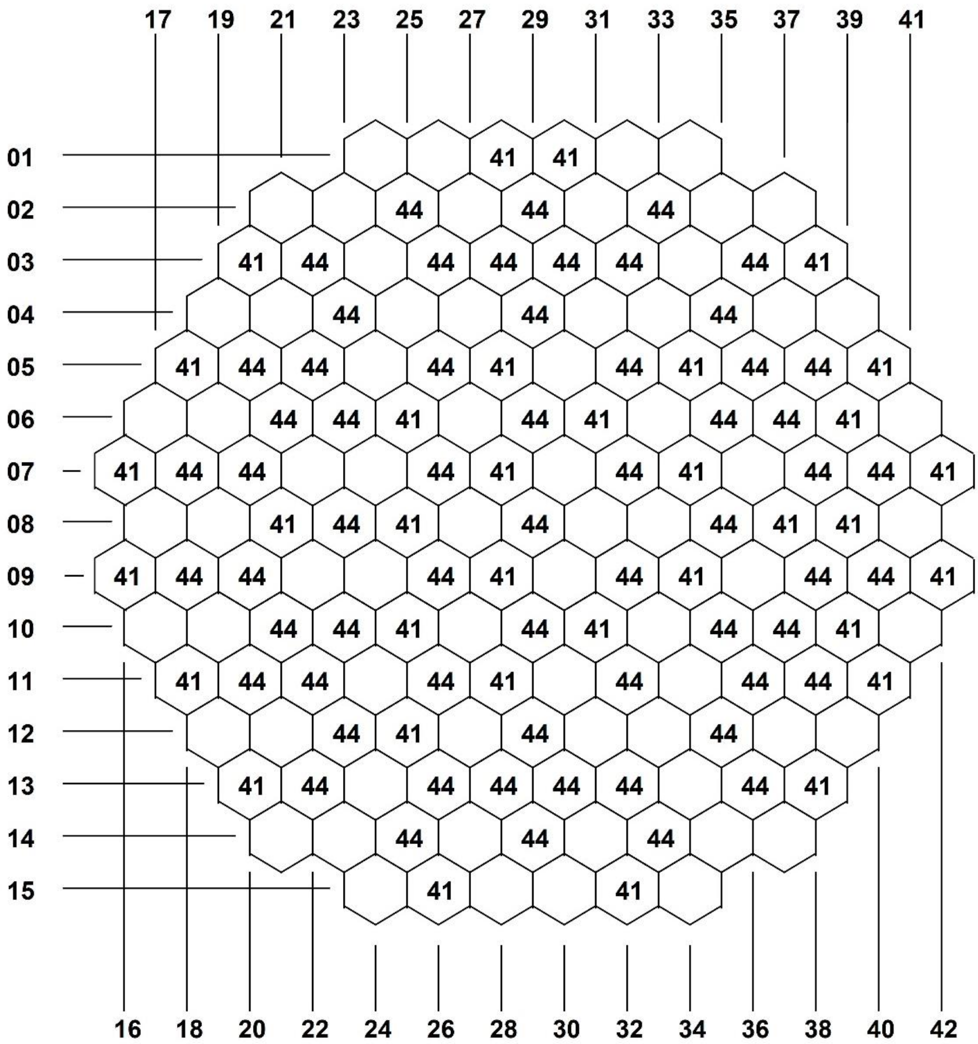

Figure 4.6 - The maximum permissible heating of the coolant on the TVSA in the locations of the TC (with 2 operating MCPs)

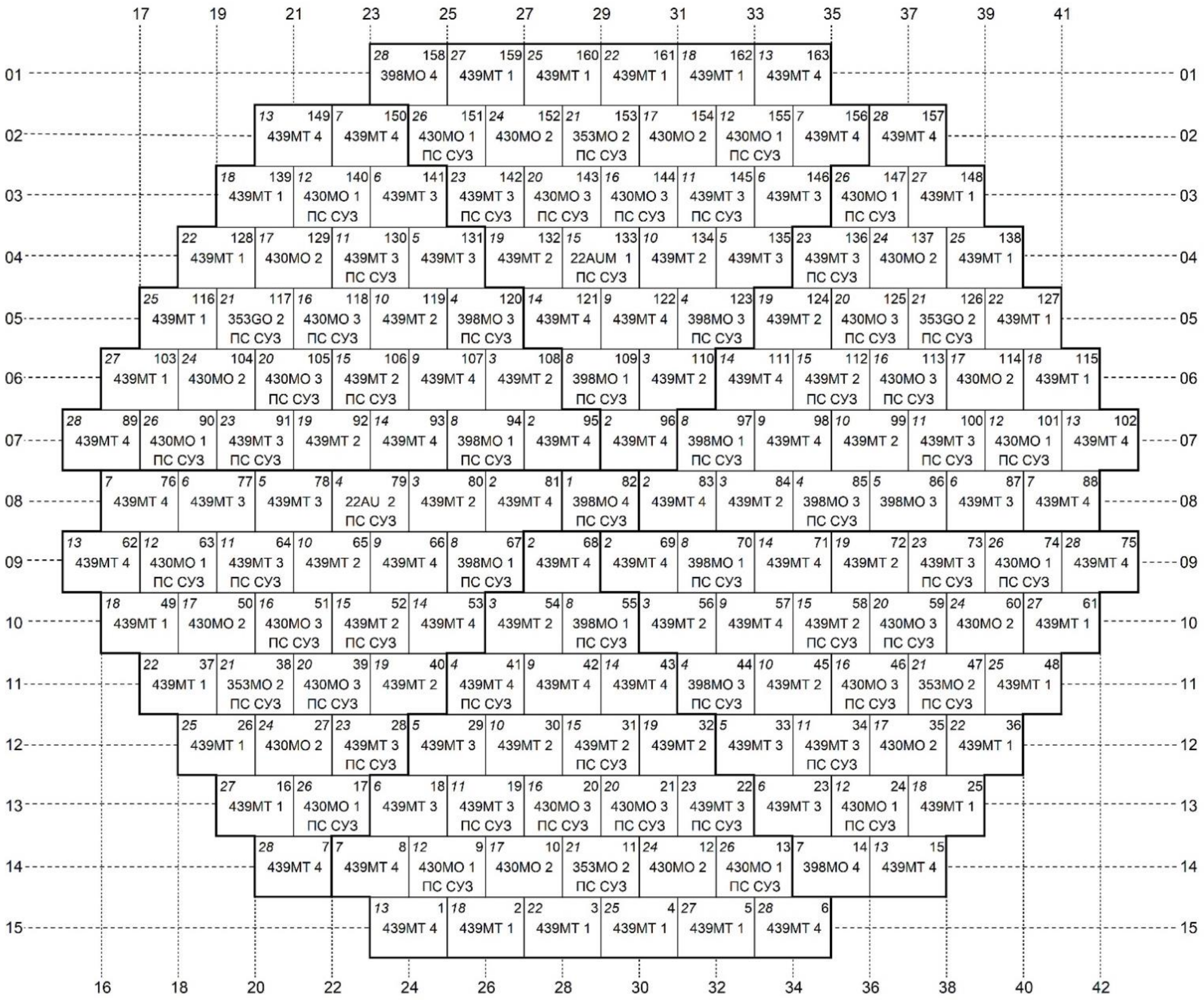

Картограмма загрузки активной зоны.

8-я топливная загрузка.

В активной зоне находится ТВС :

Тип ТВС	Топливных загрузок в активной зоне				всего
	1	2	3	4	
22AU	0	1	0	0	1
22AUM	1	0	0	0	1
353GO	0	2	0	0	2
353MO	0	4	0	0	4
398MO	6	0	5	3	14
430MC	12	12	12	0	36
439MT	24	23	23	35	105
	43	42	40	38	163

ОБОЗНАЧЕНИЯ :

20 59 - расчетный номер ТВС, 60 и 360 симетрии.
430MO 3 - Тип ТВС и срок эксплуатации в а.з. (в топливных кампаниях)
ПС СУЗ - поглотитель

Figure 4.7 - Active zone loading cartogram

4.1.Changes in the main parameters of the RC during the operation of the fuel load

Cartogram of the distribution of average burnup in TVSA at the beginning and end of the campaign is presented in Figure 4.8.

Cartogram of the distribution of relative energy release in fuel assemblies (Kqi) at the beginning and end of the campaign is presented in Figure 4.9.

On the curve changes the maximum value of Kq indicates the number of cells of the active zone (in the sector of 360°), in which Kq is achieved at the corresponding point of the campaign.

The curve for the change in the maximum Kv value shows the numbers of cells (in the 360° sector) and the layers of the core (a total of 10 layers are accepted) in height, in which this Kv is reached.

Graphs of changes in the critical concentration of boric acid during the operation of the fuel load for various states of the reactor plant are shown in Figure 4.12. The states with the following parameter values are considered:

A-N = 100%, Xe poisoning is stationary;

B - N = 50%, Xe poisoning corresponds to a power of 50;

C - N = 100%, no Xe poisoning;

D - N = 0%, no Xe poisoning, temperature 279°C;

E - N = 0%, no Xe poisoning, temperature 20°C.

Graphs of changes in the effective fraction of delayed neutrons during the operation of the fuel load are shown in Figure 4.13.

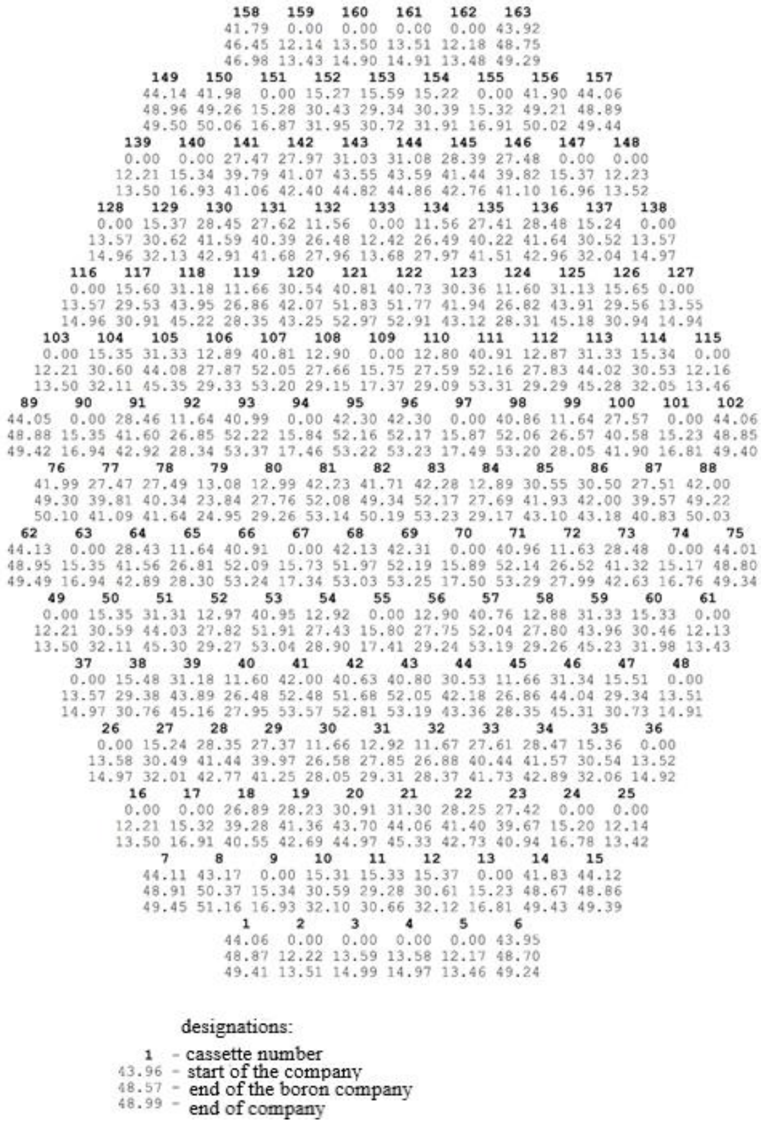

Figure 4.8 - Cartogram of the distribution of the average burnout (MW•day/ kg U) by cassettes at the beginning and end of the campaign for the 360-degree symmetry sector

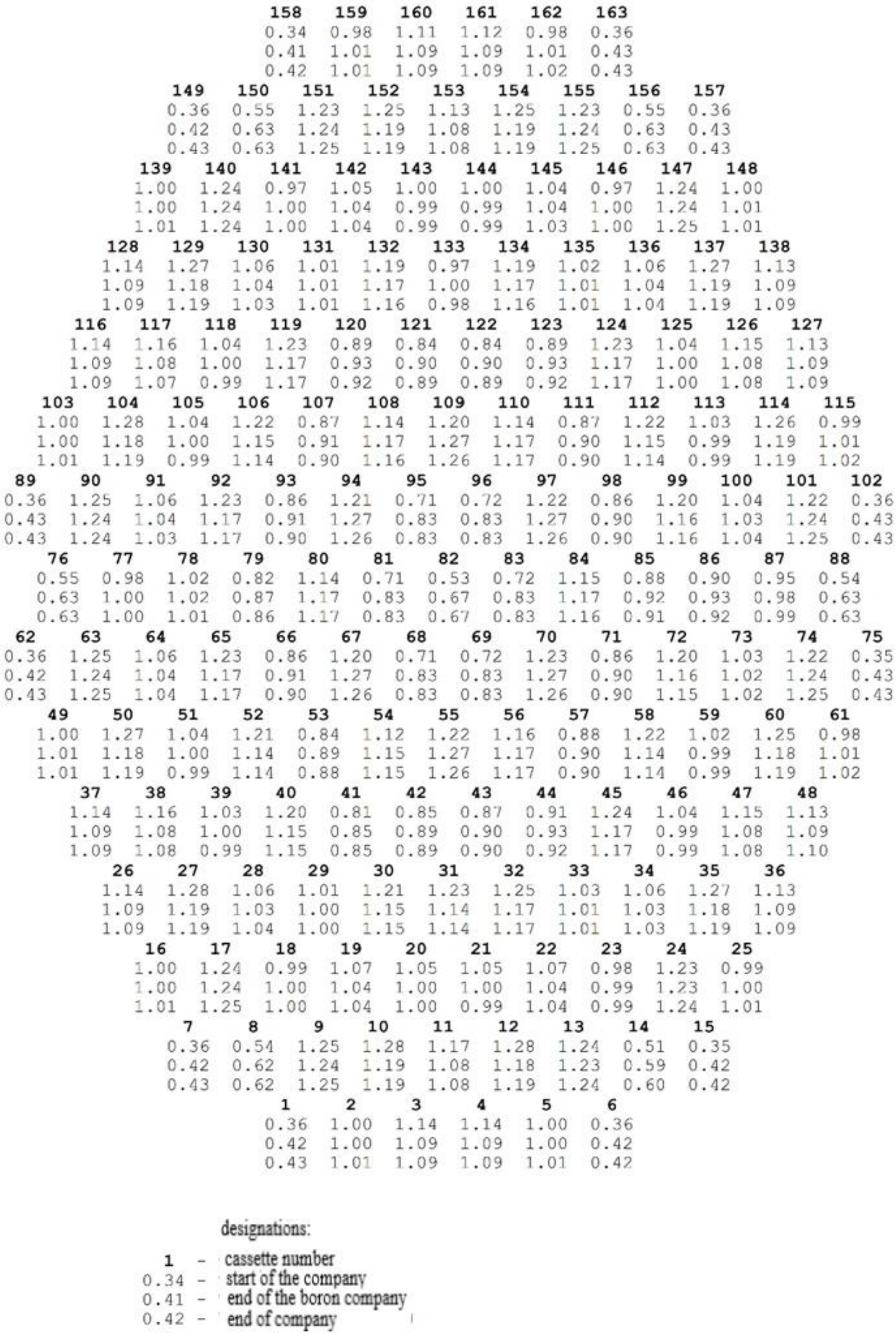

Figure 4.9 - Cartogram of the distribution of relative energy releases by cassettes at the beginning and end of the campaign for the 360-degree symmetry sector

158	159	160	161	162	163
0.34	1.01	1.15	1.15	1.01	0.35
0.33	0.99	1.14	1.14	1.00	0.35
0.33	0.98	1.12	1.12	0.99	0.34

149	150	151	152	153	154	155	156	157
0.36	0.54	1.26	1.27	1.14	1.28	1.26	0.54	0.36
0.35	0.53	1.24	1.26	1.13	1.26	1.25	0.54	0.35
0.35	0.53	1.23	1.25	1.12	1.25	1.23	0.53	0.35

139	140	141	142	143	144	145	146	147	148
1.04	1.28	0.98	1.04	0.96	0.96	1.03	0.98	1.29	1.04
1.03	1.27	0.97	1.03	0.96	0.96	1.03	0.97	1.27	1.03
1.01	1.26	0.96	1.03	0.96	0.96	1.03	0.96	1.26	1.02

128	129	130	131	132	133	134	135	136	137	138
1.19	1.32	1.07	0.99	1.14	0.85	1.14	1.00	1.07	1.32	1.19
1.18	1.31	1.06	0.99	1.15	0.87	1.15	1.00	1.06	1.31	1.18
1.17	1.30	1.06	0.99	1.15	0.90	1.16	1.00	1.06	1.30	1.16

116	117	118	119	120	121	122	123	124	125	126	127
1.20	1.19	1.03	1.21	0.84	0.77	0.77	0.85	1.21	1.03	1.18	1.18
1.18	1.18	1.03	1.22	0.85	0.77	0.78	0.85	1.22	1.03	1.17	1.17
1.17	1.17	1.04	1.23	0.85	0.78	0.79	0.86	1.23	1.04	1.17	1.16

103	104	105	106	107	108	109	110	111	112	113	114	115
1.05	1.33	1.03	1.14	0.81	1.09	1.14	1.09	0.81	1.14	1.02	1.31	1.03
1.03	1.32	1.03	1.18	0.82	1.09	1.15	1.10	0.82	1.18	1.02	1.30	1.02
1.02	1.31	1.04	1.22	0.83	1.10	1.15	1.10	0.84	1.22	1.03	1.29	1.01

89	90	91	92	93	94	95	96	97	98	99	100	101	102
0.36	1.30	1.07	1.21	0.80	1.16	0.66	0.66	1.17	0.81	1.18	1.05	1.27	0.35
0.36	1.28	1.07	1.22	0.82	1.17	0.66	0.67	1.18	0.82	1.19	1.05	1.26	0.35
0.35	1.27	1.07	1.23	0.83	1.17	0.67	0.67	1.18	0.84	1.21	1.05	1.25	0.35

76	77	78	79	80	81	82	83	84	85	86	87	88
0.55	1.00	1.01	0.77	1.09	0.66	0.48	0.67	1.11	0.84	0.88	0.95	0.54
0.55	0.99	1.01	0.78	1.10	0.67	0.48	0.68	1.12	0.85	0.89	0.95	0.53
0.54	0.98	1.01	0.78	1.10	0.67	0.48	0.68	1.13	0.86	0.89	0.94	0.53

62	63	64	65	66	67	68	69	70	71	72	73	74	75
0.36	1.30	1.07	1.20	0.80	1.16	0.67	0.68	1.19	0.82	1.18	1.03	1.26	0.35
0.36	1.29	1.07	1.22	0.81	1.16	0.67	0.68	1.20	0.83	1.19	1.03	1.25	0.35
0.35	1.27	1.07	1.23	0.83	1.17	0.67	0.68	1.20	0.84	1.21	1.03	1.24	0.35

49	50	51	52	53	54	55	56	57	58	59	60	61
1.05	1.33	1.03	1.13	0.79	1.08	1.18	1.13	0.83	1.15	1.02	1.30	1.03
1.04	1.32	1.03	1.18	0.80	1.09	1.19	1.14	0.84	1.19	1.02	1.30	1.02
1.02	1.31	1.04	1.22	0.82	1.10	1.19	1.15	0.86	1.23	1.03	1.29	1.01

37	38	39	40	41	42	43	44	45	46	47	48
1.20	1.20	1.03	1.19	0.77	0.81	0.83	0.89	1.23	1.03	1.18	1.18
1.19	1.19	1.04	1.20	0.78	0.82	0.84	0.90	1.25	1.04	1.18	1.17
1.18	1.18	1.04	1.22	0.79	0.83	0.86	0.90	1.26	1.04	1.17	1.16

26	27	28	29	30	31	32	33	34	35	36
1.20	1.34	1.08	1.01	1.20	1.16	1.24	1.03	1.08	1.32	1.19
1.19	1.33	1.08	1.01	1.22	1.21	1.26	1.04	1.08	1.31	1.18
1.18	1.32	1.08	1.01	1.23	1.25	1.27	1.04	1.08	1.31	1.17

16	17	18	19	20	21	22	23	24	25
1.05	1.30	1.01	1.09	1.05	1.05	1.09	1.00	1.29	1.04
1.04	1.29	1.00	1.09	1.06	1.06	1.09	0.99	1.28	1.03
1.03	1.28	1.00	1.09	1.06	1.06	1.09	0.99	1.27	1.02

7	8	9	10	11	12	13	14	15
0.36	0.55	1.31	1.35	1.22	1.34	1.30	0.52	0.35
0.36	0.54	1.30	1.34	1.21	1.34	1.29	0.51	0.35
0.35	0.54	1.29	1.33	1.21	1.33	1.28	0.51	0.35

1	2	3	4	5	6
0.36	1.06	1.22	1.21	1.05	0.36
0.36	1.05	1.20	1.20	1.04	0.35
0.36	1.04	1.19	1.19	1.03	0.35

designation:

1 - casset number
0.33 - relative energy release in the fuel assembly at H10=70%
0.33 - relative energy release in the fuel assembly at H10=80%
0.33 - relative energy release in the fuel assembly at H10=90%

Figure 4.10 - Cartogram of the distribution of relative energy releases by cassettes at the beginning of the campaign at the power level of 75%Nnom, for a sector of 360-degree symmetry, Xe=0

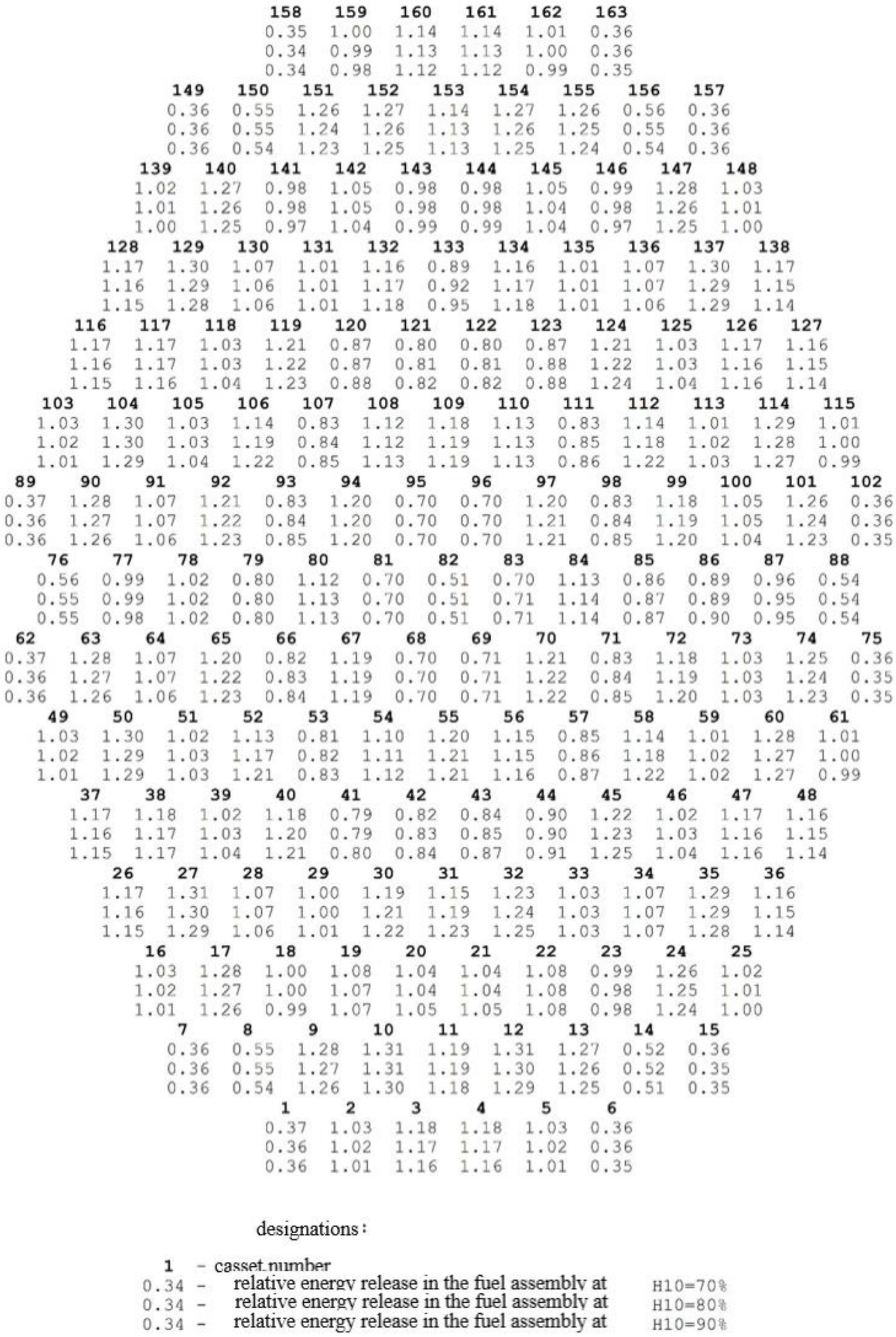

Figure 4.11 - Cartogram of the distribution of relative energy releases by cassettes at the beginning of the campaign at the power level of 75%Nnom, for a sector of 360-degree symmetry, Xe=1

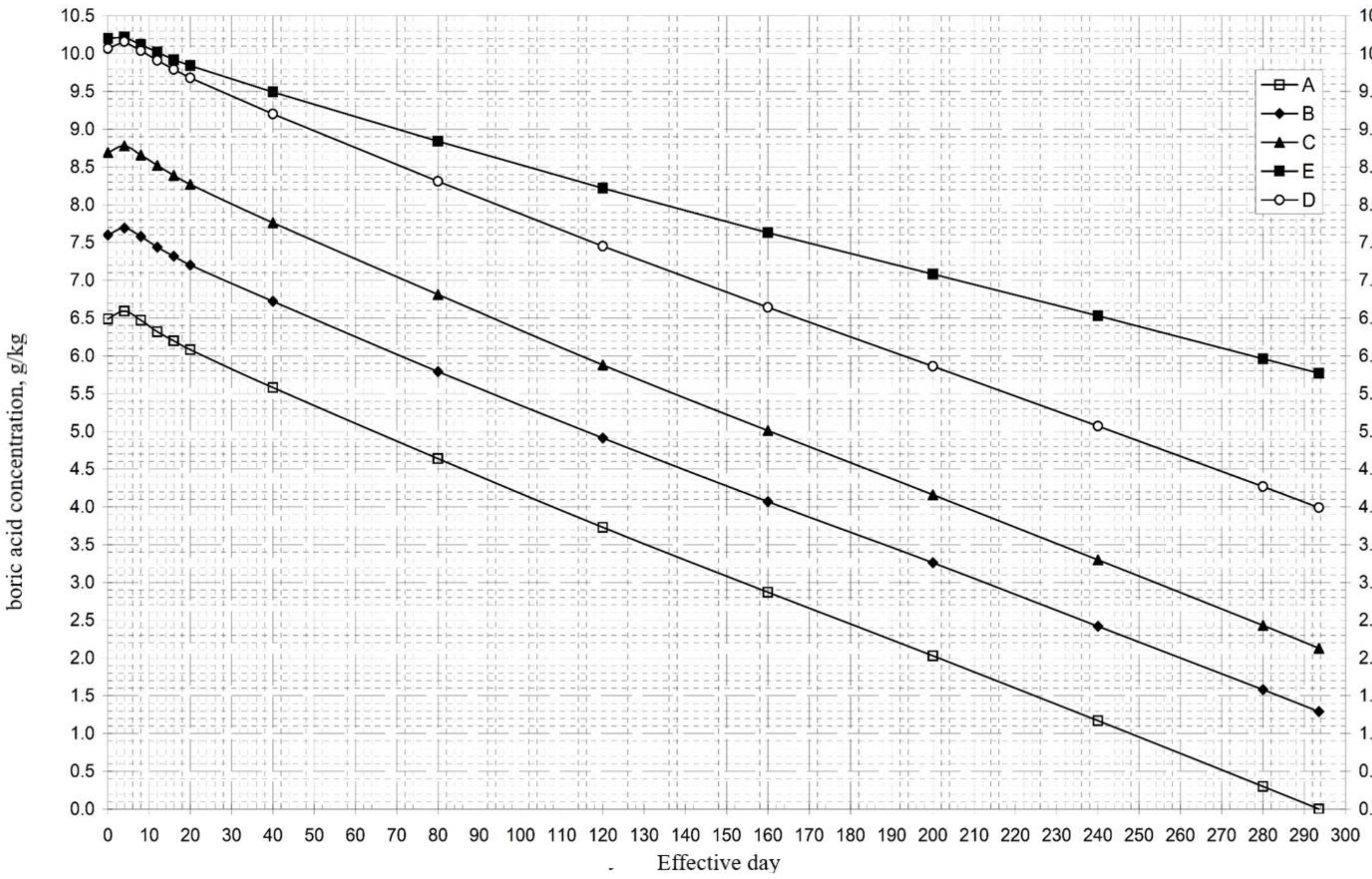

Figure 4.12 - Change in the critical concentration of boric acid during the operation of the fuel load

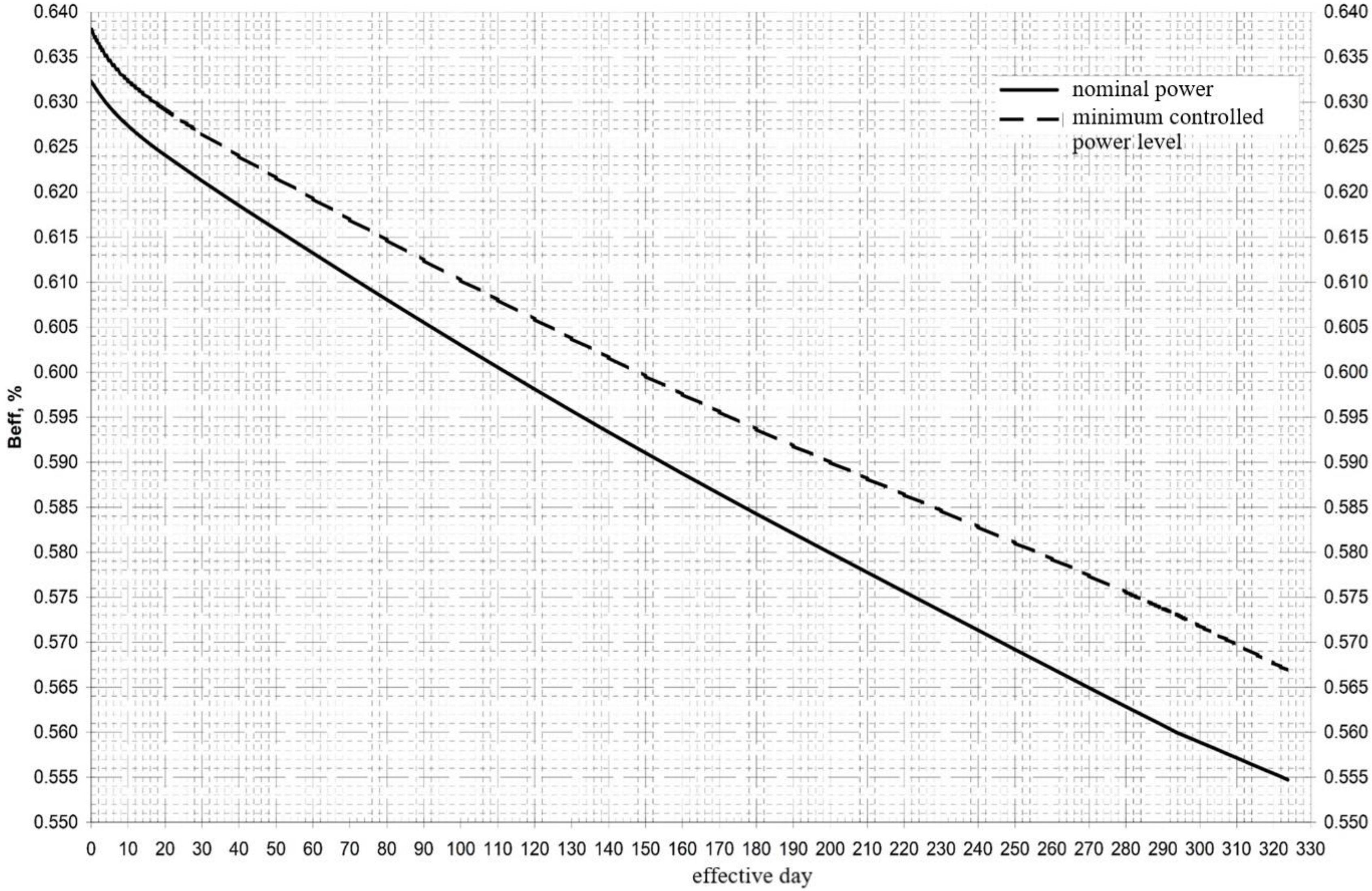

Figure 4.13 - Change in the effective fraction of delayed neutrons (Beff) during the operation of the fuel load

4.2.Effects and reactivity coefficients

Figure 4.14 shows the graphs of the total (power + temperature) reactivity effect when the power changes from the level N to zero, and the temperature-from the value corresponding to the power level N to 279°C, at the position of the working group 90% from the bottom of the core.

Figure 4.15 shows the graphs of the total (power + temperature) reactivity effect when the power changes - from zero to level N, and the temperature - from 279°C to the value corresponding to the power level N, at the position of the working group 90% from the bottom of the core.

Figure 4.16shows graphs of changes in the values of the power reactivity coefficient and the reactivity coefficient for the temperature of the coolant at the nominal parameters during the campaign.

Figure 4.17 shows the change in the value of the reactivity coefficient for the temperature of the coolant in the state on the MPL at different positions of the CPS AR during the campaign.

Graphs of changes in the value of boric acid efficiency during the campaign for different states of the reactor plant are shown in Figure 4.18.

States with the following parameter values are considered:

- A - N=100%, Xe poisoning is stationary;
- B - N=50%, Xe poisoning corresponds to 50% power;
- C - N=100%, no Xe poisoning;
- D - N=0%, no Xe poisoning, temperature 279°C;
- E - N=0%, no Xe poisoning, temperature 20°C.

Figure 4.19 shows the change in the value of the reactivity margin during the campaign with the absorbers removed. The graph designations are as follows:

- A burnout reactivity margin;
- B reactivity margin for burnout and stationary poisoning Xe135;
- C reactivity margin for burnout and stationary poisoning Xe135, power (from 0% to 100%) and temperature (from 279°C to 302°C) reactivity effects;
- D reactivity margin for burnout and stationary poisoning Xe135, power (from 0% to 100%) and temperature (from 20°C to 302°C) reactivity effects.

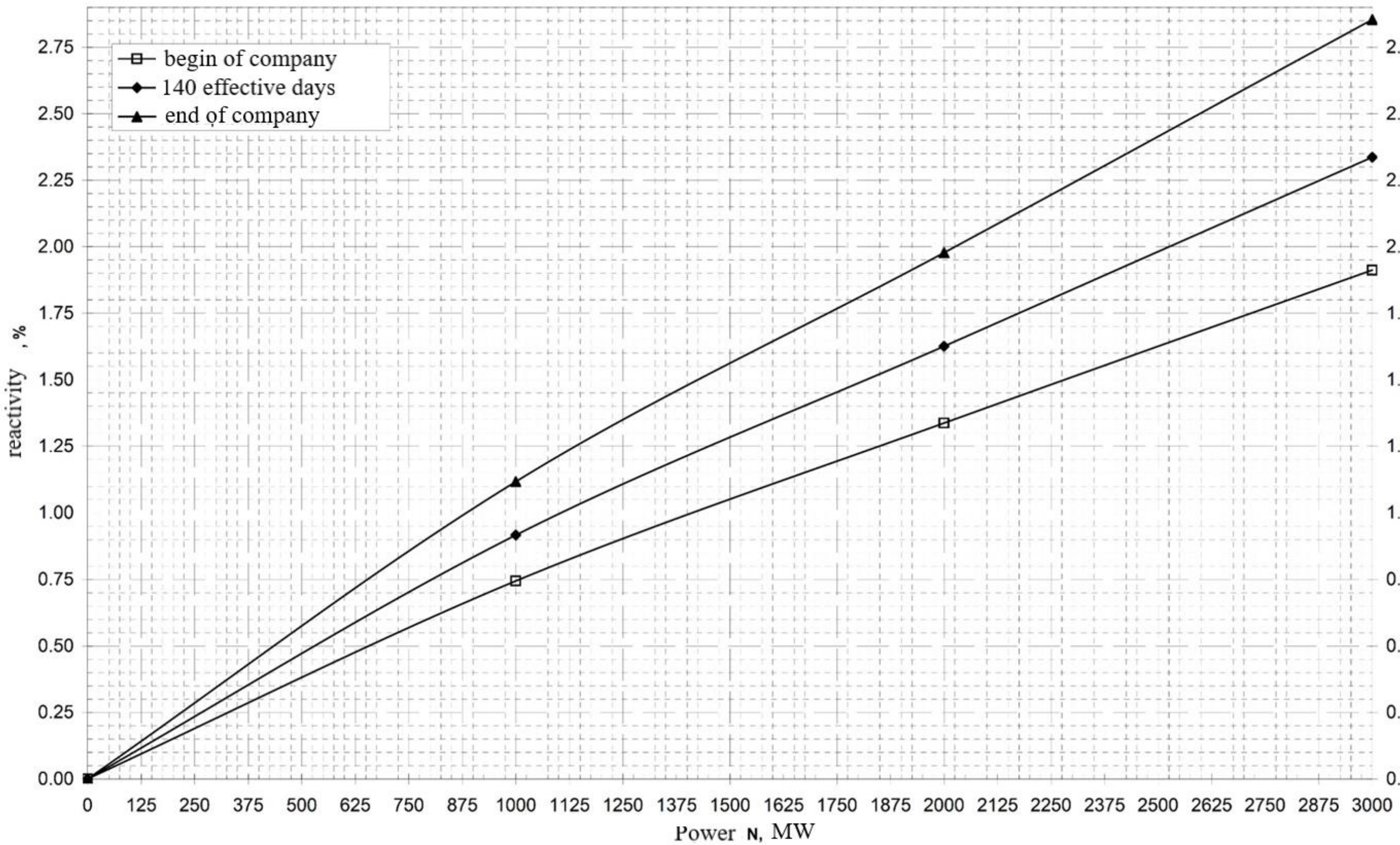

Figure 4.14 - The total effect of reactivity when the power changes from the level N to zero and the temperature changes from the value corresponding to the power level N to 279 °C

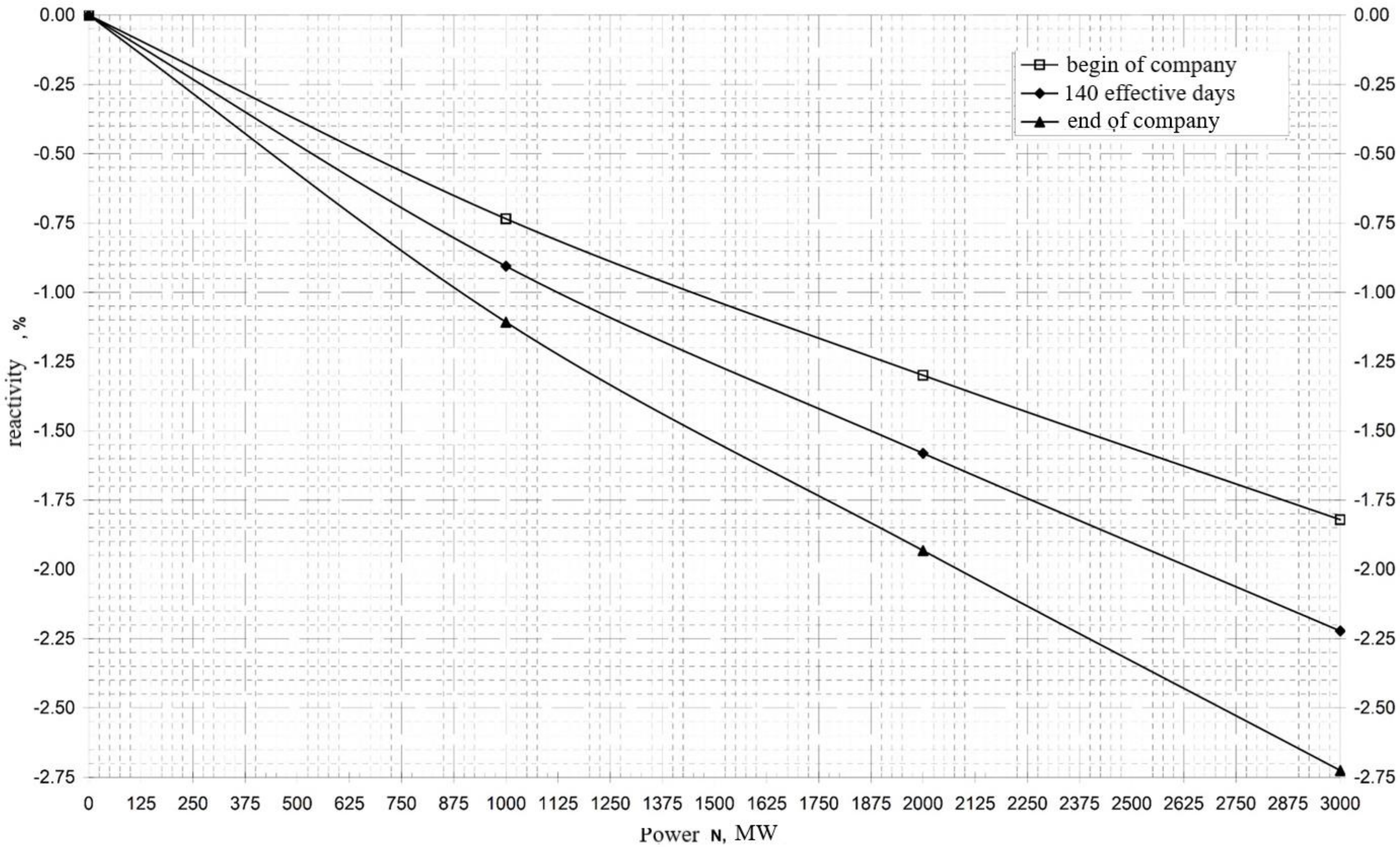

Figure 4.15 - The total effect of reactivity when the power rises from zero to the N level and the temperature rises from 279 °C to the value corresponding to the power level N

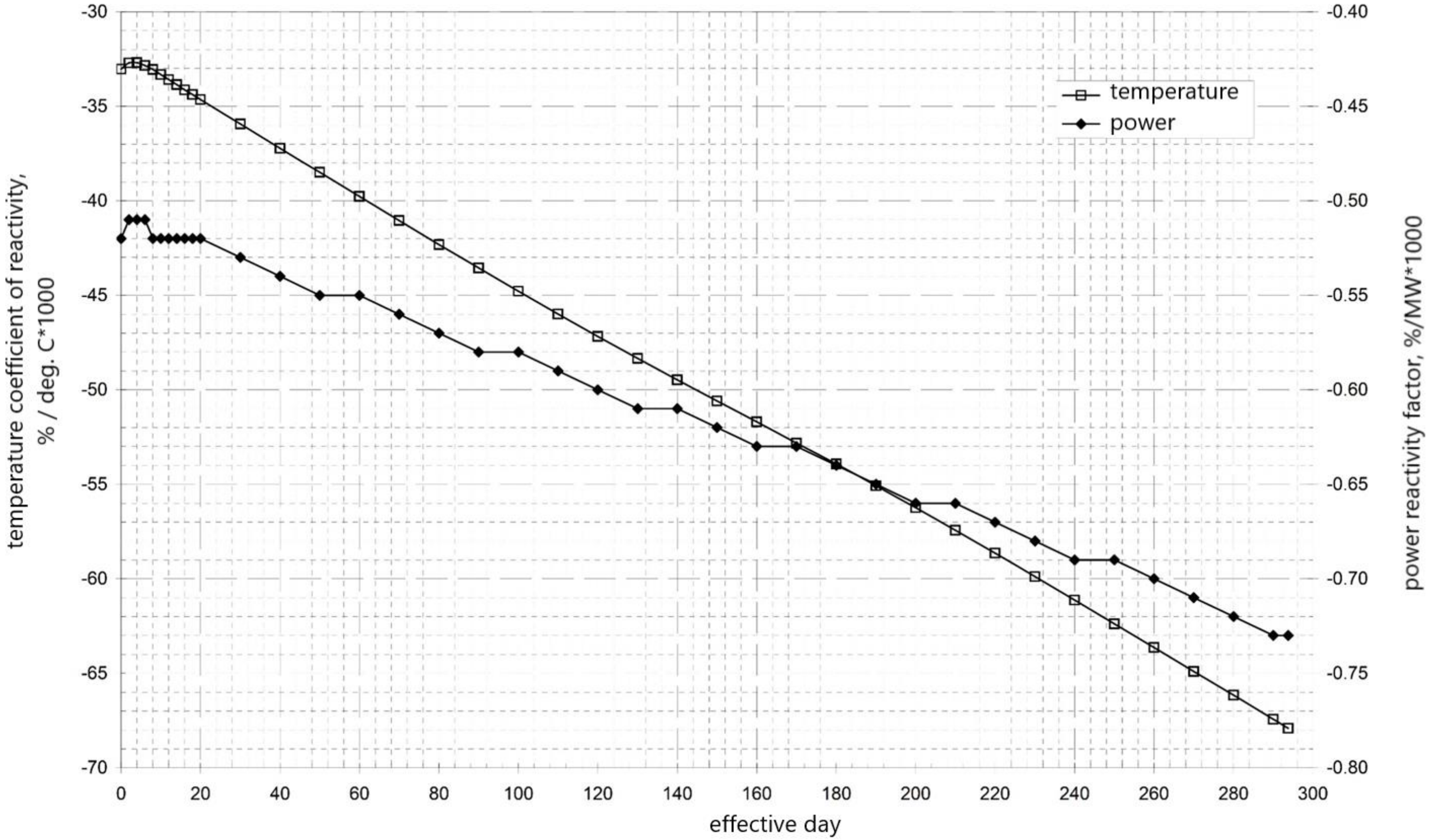

Figure 4.16 - Change in the values of the power reactivity coefficient and the reactivity coefficient for the temperature of the coolant at the nominal parameters

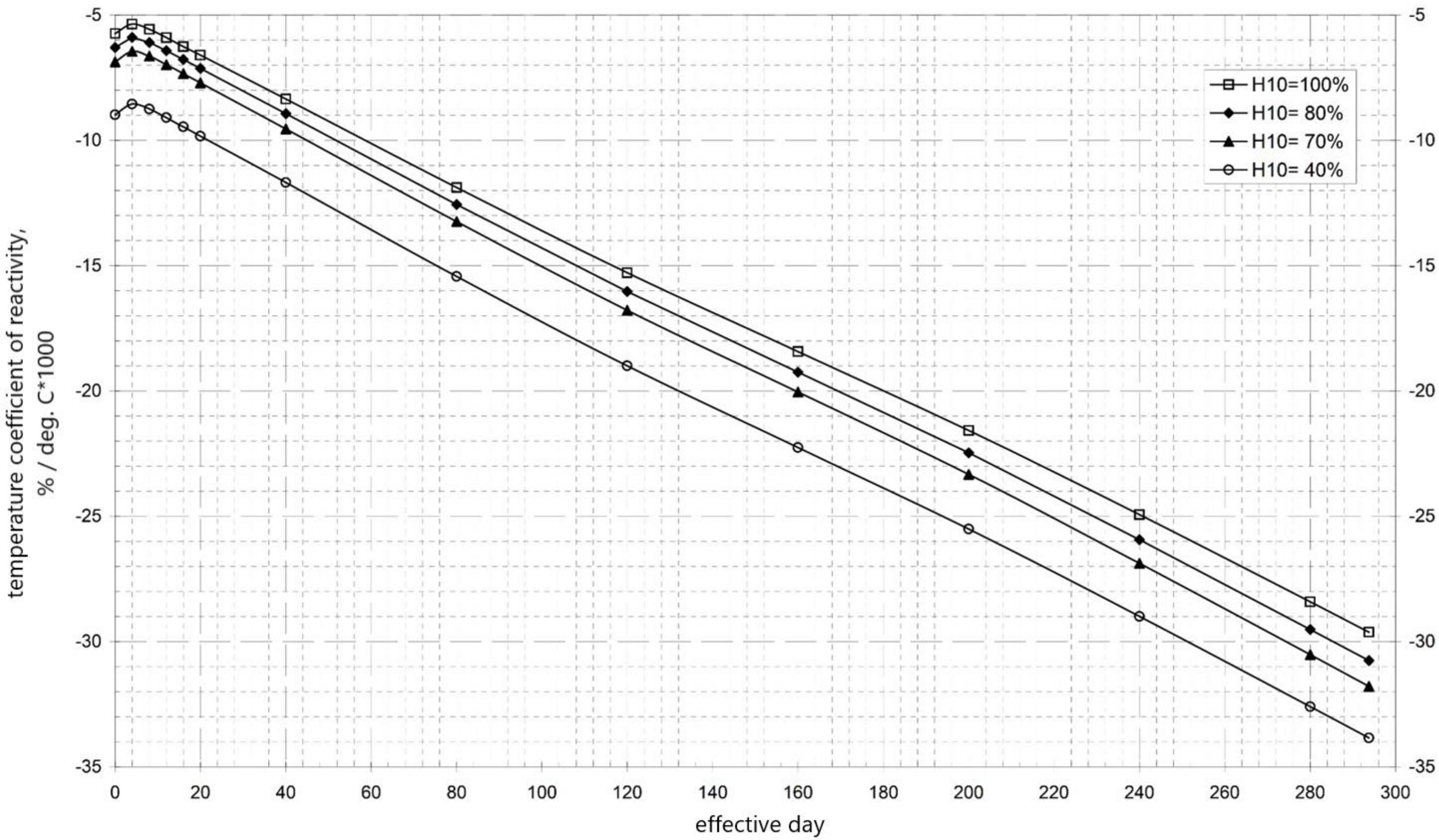

Figure 4.17 - Change in the value of the reactivity coefficient for the temperature of the coolant in the state on the minimum-controlled power level at different positions of the CR CPS during the campaign

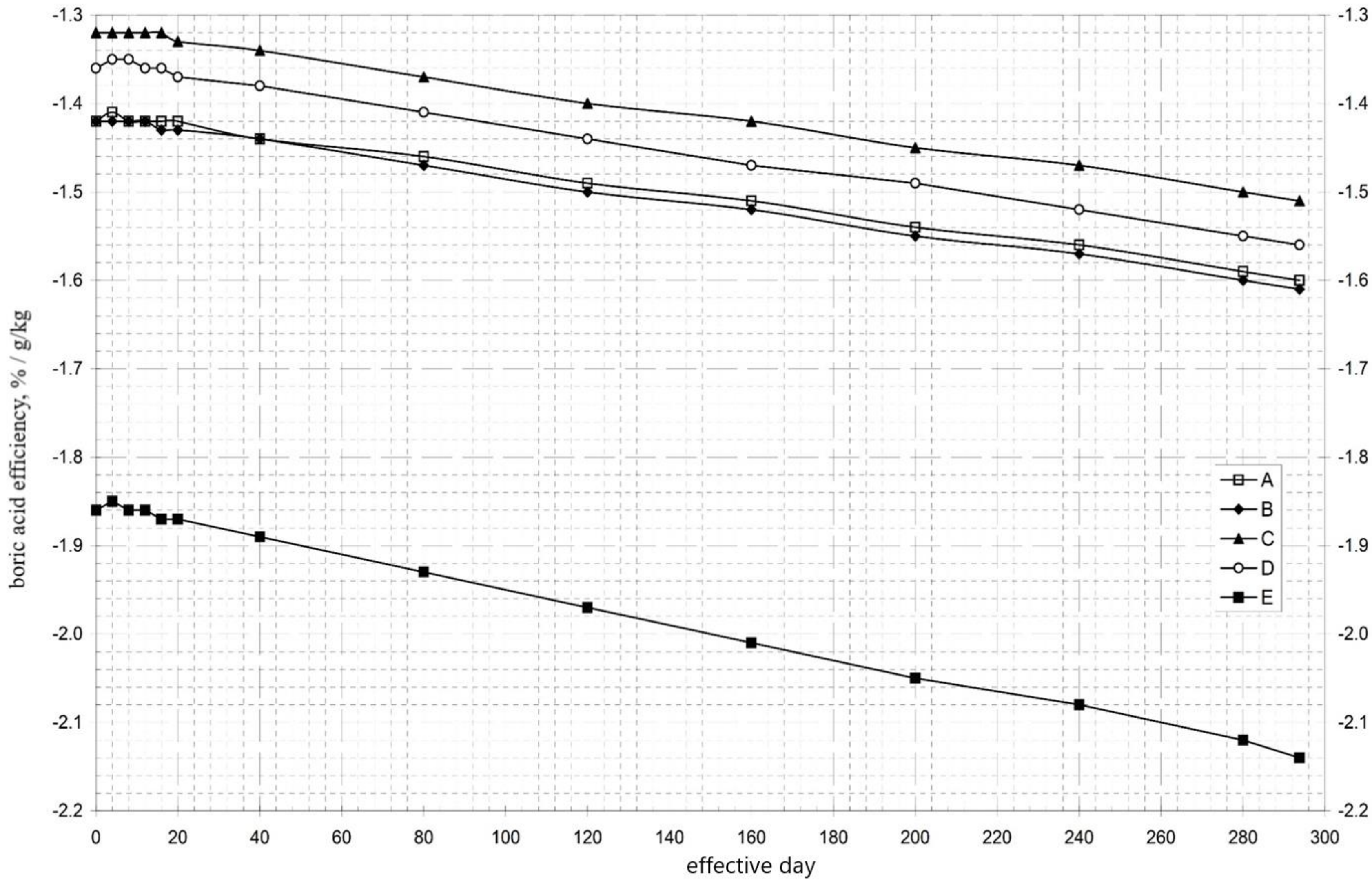

Figure 4.18 - Changes in the effectiveness of boric acid during the campaign

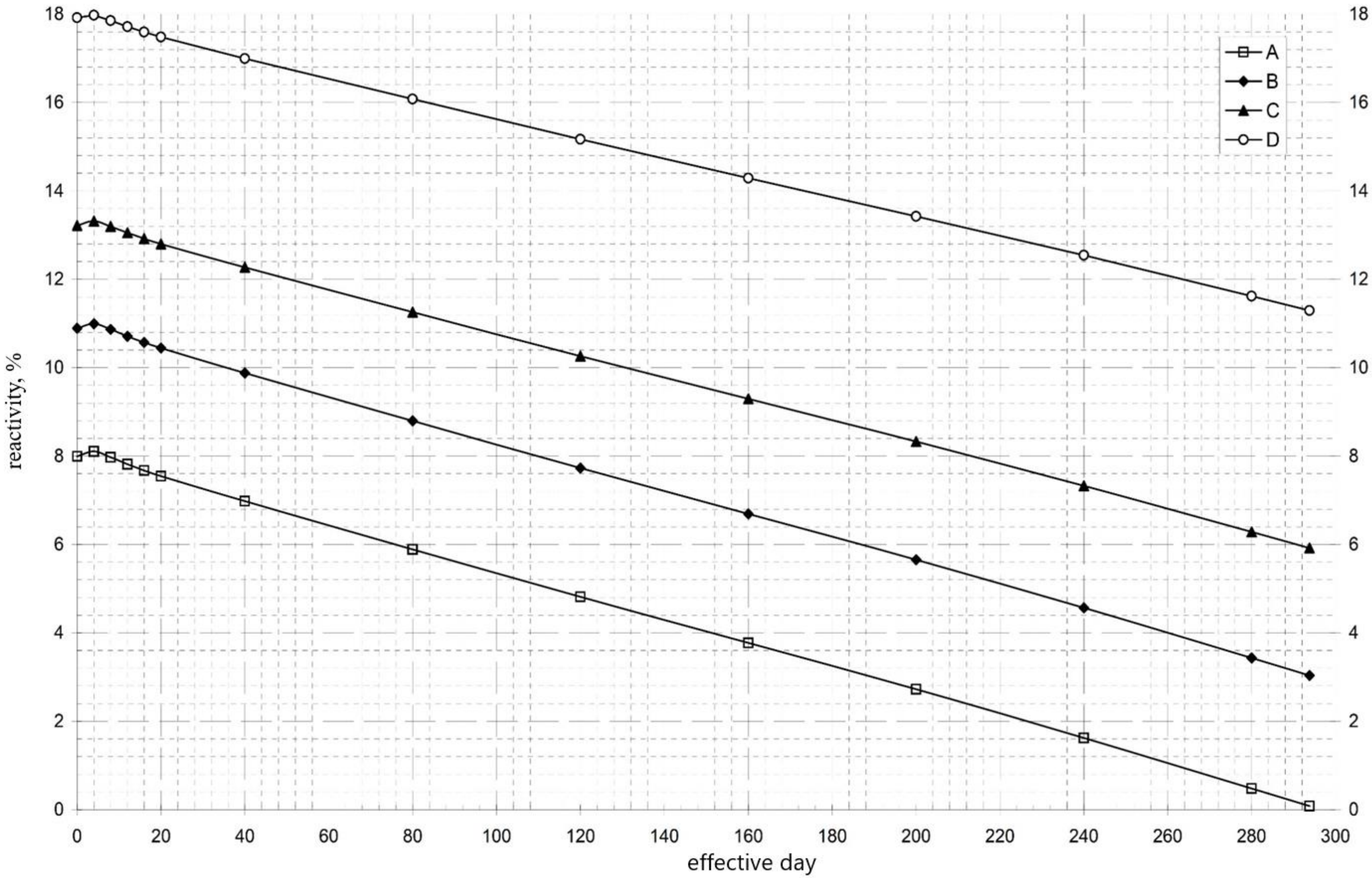

Figure 4.19 - Change in the value of the reactivity margin during the campaign with the absorbers removed

REFERENCES

1. CAMIVVER – Codes and Methods improvements for VVER comprehensive safety assessment. – H2020 Proposal ID 945081.
2. T. Lötsch, V. Khalimonchuk, A. Kuchin, PROPOSAL OF A BENCHMARK FOR CORE BURNUP CALCULATIONS FOR A VVER-1000 REACTOR CORE, 2009; 57 p; 19. AER Symposium on VVER Reactor Physics and Reactor Safety; Varna (Bulgaria); 21-25 Oct 2009.
3. T. Lötsch, S. Kliem, E. Bilodid, V. Khalimonchuk, A. Kuchin, Yu. Ovdienko,M. Ieremenko, R. Blank, G. Schultz, THE X2 BENCHMARK FOR VVER-1000 REACTOR CALCULATIONS. RESULTS AND STATUS, International Conference “Novel Vision of Scientific & Technical Support for Regulation of Nuclear Energy Safety: Competence, Transparency, Responsibility” dedicated to the 25th Anniversary of the SSTC NRS, Kiev, Ukraine, 22 – 23 March 2017.
4. Y. Bilodid, E. Fridman, T. Lötsch, X2 VVER-1000 benchmark revision: Fresh HZP core state and the reference Monte Carlo solution, Annals of Nuclear Energy, Volume 144, 1 September 2020, 107558, X2 benchmark dataset: https://rodare.hzdr.de/record/200.
5. S.Nikonov, K.Velkov, S.Langenbuch, M.Lizorkin, A.Kotsarev, Optimal Nodalization Schemas of VVER-1000 Reactor Pressure Vessel for the Coupled Code ATHLET-BIPR8KN, 16th Symposium of AER on VVER Reactor Physics and Reactor Safety, Slovakia, Bratislava, Sept. 25-29, 2006.
6. B. Ivanov, K. Ivanov, E. Royer, S. Aniel, Y. Kozmenkov, U. Grundmann, ANALYSIS OF THE NEUTRONIC SPECIFICATIONS OF THE OECD/DOE/CEA V1000CT-1 EXERCISE 2 BENCHMARK.
7. B.Ivanov, K.Ivanov, P.Groudev, M.Pavlova, V.Hadjiev, VVER-1000 Coolant Transient Benchmark - Phase 1 (V1000CT-1), Vol. I: Main Coolant Pump (MCP) Switching On - Final Specifications, NEA/OECD 2002, NEA/NSC/DOC(2002)6.
8. N .Kolev, E. Royer, U.Bieder, S.Aniel, D. Popov and Ts. Topalov, VVER-1000 Coolant Transient Benchmark Volume II: Specifications of the VVER-1000 Vessel Mixing Problems, NEA/OECD NEA/NSC/DOC (2004).
9. N.P. Kolev, I. Spasov INRNE, Bulgaria E. Royer, VVER-1000 Coolant Transient Benchmark Phase 2 (V1000CT-2) Summary Results of Exercise 1 on Vessel Mixing Simulation, OECD 2010 NEA No. 6964.
10. N. Kolev, N. Petrov, J. Donov, D. Angelova, S. Aniel, E. Royer, B. Ivanov, K. Ivanov, E. Lukanov, Y. Dinkov, D. Popov, S. Nikonov, VVER-1000 Coolant Transient Benchmark, PHASE 2 (V1000CT-2), Vol. III: MSLB Problem – Final Specifications, NEA/NSC/DOC(2006).
11. Pavlin Groudev, Malinka Pavlova, RELAP5/MOD3.2 INVESTIGATION OF A VVER-1000 MCP SWITCHING ON PROBLEM, ICONE10-22443, Proceedings of ICONE 10, The Tenth International Conference on Nuclear Engineering April 14-18, 2002, Arlington, Virginia, USA.
12. B. Ivanov, K. Ivanov S. Aniel, E. Royer N. Kolev, P. Groudev, OECD/DOE/CEA VVER 1000 Coolant Transient (V1000CT) Benchmark for Assessing Coupled Neutronics/Thermal-Hydraulics System Codes for VVER-1000 RIA Analysis, PHYSOR 2004 -The Physics of Fuel Cycles and Advanced Nuclear Systems: Global Developments Chicago, Illinois, April 25-29, 2004, on CD-ROM, American Nuclear Society, Lagrange Park, IL. (2004).

13. Ulrich Bieder, Gauthier Fauchet, Sylvie Bétin , Nikola Kolev, Dimitar Popov, SIMULATION OF MIXING EFFECTS IN A VVER-1000 REACTOR, Nuclear Engineering and Design 237(15-17):1718-1728.
14. B. Ivanov, K. Ivanov, E. Royer, S. Aniel, U. Bieder, N. Kolev, P. Groudev, OECD/DOE/CEA VVER-1000 coolant transient (V1000CT) benchmark - A consistent approach for assessing coupled codes for RIA analysis, Progress in Nuclear Energy 48 (2006) 728-745.
15. A. Stefanova, P. Groudev, Comparison of RELAP5 calculations of VVER-1000 coolant transient benchmark phase 1 at different power, Progress in Nuclear Energy 48 (2006) 790-805.
16. K. Ivanov, M. Avramova, S. Kamerow, I. Kodeli, E. Sartori, E. Ivanov, O. Cabellos, BENCHMARKS FOR UNCERTAINTY ANALYSIS IN MODELLING (UAM) FOR THE DESIGN, OPERATION AND SAFETY ANALYSIS OF LWRs Volume I: Specification and Support Data for Neutronics Cases (Phase I) Version 2.1 (Final Specifications), NEA/NSC/DOC(2013)7.
17. P V Gordienko, P K Kiryukhin, and A A Shcherbakov, Benchmark calculation AER VVER-1000 - ETE using BIPR8, ICNRP Volga-2018, IOP Conf. Series: Journal of Physics: Conf. Series 1133 (2018) 012043.
18. Spasov, S. Mitkov, N.P. Kolev, S. Sanchez-Cervera, N. Garcia-Herranz, A. Sabater, D. Cuervo, J. Jimenez, V.H. Sanchez L. Vyskocil, Best-estimate simulation of a VVER MSLB core transient using the NURESIM platform codes, Nuclear Engineering and Design 321 (2017) 26–37.
19. Spasov, J. Donov, N. P. Kolev, and L. Sabotinov, CATHARE Multi-1D Modeling of Coolant Mixing in VVER 1000 for RIA Analysis, Science and Technology of Nuclear Installations, Volume 2010, Article ID 457094.
20. Ovdiienko, M. Ieremenko, Y. Bilodid, Jelena Krhounkova, Experience and perspective of best-estimate approach application for RIA analysis, Nuclear and Radiation Safety, November 2016.
21. R. Ferrer and T. Bahadir, Validation of new CMS5-VVER nuclear data library using critical experiments and X2 full-core benchmark, Kerntechnik, Volume 85, Issue 4, September 2020.
22. VALIDATION MATRIX FOR THE ASSESSMENT OF THERMAL-HYDRAULIC CODES FOR VVER LOCA AND TRANSIENTS, A Report by the OECD Support Group on the VVER Thermal-Hydraulic Code Validation Matrix, NEA/CSNI/R(2001)4.
23. Ivan Tóth, The VVER Code Validation Matrix and VVER Specificities, THICKET 2008 – Session III – Paper 05.
24. Del Nevo, M. Adorni, F. D'Auria, O. I. Melikhov, I. V. Elkin, V. I. Schekoldin, M. O. Zakutaev, S. I. Zaitsev, and M. Benčík, “Validation of Advanced Computer Codes for VVER Technology: LB-LOCA Transient in PSB-VVER Facility”, Science and Technology of Nuclear Installations, Volume 2012, Article ID 480948.
25. V. Alekseev, O. I. Dreganov, A. L. Izhutov, I. V. Kiseleva,V. N. Shulimov, Outcomes of the “steady-state crisis” experiment in the MIR reactor channel, Nuclear Energy and Technology 5(3): 207–212.
26. A.A. Falkov, O.B. Samoilov, A.V. Kupriyanov, V.E. Lukyanov, O.N. Morozkin, D.L. Shipov, EXPERIMENTAL INVESTIGATION AND ANALYSIS OF THERMAL HYDRAULIC CHARACTERISTICS OF WWER-1000 ALTERNATIVE FA, 6 th

International Conference on WWER Fuel Performance, Modeling and Experimental Support, Albena, Bulgaria.

27. J. Höglund, S. Andersson, F. Waldermarsson, S. Slyeptsov, DNB measurements in the Westinghouse Critical Heat Flux Test Facility – ODEN to provide an improved correlation to increase DNB margin for the Westinghouse WWER-1000 fuel design (2013).
28. AER Benchmark book, Atomic energy research (AER), Budapest, 1999 P. Dařilek, Korpás,J. Kyncl,L. Maiorov,M. Makai, P. Siltanen.
29. AER Benchmark Specification Sheet, Test ID: AER-FCM-101.
30. AER Benchmark Solution Sheet, Test ID: AER-FCM-101, Forschungszentrum Rossendorf Institute of Safety Research, Germany, 02.06.2005 Ulrich Grundmann.
31. AER Benchmark Solution Sheet, Test ID: AER-FCM-101, Nuclear Research Institute Rez plc 250 68 Rez, Czech Republic, 16.06. 2006, Jan Hádek.
32. AER Benchmark Specification Sheet, Test ID: AER-FCM-102, G. Alekova, R. Prodanova.
33. AER Benchmark Specification Sheet, Test ID: AER-HOM-101, Mihály Makai.
34. Validation of coupled neutronic/thermal-hydraulic codes for VVER reactors. Final Report - FIKS-CT-2001-00166, S. Mittag, U. Grundmann, S. Kliem, Y. Kozmenkov, U. Rindelhardt, U. Rohde, F.-P. Weiß, S. Langenbuch, B. Krzykacz-Hausmann, K.-D. Schmidt T. Vanttola, A. Hämäläinen, E. Kaloinen , A. Keresztúri , G. Hegyi , I. Panka , J. Hádek , C. Strmensky , P. Darilek, P. Petkov, S. Stefanova, A. Kuchin, V. Khalimonchuk, P. Hlbocky , D. Sico, S. Danilin, V. Ionov, S. Nikonov, and D. Powney.
35. Validation of coupled neutron kinetic/thermal-hydraulic codes. Part 1: Analysis of a VVER-1000 transient (Balakovo-4), Annals of Nuclear Energy 28 (2001) 857-873, S. Mittaga, S. Kliema, F.P. Weißa, R. Kyrki-Rajamaki, Hamalainen, S. Langenbuch, S. Danilin, J. Hadek, G. Hegyi, A. Kuchin, D. Panayotov.
36. Development of CrossSection Library for DYN3D Code. I. Ovdiienko, M. Ieremenko, A. Kuchin, V. Khalimonchuk.
37. DEVELOPMENT OF A THREE-DIMENSIONAL MODEL OF THE VVER-1000 REACTOR USING SERPENT MONTE CARLO CODE FOR NEUTRON-PHYSICAL MODELING. V. Gulik, PhD,V. Galchenko, PhD, I. Shlapak, D. Budik.
38. Explicit decay heat calculation in the nodal diffusion code DYN3D. Y. Bilodid, E. Fridman, D. Kotlyar, E. Shwageraus.
39. Power coefficient of reactivity: definition, interconnection with other coefficients of reactivity, evaluation of results of transients in power nuclear reactors. Yury A. Kazansky, Ya.V. Slekenichs.
40. Solution of Point Reactor Neutron Kinetics Equations with Temperature Feedback by Singularly Perturbed Method. Wenzhen Chen, Jianli Hao, Ling Chen, and Haofeng Li.
41. Validation of Pin Power Calculations Using DYN3D on MIDICORE Benchmark Kuchyn O., Ovdiienko I., Khalimonchuk V., Ieremenko M.